

DOE/ESF/70030 - T33

Attachment to Letter No.

XL-611-00026

EVALUATION OF LLTR SERIES II TESTS

A-1A & A-1B TEST RESULTS

MASTER

AT03-765F70030
BY

B. F. SHOOPAK
J. C. AMOS
T. J. NORVELL

Advanced Reactor Systems Department
General Electric Company
Sunnyvale, California

March 1980

Prepared for

U. S. Department of Energy
Under Contract No. DE-AT03-765F70030
Work Package AF 15 10 05, WPT No. SG037

DISCLAIMER

This book was prepared as an account of work sponsored by an agency of the United States Government. Neither the United States Government nor any agency thereof, nor any of their employees, makes any warranty, express or implied, or assumes any legal liability or responsibility for the accuracy, completeness, or usefulness of any information, apparatus, product, or process disclosed, or represents that its use would not infringe privately owned rights. Reference herein to any specific commercial product, process, or service by trade name, trademark, manufacturer, or otherwise, does not necessarily constitute or imply its endorsement, recommendation, or favoring by the United States Government or any agency thereof. The views and opinions of authors expressed herein do not necessarily state or reflect those of the United States Government or any agency thereof.

DISTRIBUTION OF THIS DOCUMENT IS UNLIMITED

fey

DISCLAIMER

This report was prepared as an account of work sponsored by an agency of the United States Government. Neither the United States Government nor any agency thereof, nor any of their employees, makes any warranty, express or implied, or assumes any legal liability or responsibility for the accuracy, completeness, or usefulness of any information, apparatus, product, or process disclosed, or represents that its use would not infringe privately owned rights. Reference herein to any specific commercial product, process, or service by trade name, trademark, manufacturer, or otherwise does not necessarily constitute or imply its endorsement, recommendation, or favoring by the United States Government or any agency thereof. The views and opinions of authors expressed herein do not necessarily state or reflect those of the United States Government or any agency thereof.

DISCLAIMER

Portions of this document may be illegible in electronic image products. Images are produced from the best available original document.

CONTENTS

	<u>Page No.</u>
I INTRODUCTION & OBJECTIVES	1
II SUMMARY & CONCLUSIONS	2
III TEST AND FACILITY DESCRIPTION	3
A. FACILITY DESCRIPTION	3
B. TEST CONDITIONS	7
C. INTER-TEST EVALUATION	8
IV ANALYTICAL METHODS & MODELS	26
A. OVERALL APPROACH	26
B. RUPTURE TUBE MODELING WITH NONSAP & RELAP COMPUTER CODES	26
C. SODIUM SYSTEM MODELING WITH TRANSWRAP	27
V EVALUATION OF TEST RESULTS	53
A. LLTV & SYSTEM PRESSURES	53
B. RELIEF SYSTEM PERFORMANCE	55
C. PRETEST PREDICTIONS	56
VI REFERENCES	90
VII APPENDICES	
A1 A-1A RESULTS TO 100 MSEC	
A2 A-1A RESULTS TO 1 SECOND	
B. A-1B RESULTS TO 1 SECOND	
C. A-1A AND A-1B PRESSURE DATA TO 20 MSEC	
D. RELAP INPUT LISTINGS	
E. TRANSWRAP INPUT LISTINGS	
F. RUPTURE DISC DYNAMIC MODEL LISTING	

I. INTRODUCTION & OBJECTIVES

This report presents an evaluation of the first two tests (A-1a and A-1b) in the Series II Large Leak Test Program being performed at the Energy Technology Engineering Center in the Large Leak Test Rig (LLTR). This test program will evaluate the effects of intermediate size to large size leaks produced by a double-ended guillotine (DEG) rupture of a single tube. Tests A-1a and A-1b were inert gas injection tests and were conducted in July 1979 and October 1979 respectively. The balance of the tests currently planned are sodium-water reaction tests. The test article employed in Series II simulates the CRBR steam generator but is of shorter length.

The principal objectives of the Series II program are to define the potential for secondary tube failures in order to establish a basis for selection of design basis leaks (DBL's), to determine experimentally the peak pressures produced from large leak events and, to provide data for confirming or modifying design analysis methods. Test A-1a provided the opportunity to shakedown the LLTR systems and instrumentation which had been modified after the Series I program. Test A-1a and Test A-1b also allowed comparison of the effects of using a single rupture disc and double rupture disc assembly in the relief system. Use of pressured nitrogen rather than water/steam in the ruptured tube permitted assessment of analytical modeling methodology separated from the complicating phenomena introduced by the chemical processes of a sodium-water reaction.

The major objectives of this report are to assess and extend the analytical methodology, established during Series I testing, to predict the thermal-hydraulic phenomena (exclusive of sodium-water reaction chemistry) of importance to LMFBR design for large leaks in steam generators. Of particular interest is the ability to predict:

- o peak leak site pressures
- o propagation of pressure waves in the sodium system
- o performance of both single and double rupture discs
- o and performance of the relief system

This report also summarizes the inter-test examinations and activities performed after Tests A-1a and A-1b.

II. SUMMARY & CONCLUSIONS

The standard methodology developed from the Series I testing and analysis was applied to the evaluation of Series II tests A-1a and A-1b. A dynamic rupture model of a double rupture disc assembly, which was developed from the SWAAM code, was also incorporated into TRANSWRAP to permit post-test evaluation of the data. The analyses leads to the following conclusions:

1. The standard methodology, with minor modifications described below, provides conservative yet realistic predictitons of leaksite and other sodium system pressures in the LLTR Series II vessel and piping.
2. The good agreement between predicted and measured pressures indicates that the TRANSWRAP/RELAP modeling developed from the Series I tests is applicable to larger scale units prototypical of the Clinch River steam generator design. In particular, these results add further justification for use of the one-dimensional flow model in the TRANSWRAP II computer code for large scale units.
3. Calculated sodium system pressures are sensitive to several modeling parameters including rupture disc modeling, acoustic velocity in the test vessel, and flow rate from the rupture tube. The acoustic velocity which produced best agreement with leaksite pressures was calculated based on the shroud diameter and shroud wall thickness. The corresponding rupture tube discharge coefficient was that of the standard design methodology developed from Series I testing. Stronger pressure pulses from the sodium-water reaction in Test A-2 may premit better determination of acoustic velocity within the test vessel. A reevaluation of the above modeling parameters is planned as part of the test A-2 evaluation.
4. As was found in Series I testing, the Series II data suggests that the leading edge of the flow in the relief line is two phase for a single, doubled-ended guillotine tube rupture.
5. The steam generator shroud acts as if it is relatively transparent to the transmission of radial pressures to the vessel wall.
6. No firm conclusions on elbow attenuation effects of pressure pulses could be determined from these tests because of the complex wave patterns resulting from internal reflections in the piping system. Further studies are planned in this area as part of the test A-2 evaluation.

7. Slightly lower sodium system maximum pressures measured during Test A-1b compared to Test A-1a are attributed to premature failure (failure at a lower pressure) of the rupture disc in contact with the sodium for test A-1b, though the reason for this early failure is currently unknown.

The delay in failure of the second disc in Test A-1b, which was successfully modeled with TRANSWRAP, is attributed to the limited energy in the nitrogen injection which was not sufficient to fail the second disc. It is believed that initial tearing of the first disc results from the relatively low energy pulses generated by nitrogen injection. Further tearing of this disc to the post-test observed condition of 50% open is believed to have resulted from sodium flow occurring when the second disc ruptured at 12.7 seconds. This limited rupture disc opening is consistent with the findings of recent rupture disc tests at SRI (reference 12) which indicated that the disc opening area decreases as the acoustic pressure pulse energy decreases.

III. TEST AND FACILITY DESCRIPTION

A. FACILITY DESCRIPTION

The LLTR consists of a test article having representative Clinch River steam generator geometry and those systems required to prepare for, conduct, and recover from large sodium-water reaction tests. These systems are the sodium system, the water/steam injection system, the reaction products relief system, and the instrumentation and control system. Each is briefly described in the following sections. A simplified schematic is shown as Figure III-I.

1. Test Article Description

The Series II test article shown in Figure III-2 consists of two major assemblies; the permanently installed Large Leak Test Vessel (LLTV) and the removable Large Leak Test Internals (LLTI). These assemblies, when combined, are representative of a full-scale LMFBR steam generator from the standpoint of the sodium/water reaction event. The vessel is comparable to the inside diameter of the CRBRP steam generators. The LLTI tube size, number and pitch is the same as the CRBRP; however, the LLTI tube bundle length is slightly less than half the length of the CRBRP tube bundle. Full scale test article diameter is considered necessary to obtain representative sodium ejection velocities and hydrogen bubble geometries

under sodium-water reaction conditions which could be quite different in a scaled down diameter. Representative test article length is less important since the analysis code can be readily adjusted for length. The test article assemblies are constructed of 2-1/4Cr-1 Mo.

The LLTV consists of a top hemispherical head, a cylindrical shell and a bottom hemispherical head. The top head secures the LLTI tubesheet in place and acts as a steam head for the LLTI secondary tubes. A gasket between the top head and the LLTI tubesheet provides the steam seal. The top head has three nozzles. One nozzle is for instrumentation, and the other two are positioned over the central and peripheral rupture tube locations for attachment to the Large Leak Injection Device and the secondary tube steam supply line.

A seal ring provides the primary seal between the shell upper flange and the LLTI tubesheet. Provision is also made for a backup seal should sodium leakage be experienced at this location. The bottom head flange seal includes a metal O-ring and welded seal. Since removal of the bottom head would be required only if an adequate LLTV sodium drain is not obtained, the lower seal is welded in place.

The LLTI consists of a thick upper tubesheet with tubes attached by full penetration internal bore welds similar to the welds planned for the CRBRP steam generator units. Additional tubes consisting of removable instrumentation tubes, removable dummy tubes and rupture tubes complete the tube array which simulates the full scale CRBRP tube bundle. The instrument tubes include pressure transducers, strain gage tubes and thermocouple tubes.

LLTI secondary tubes are capped at the bottom. However, a simulated tubesheet is located at the bottom of the LLTV to react to sodium pressure waves similarly to a steam generator lower tubesheet. The LLTI tubes are enclosed in a shroud prototypical of the CRBRP steam generator shroud except for length and axial bolting flanges are provided to allow removal of the shroud in two clam shell halves for inspection and maintenance of the tube bundle. The LLTI contains thick spacer plates attached to the shroud similar to the CRBRP units. The LLTI shroud includes prototypic windows located with the same relation to the sodium inlet and outlet nozzles as the CRBRP units.

The LLTV sodium inlet nozzle is located such that the LLTI regions representing the CRBRP hockey stick and the vertical section are both proportionately shortened. The alternate LLTV sodium inlet nozzle is provided so that by modifying the LLTI shroud, the full length of the CRBRP hockey stick region could be represented at the expense of substantially shortening the part of the LLTI which represents the vertical section. This modification is not planned as part of the Series II testing.

2. Sodium System

Figure III-3 shows a pictorial representation of the sodium and relief system major components and piping. The main sodium piping is fabricated from 304 stainless steel and is designed for normal operation between 600° F and 900° F. The upper sodium line is 10 in. Schedule 80 pipe and has a total length of approximately 40 ft. The upper header is 18 in. Schedule 100 pipe and is approximately 25 ft. in length. Nozzles to the rupture disc attachment flanges are 18 in. diameter. A blank flange was installed at the upper disc location (RD-2) for Test A-1a and A-1b. The system includes provisions for sodium filling from a 10,000 gal. drain tank, and for rapid sodium drain to the Reaction Products Tank (RPT).

Also shown on Figure III-3 are the locations of sodium system pressure and temperature instrumentation. The instrumentation consists of thermocouples for measurement of fluid temperature, fast-response pressure transducers, a low-level pressure transducer to provide an accurate measure of initial sodium pressure, strain gages, and three drag-disc flowmeters (located in the relief lines and designated as sensors F506, F511, and F510 on Figure III-3) to provide information on sodium ejection velocities and bubble growth at the rupture site. Spark plug type flow meters (sensors F508A to F508H) provide information on the location of the fluid slug in the relief line. Figure III-4 shows locations of pressure transducers installed to measure radial and axial pressure distributions within the Large Leak Test Vessel (LLTV) and Large Leak Test Internals (LLTI).

3. Water Injection System

The water/injection system is filled with 2000 psig nitrogen for tests A-1a and A-1b. This system (Figure III-1) consists of water/nitrogen supply

tanks (T1 and T2) and piping to and from the test article, the Large Leak Injection Device (LLID) which is used to induce tube rupture, and a downstream flow control valve and condenser tank which can be used to initiate and control pretest water flowrate. The main water supply tanks, the interconnecting piping, and the LLID are electrically heated to condition water temperatures and pressures to required test levels. Piping and components are fabricated of 2-1/4 Cr-1Mo material and are designed for operating temperatures between 500° F and 925° F.

The system contains two 25 ft³ supply tanks: Tank T-1 is connected to the normal water inlet and the bottom of the LLTV and Tank T-2 piping is connected to the LLID at the upper section of the primary rupture tube. The water injection system contains pressure and temperature instrumentation similar to that described for the sodium system and flowmeters of several types and sizes.

The LLID (Figure III-5) is a piston-cylinder device which is used to apply an axial load that causes separation of the notched rupture tube to which it is attached. The cylindrical body of the mechanism is rigidly attached to the shell of the LLTV via a series of mounting flanges; the piston rod extension is welded directly to the rupture tube. A bellows seal between the fixed mechanism and the piston rod maintains the integrity of the sodium boundary during the piston stroke. The piston rod is tubular and serves as an extension of the rupture tube. The LLID is pressurized with nitrogen gas to initiate tube rupture. Gas pressures between 1600 and 1800 psig (which yield forces of 7000 to 8000 lb) are utilized. A crushable structure is included at the top of the cylinder to absorb the kinetic energy of the piston rod and attached tube segment after rupture occurs. Pressure and displacement information from the LLID are monitored. Typical opening times to simulate an equivalent double-ended guillotine break are 0.001 sec.

3. Reaction Relief System

The reaction relief system (Figure III-2) starts at the two 18 in. reverse buckling rupture discs (RD-1), which protects the sodium system, and consists of the downstream piping, a large reaction products tank (RPT) to which the sodium and reaction products are relieved after a sodium-water reaction (SWR)

event, and a stack, with igniter, for burning the hydrogen evolved during the SWR. A single rupture disc was employed for RD-1 in Test A-1a. For Test A-1b, RD1 consisted of two rupture discs. A blind flange replaced the upper rupture disc (RD-2) during Series II Tests A-1a and A-1b. Thus, the only relief path during this test will be through the lower rupture disc (RD-1) (Figure III-1). The relief system line is approximately 53 ft. in length and is 16 inches in diameter. The relief system in the LLTR is instrumented with spark plug detectors in the piping downstream of the rupture discs to monitor sodium velocities. Piping wall temperatures are monitored, as are inlet and outlet pressures. Contact-type sensors are also provided downstream of each rupture disc to indicate the timing of disc actuation.

B. TEST CONDITIONS

Tests A-1a and A-1b were performed in accordance with GE Test Request (Reference 1) under very similar test conditions. The major differences were that A-1a used a single rupture disc at location RD-1 and A-1b used a double disc, and there were minor differences in rupture-tube leak location. Descriptions of the tests, test data, and post-test examinations have been reported in references 2 thru 5. Test conditions were as follows:

- o DEG rupture of a single tube with the break site located 127.75 in. above the lower end of the LLTI shroud for Test A-1a and 122.25 in. for Test A-1b. The tests were non-reactive (nitrogen) with no flow prior to rupture. The LLTI/LLTV was in "evaporator startup power mode," (i.e., 580° F and 125 psig) the sodium system was soft (i.e., surge tank pressurized with gas).
- o Injection medium: Nitrogen (580F).
- o Rupture Tube Supply Pressure: 2000 \pm 50 psig.
- o Water/Steam Secondary System: 1000 \pm 50 psig (N₂).
- o Water/Steam Tubes and Lines: 580 \pm 10F.
- o Sodium Pressure (P-531): 125 $\begin{matrix} +5 \\ -0 \end{matrix}$ psig.
- o LLTV with a linear temperature gradient from 570 \pm 10F at the lower tubesheet to 590 \pm 10F at the upper tubesheet.

- o The RD-1 rupture disc assembly was preheated with a temperature gradient from 565F at the upstream end to 375F at the downstream end.

C. INTER-TEST EXAMINATIONS

1. General

Following both Series II Test A-1a and A-1b, non-destructive examinations were performed as required by the LLTR Series II Test Request (Reference 1) to identify and evaluate any structural damage or other test consequences resulting from the previous test. Since these tests were non-reactive gas tests, it was not necessary to examine for sodium water reaction product (SWRP) buildup or steam tube wastage which could result only from sodium-water reaction conditions. Examination of the transient test data confirmed that pressures, temperatures, and strains were well below the test article design values. Therefore, structural damage would not be expected to result from these tests. Absence of such damage was verified following each test by non-destructive examinations, including mass spectrometer leak tests of the LLTI secondary tubes, radioactive isotope scanning tests for tube bowing, visual and borescope examination of the LLTI interior, and radiographic examination of the drain line at the 8" tee.

During checkout prior to Test A-1a, six (6) of the nineteen (19) fast response test article pressure transducers were found to be inoperative. Since Tests A-1a and A-1b were duplicate tests with the exception of the number of rupture disc membranes installed in the RD-1 rupture disc, it was decided to proceed with Test A-1a with the available instrumentation and remove the LLTI from the LLTV and refurbish the instrumentation between Test A-1a and A-1b. An in-place alcohol cleaning operation was performed to remove residual sodium from the test article prior to removal of the LLTI from the LLTV. Visual inspection after LLTI removal indicated that the cleaning operation successfully removed all of the residual sodium. Removal of the LLTI for instrumentation refurbishment following Test A-1b was not necessary. Details of the intertest activities conducted following Test A-1a and A-1b are reported by ETEC in References 3 and 5, respectively.

2. Prototype Rupture Disc Operation

Test A-1a

A single rupture disc was installed in the prototypical CRBR double membrane rupture disc assembly RD-1 for Test A-1a. The disc burst at approximately 325 psig about 45 milliseconds after leak initiation. The open area of the membrane is estimated to be approximately 30%. The Linear Voltage Displacement Transducer (LVDT) installed to detect membrane rupture failed to operate during this test due to bending of the moving contact rod. Further details of rupture disc operation during Test A-1a are given in References 3 and 6. Figure III-6 shows the rupture disc assembly after test.

Test A-1b

This test utilized the prototype double membrane rupture disc arrangement. The upstream disc ruptured 30 milliseconds after leak initiation at a pressure of about 280 psig. The downstream disc ruptured approximately 12-3/4 seconds later at a pressure of 320 psig. The specified tolerance on the disc steady-state rupture pressure is \pm 5% (~15 psi). Post-test measurements showed that the upstream disc opening area was about 50% and the downstream disc opening was about 65% of the total area. Figures III-7 and III-8 show the rupture discs after test. The reason for the reduced burst pressure for the upper rupture disc is not understood at this time. The discs were formed by the manufacturer from the same material and there was no significant difference in thicknesses of the discs.

LVDT's were installed in the RD-1 rupture disc assembly to detect movement of each rupture membrane (Z-502 upstream and Z-505 downstream). Post-test examination showed both LVDT plunger rods were bent by disc rupture. The upstream LVDT did not produce an output signal when the upstream disc ruptured. The downstream LVDT provided a signal to the sequencer to signify RD-1 operation. However, the tape on which this signal was recorded did not show any recorded signal.

It was recognized when this device was selected for rupture disc application that it would be destroyed by each test. However, since the test experience indicates that it does not reliably provide an output signal prior to its destruction, a different type of device, i.e., a contact probe, should be considered for signaling rupture disc operation.

3. Helium Leak Check of LLTI Secondary Tubes

Following test article cooldown after each test, the shell side of the LLTV/LLTI was flooded with helium and helium leak detection (sniffing method) was applied to the LLTV steam head. Since no leak indication was obtained, it was not necessary to proceed with vacuum probe leak detection of individual tubes.

4. Isotope Scanning Test (IST)

Tube bowing had been detected in one of the Series I tests by radiography through the MSG 1" thick shell. Since the LLTV Series II shell is 4-1/2 inches thick, radiography is not suitable for detecting tube bowing in Series II. Therefore, a special isotope scanning test was developed to non-destructively examine the LLTI tubes for bowing. This technique will also detect spacer deformation. The technique consists of inserting a cobalt 60 or 57 gamma source in a straight tube installed in place of the injection system rupture tube. A gamma detector is inserted in tubes surrounding the source tube to measure the gamma attenuation. A source/detector drive system moves the source and detector simultaneously up and down their respective tubes at a rate of 0.1 in/sec. The measurements are based on the inverse square law, where the intensity of a point source varies inversely with the square of the distance from the source.

This very sensitive technique will measure tube spacing to better than 0.1 inches. Figure III-9 shows a typical IST tube scan. The peaks indicate the location of the tube spacers. Inspection of a minimum of four tubes surrounding the rupture tube was specified. Since the LLTV upper head was removed after Test A-1a, a total of ten (10) tubes were inspected. Four (4) tubes were inspected by IST after Test A-1b.

No evidence of tube bowing or spacer deformation was found by this technique. Borescopic examination of the interior of the LLTI also indicated an absence of tube bowing.

5. Visual and Radiographic Examinations for Flow Restrictions

Visual examination of the relief line following removal of the RD-1 rupture discs and radiographic examination of the 8" tee in the drain line

indicated only a small amount of residual sodium with no significant reduction in flow areas.

6. Dye Penetrant Examination of Relief Line Weld Areas

Dye penetrant examination of selected weld areas in the relief line near the rupture disc assembly did not indicate any cracking.

7. Base Line Ultrasonic Examination of Relief Line

Ultrasonic examination (UT) of heat affected zones of dissimilar metal welds in the LLTR relief line will be performed after each sodium water reaction test to detect evidence of stress corrosion cracking. A base line examination of these weld areas was performed as part of the A-1b intertest examination to provide a basis for comparison with later UT results. Results were as follows:

No indications which exceeded 40% of a 2% circumferential and longitudinal reference standard notches were found at the carbon steel to carbon steel weld (#24) upstream of the RPT nozzle or the carbon to stainless weld (#8) upstream of the RD-1 rupture disc assembly.

Several indications greater than 40% of the 2% circumferential reference standard notch were found at the carbon steel to stainless steel weld (#46A) upstream of the RPT. No longitudinal indications which exceeded 40% of the 2% longitudinal reference standard were found at this weld. The weld is a new weld made during the Series II modification. The indications do not represent significant defects. However, their identification is important to prevent erroneous conclusions from future examinations that these defects are the result of stress corrosion cracking.

8. LLTI/LLTV Cleaning and Instrumentation Refurbishment

Since less than the minimum required LLTI pressure transducers were functioning, it was necessary to remove the LLTI from the LLTV and refurbish the internal instrumentation prior to performing Test A-1b. The test article was cleaned with organic solvents to remove the residual sodium prior to removal of the LLTI. The cleaning procedure included circulating Dowanol containing 2% water through the test article at a flow rate of about 100 gpm. Approximately 3200 gallons of Dowanol were required to completely fill the system. After the Dowanol was circulated for three days with only minor changes in the sodium concentration, the system was

heated to about 135°F and nitrogen sparge gas added. This did not increase the sodium concentration and the system was cooled and the Dowanol drained after five days. Figure III-10 shows the sodium concentration during Dowanol circulation. Denatured ethanol containing approximately 4.2% water was then circulated through the system. The system was heated to 140°F and sparged with nitrogen. Figure III-11 shows the sodium concentration in the ethanol vs time during the three day ethanol circulation. Calculations based on the measured concentrations during the cleaning indicated that approximately 170 lbs of sodium was reacted by the cleaning operation. Visual inspection following removal of the LLTI confirmed that all the residual sodium had been removed.

Following the cleaning operation, the LLTI was removed from the LLTV and placed in the vertical handling stand where the handling fixture was installed. The LLTI with handling fixture in place was then oriented horizontally in the assembly fixture where the failed instrument tubes were removed and replaced with new tubes. Six pressure transducer tubes (P-01-1, P-01-2, P-01-5, P-01-6, P-01-8, and P-01-9) and one strain gauge tube containing three strain gauges (SG-01-4, SG-01-5, and SG-01-6) were replaced. Pressure transducer tubes P-01-1, P-01-2, and P-01-5 were spare tubes provided with the spare LLTI instrumentation purchased in FY1979 and contained second generation "Kaman" transducers. Tubes P-01-6, P-01-8, and P-01-9 were tubes which were fabricated with the original LLTI and contained first generation Kaman transducers.

Destructive examination and failure analysis of the transducers removed from the LLTI indicated that all of the failures involved lead wires. Four units had open lead wires and two units had shorted leads. Failure of earlier units investigated at ETEC and HEDL attributed the cause of similar lead wire failures to impurities in the lead wire. Since the transducer vendor had new lead wire available when the second generation transducers were procured, it was assumed that the problem had been corrected.

During Test A-1a twenty-one Ailtech Model SG-425 strain gauges, which were exposed to sodium, failed. Post-test examination disclosed that sodium was penetrating the gauges at the junction of the lead wire

to the gauge. It was concluded that this model strain gauge was not suitable for immersion in sodium. Since the replacement gauges were the same type, the strain gauges were not replaced with the exception of the one strain gauge tube. The three gauges in this strain gauge tube did not give valid output for Test A-1b. No other additional strain gauges failed during Test A-1b.

9. Summary of Failed Transducers as reported by ETEC (in References 2 and 4)

Test A-1a

All 220 parameter data obtained on the data tapes were valid except for the following 44 where problems such as open or shorted circuits or faulty transducers existed.

<u>DAS*</u>	<u>ANALOG*</u>
F-501	SG-A-1
TE-SG-507	SG-A-2
TE-22-1	SG-A-3
TE-546	SG-A-4
SG-712	SG-C-3
SG-721	SG-C-5
SG-C-2	SG-C-6
SG-C-4	SG-D-2
SG-C-7	SG-D-3
PT-01-6	SG-01-4
D-503	SG-01-5
TE-21-6	SG-01-6
SG-706	SG-01-8
TE-544	SG-507B
	SG-509B
	P-01-1
	P-01-2
	P-01-4
	P-01-5
	P-01-6
	P-01-7
	P-01-9
	P-527
	Z-502
	W-511
	D-503
	P-512
	P-516
	P-517
	P-614

- * Note: F - Flow sensor
- TE - Thermocouple
- SG - Strain gage
- PT, P - Pressure transmitter
- D - Densitometer
- Z - Displacement transducer
- W - Load cell

Test A-1b

All parameter data on the data tapes were valid except for those listed below. These measurements either exhibited questionable response or malfunctioned during the test. (Details on the specific transducer may be found in Reference 4)

P-01-3	P-504
PRD-1-B	P-507
SG-C-7	P-509
SG-01-3	P-510
SG-01-4	P-512
SG-01-5	P-516
SG-01-6	P-522
SG-C-7	P-526
SG-C-8	Z-503
SG-D-3	
TE-544	

Data from Analog Tape Recorder #7 which was lost consisted of the following measurements: A-600, FSP-508H, P-506, P-527, P-618, P-01-7, SG-01-8, TE-543, SG-C-5, Z-505, P-521, SG-509B, and P-A-12.

Note that only 3 test article pressure transducers (P-01-3, P-C18 and P-A-12) failed to provide data during Test A-1b as contrasted with 8 test article pressure transducers in Test A-1a. Similar improvement with other transducer performance was experienced between A-1a and A-1b.

LARGE LEAK TEST RIG (LLTR) SERIES 2

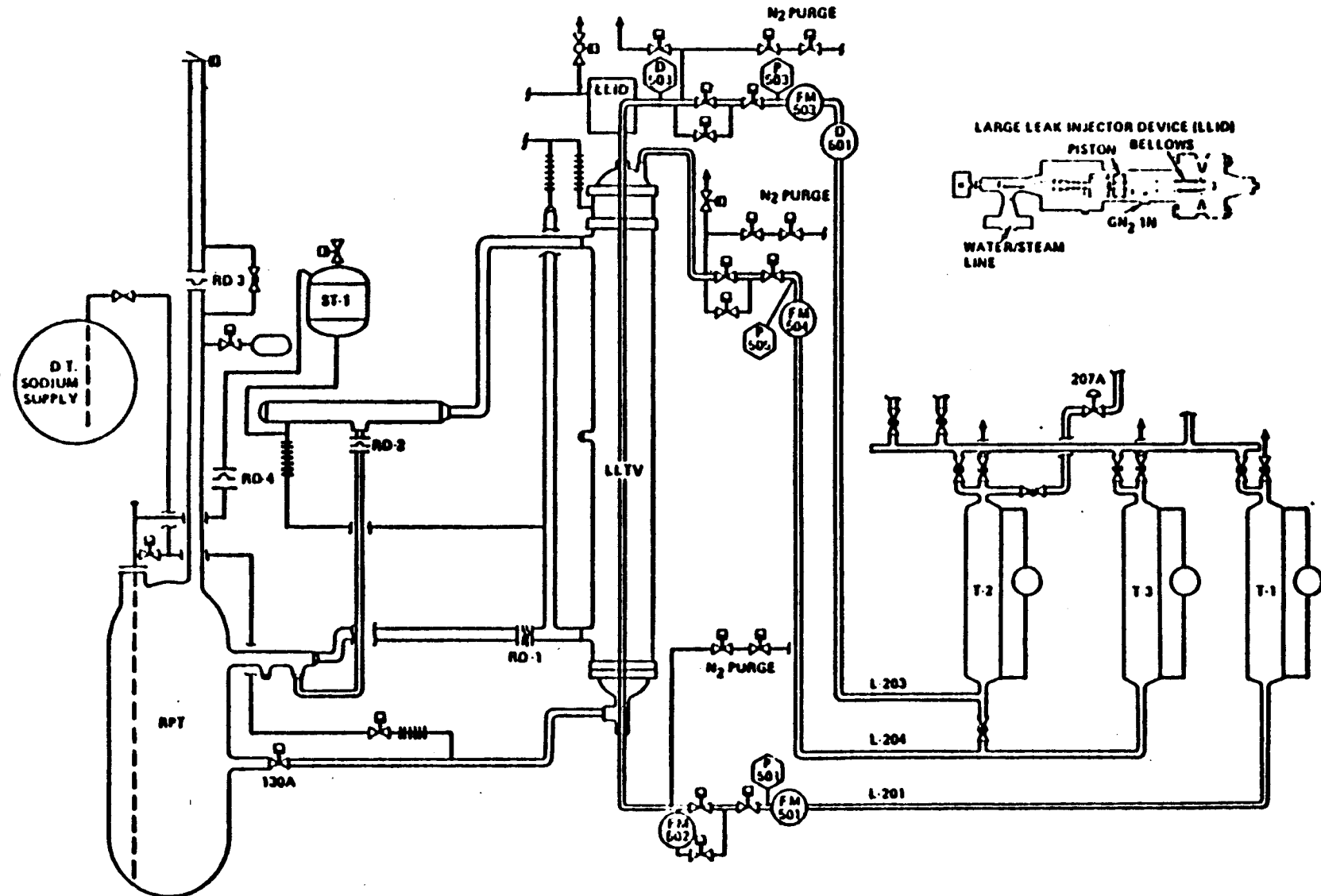
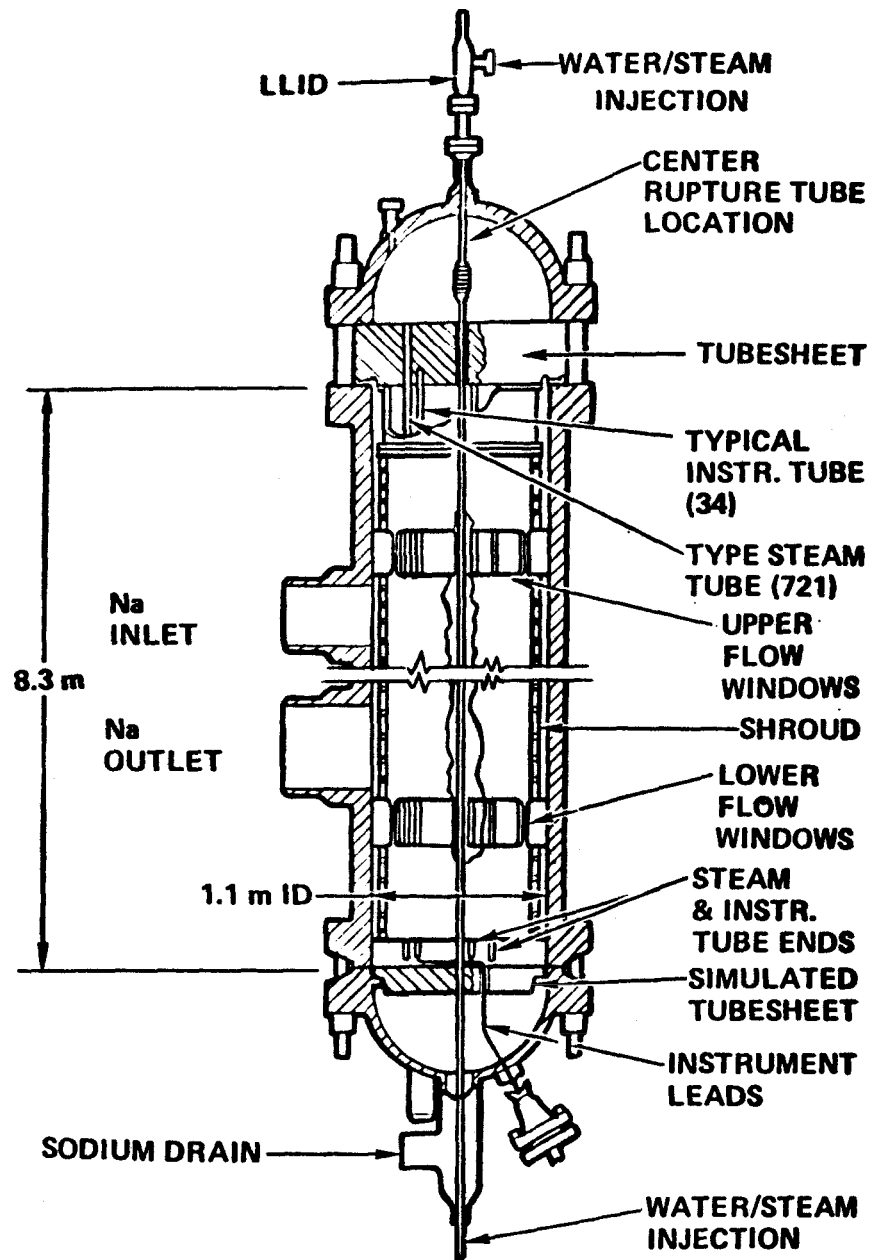
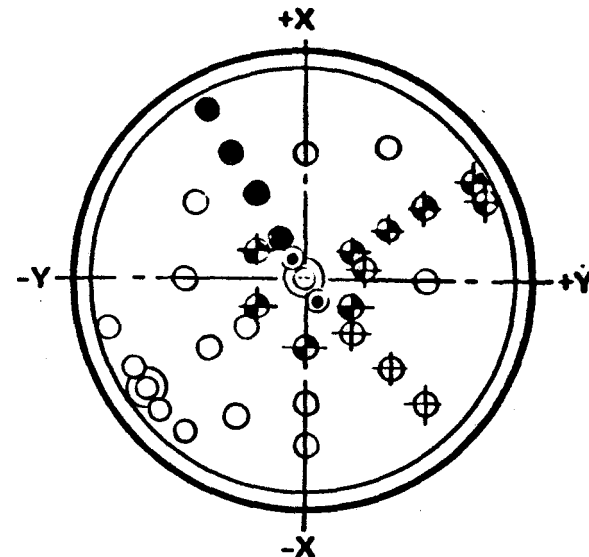


FIGURE III-1

Figure III-2



LLTI/LLTV ASSEMBLY



- PRES. TRANSDUCER
- RADIAL Na IMMersed TC
- AXIAL Na IMMersed TC
- ⊕ WALL MOUNTED TC
- ⊕ STRAIN GAGE
- ALTERNATE LOCATION

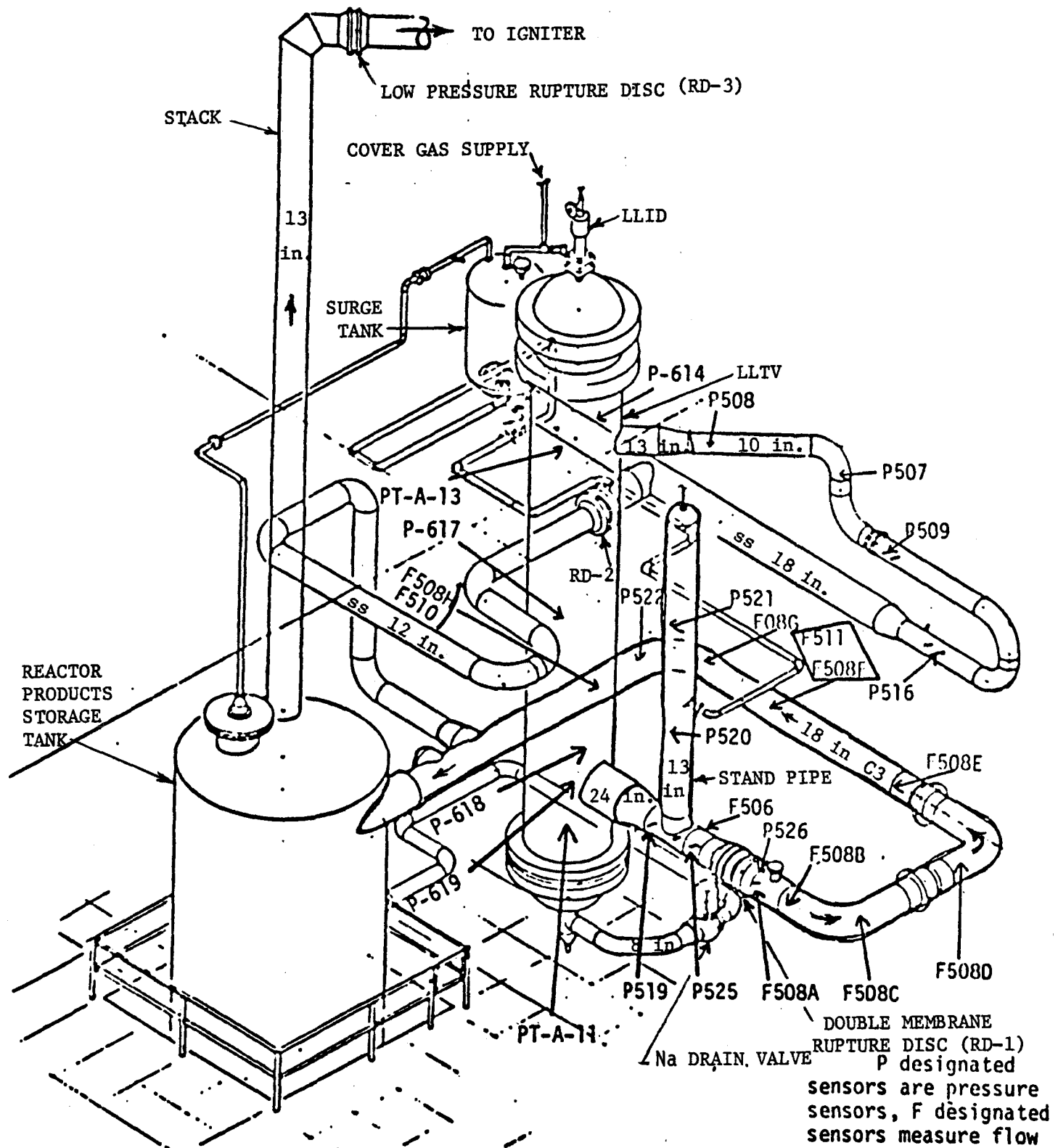
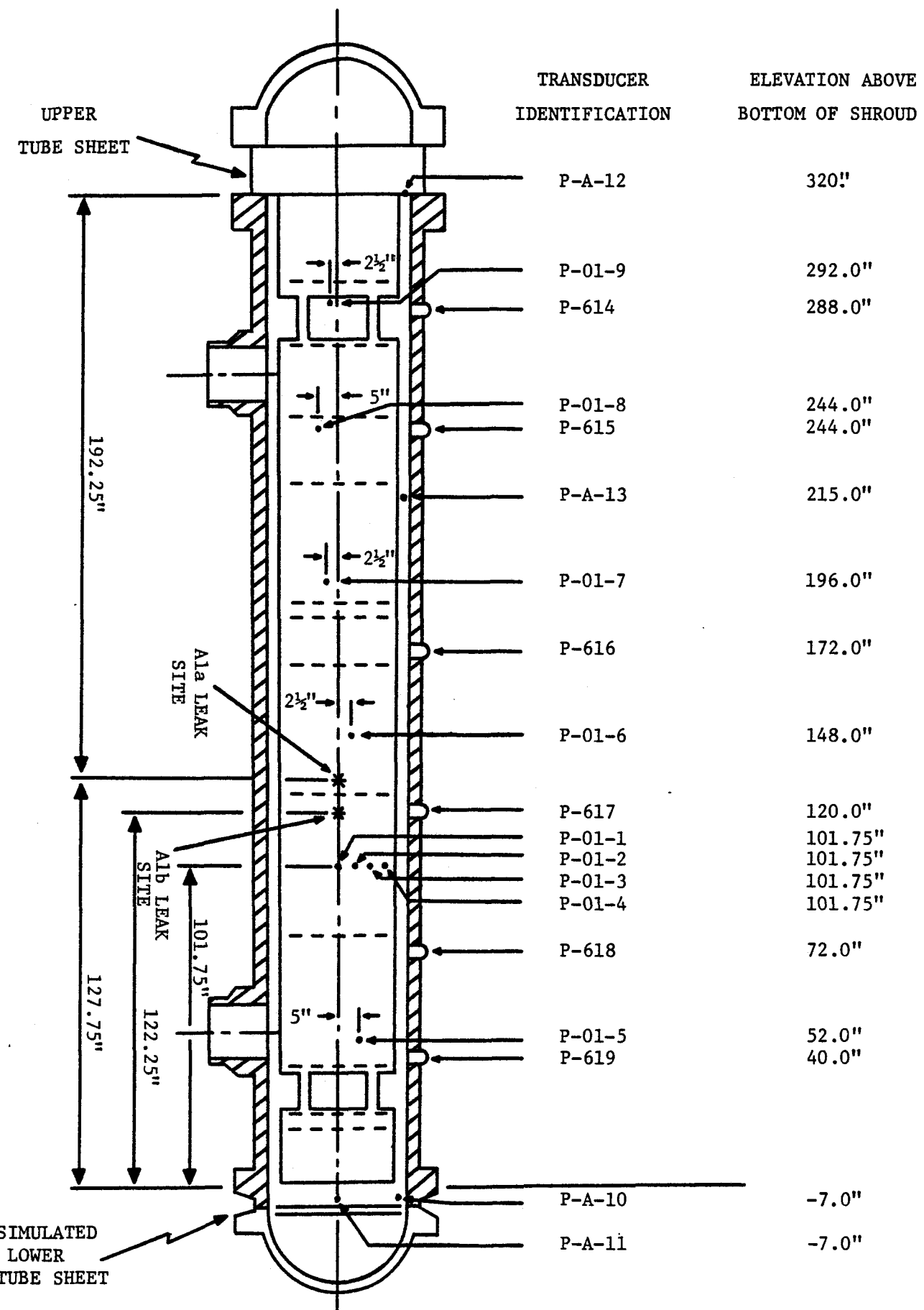


FIGURE III-3
LLTR Sodium and Relief Systems
Flow and Pressure Sensor Locations



LLTV/LLTI PRESSURE TRANSDUCER LOCATIONS

FIGURE III-4

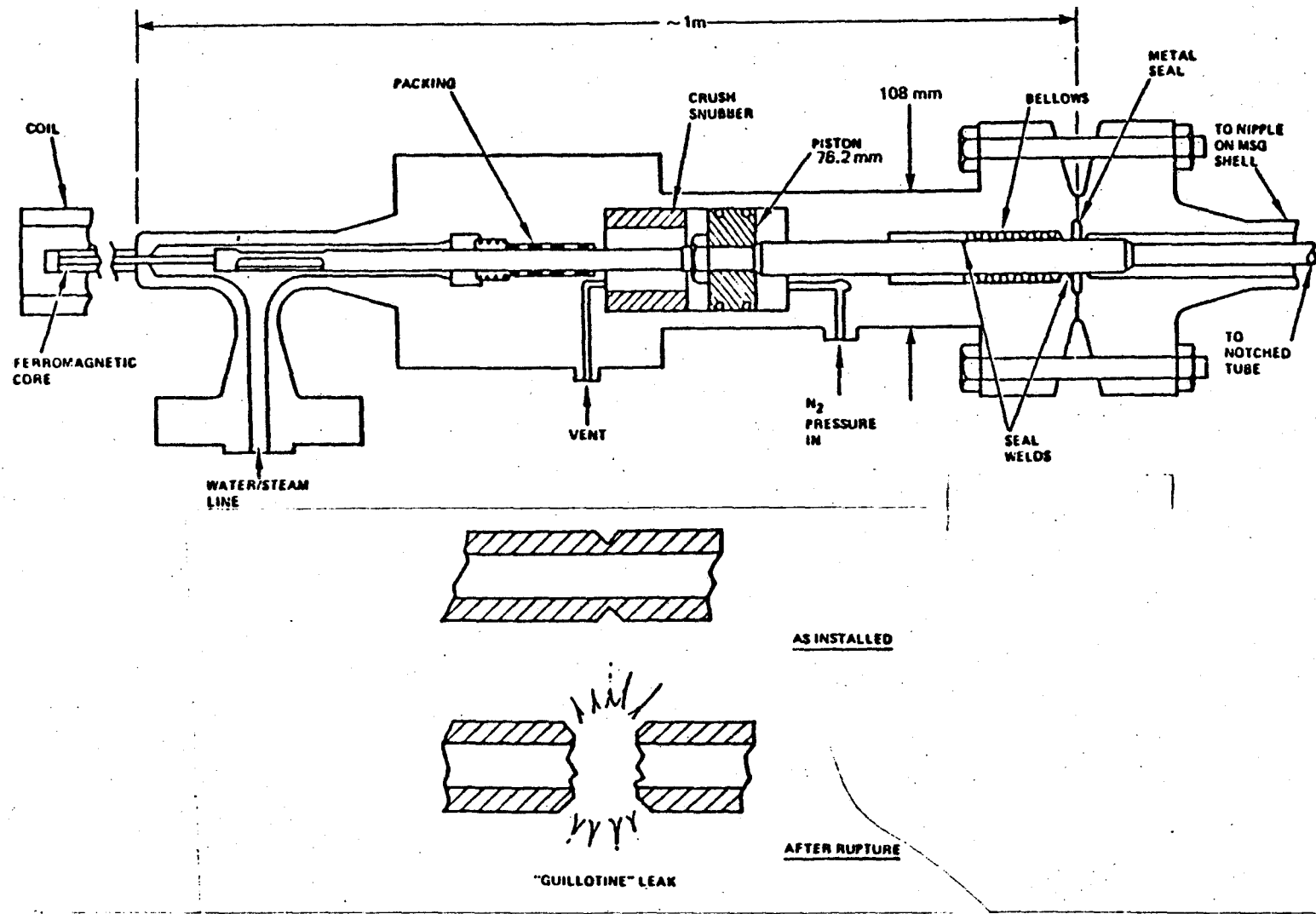
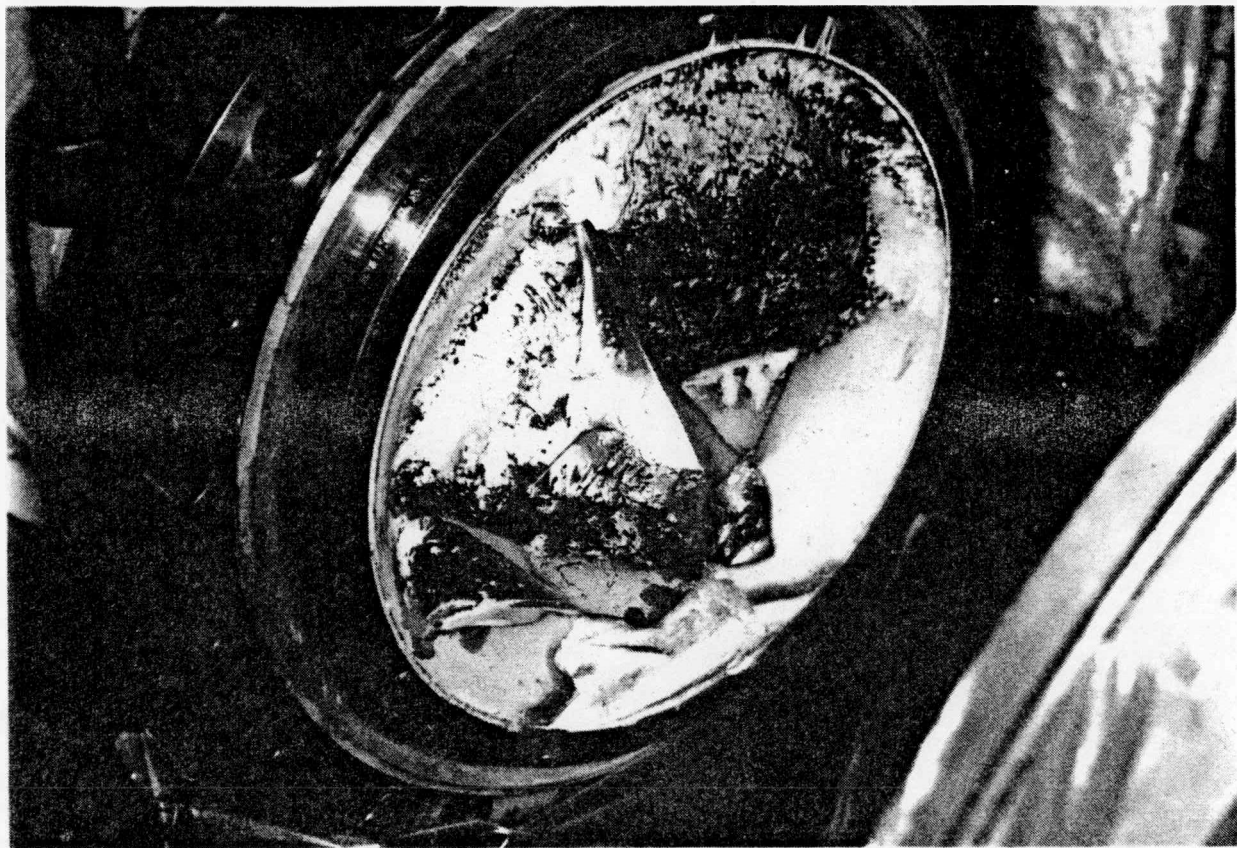
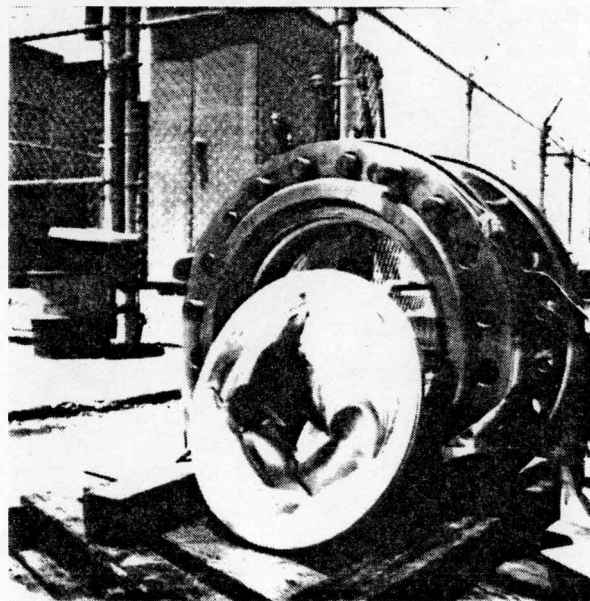


FIGURE III - 5

Large Leak Injection Device (LLID)



(a) BEFORE CLEANING



(b) AFTER MEMBRANE REMOVAL AND CLEANING

PHOTOGRAPH OF SINGLE RUPTURE DISC (DOWNSTREAM SIDE)
FOLLOWING REMOVAL AFTER TEST A1a.

FIGURE III - 6

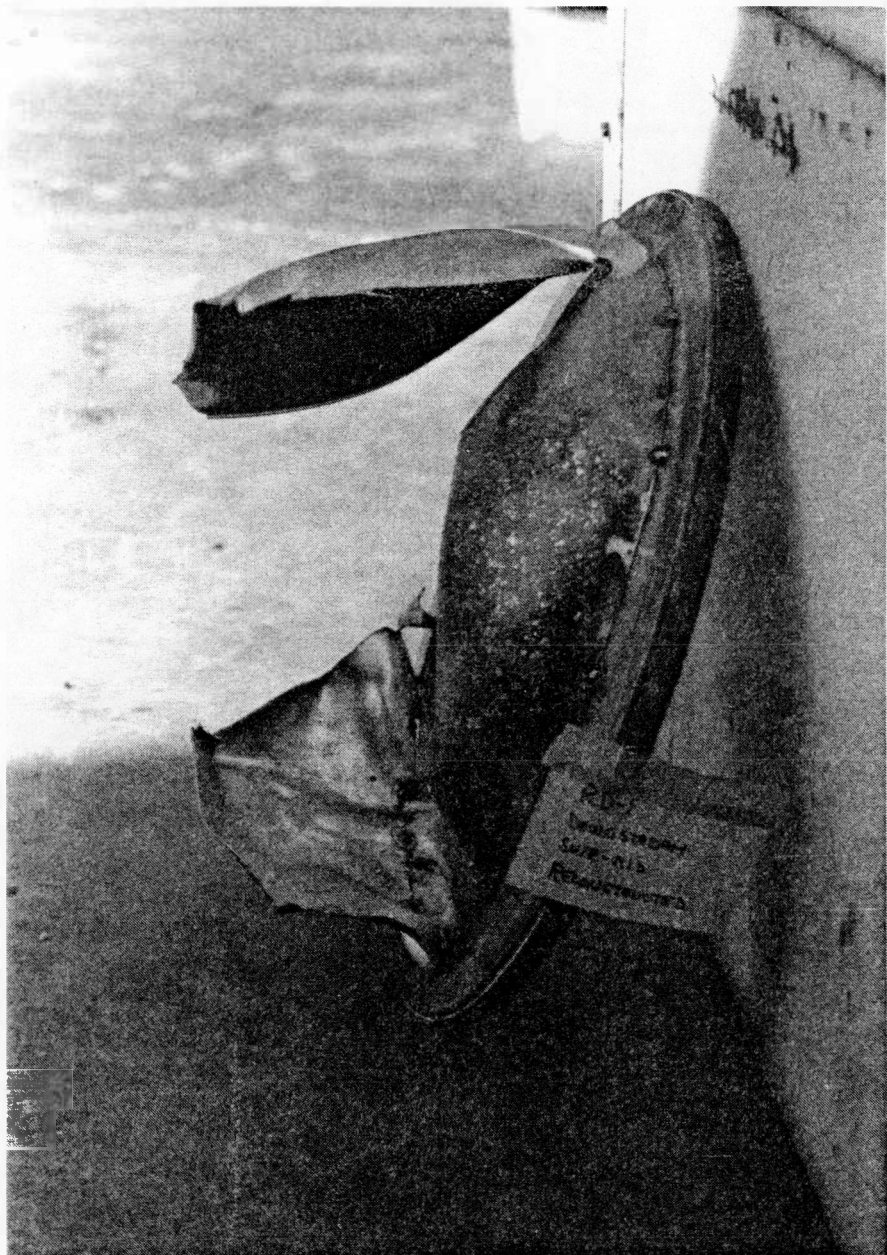
79-496-14



80-194-02

TEST A1b RD-1 UPSTREAM RUPTURE DISC MEMBRANE
AFTER REMOVAL AND CLEANING

FIGURE III - 7



80-194-01

TEST A1b RD-1 DOWNSTREAM RUPTURE DISC
MEMBRANE AFTER REMOVAL AND CLEANING

FIGURE III - 8

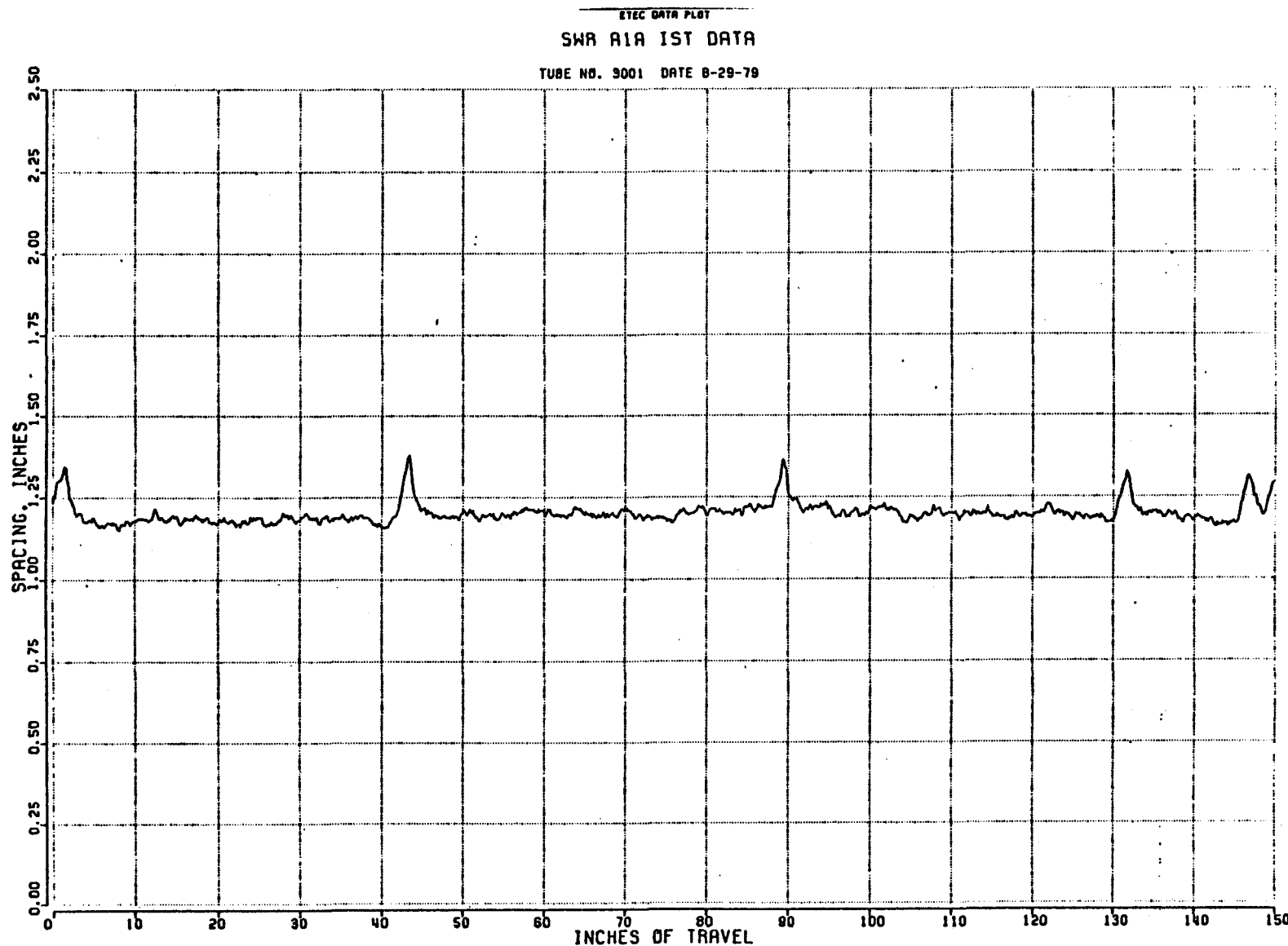


Figure - TYPICAL IST SCAN TUBE 3001

FIGURE III - 9

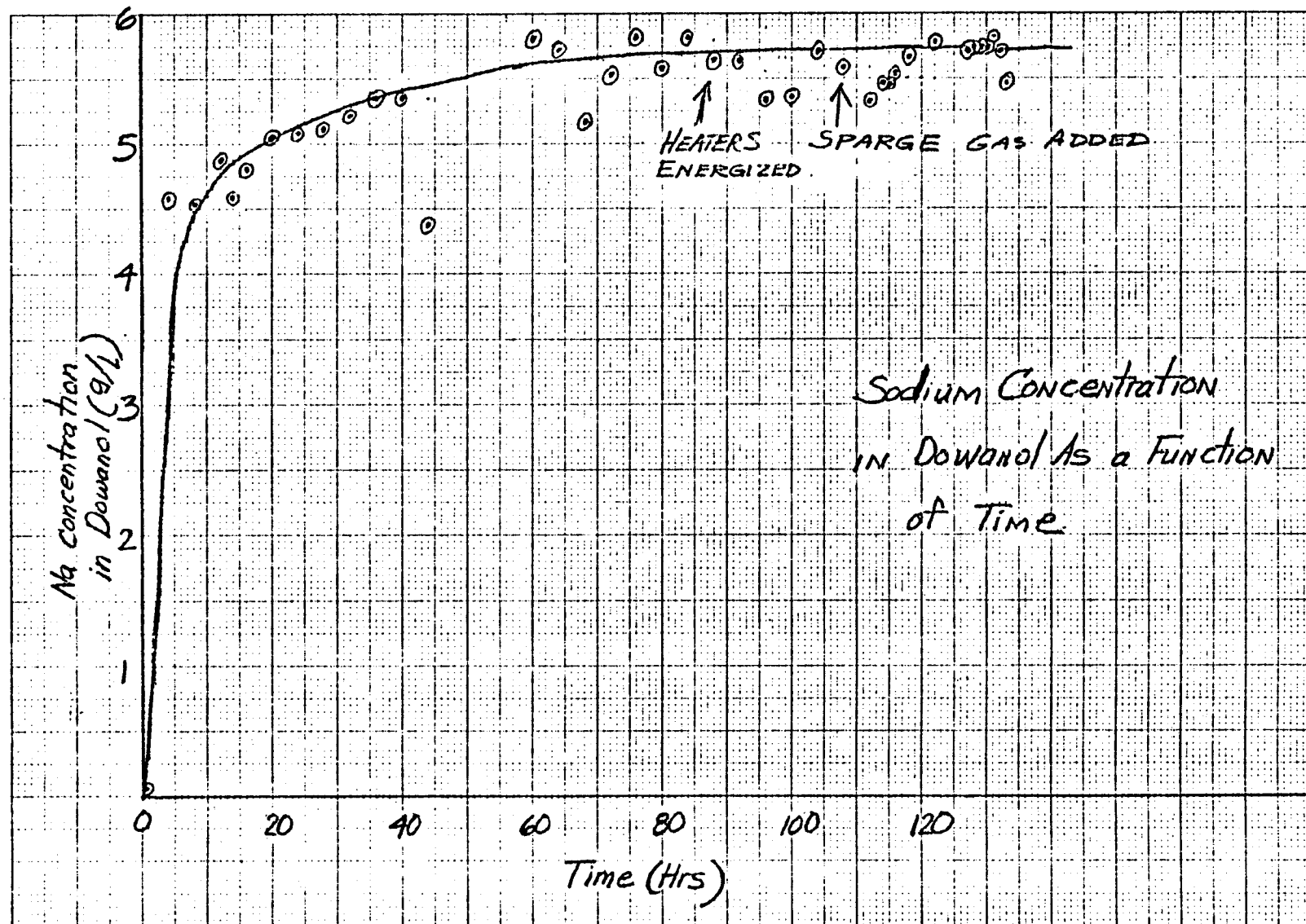


FIGURE III-10 - SODIUM CONCENTRATION DURING LLTV/LLTI DOWANOL CLEANING

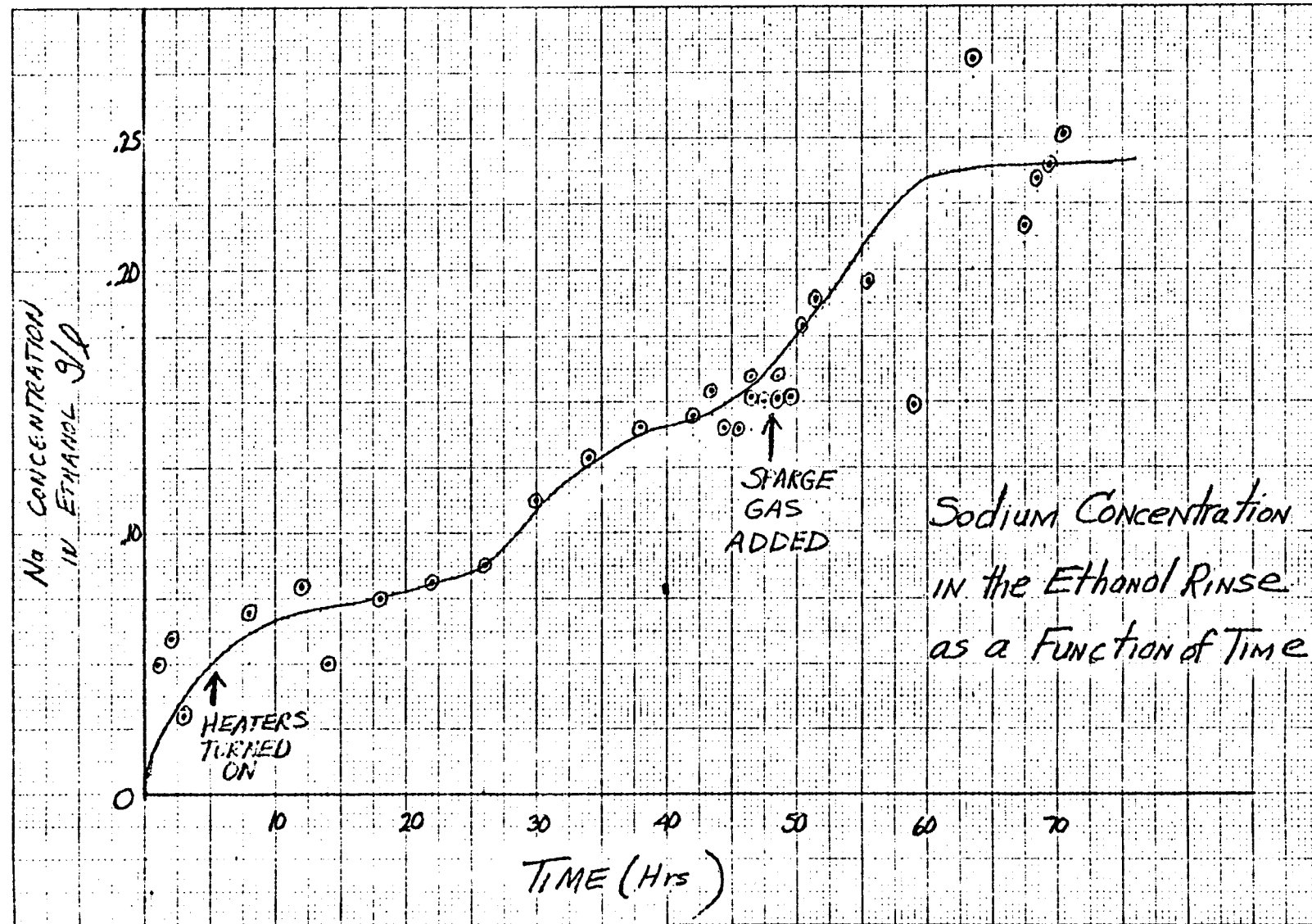


FIGURE III - 11 - SODIUM CONCENTRATION IN ETHANOL RINSE DURING LLTV/LLTI CLEANING

IV. ANALYTICAL METHODS & MODELS

A. OVERALL APPROACH

The post-test analyses of the Series II, Tests A-1a and A-1b were performed in accordance with the standard design methodology developed as a result of Series I test analyses (reference 8). Pre-test predictions made in 1978 were accomplished before the dynamic double rupture disc model was incorporated in the TRANSWRAP II code and before the standard methodology was developed from the Series I Test Program. Post-test analyses of these 2 Series II tests, therefore, expand the data base available to evaluate and extend the standard methodology.

B. RUPTURE TUBE MODELING WITH NONSAP AND RELAP COMPUTER CODES

The NONSAP computer code (ref 9) has been used to determine the rate of separation of the ends of the stressed rupture tube following failure. The results are essentially the same as found for Series I, SWR-2 NONSAP calculations: each end moves at a constant absolute velocity (i.e., the end separation is linear with respect to time) of about 150 inches per second during the tube opening period of interest for calculation of nitrogen flow rates. The time to "fully open" (i.e. to 1/2 the tube diameter) was calculated to be 0.68 msec. from the start of motion.

Fig IV-1, was used to determine the flow area for the leak used in the RELAP code input. This figure is the same as that of Appendix A, Volume 1, of the Series I report (reference 8), except the abscissa has been relabeled to permit its use for any tube separation history. The product of the "Area Fraction" times the "Discharge Factor" is then used as the variable "leak site junction" area ratio for the RELAP code inputs.

The "containment option" of RELAP 4/MOD 5 (ref 10) was used to calculate rupture tube flow rates following tube failure. The two RELAP models established for this analyses are shown in Fig IV-2 and IV-3. Each represents the circuit from either Tank T1 or Tank T2 to the rupture location (leak site). The figures show the number of volumes assigned to various parts of the circuit and the location of valves and the other changes in flow area. A listing of the RELAP inputs for these analyses is presented in Appendix D. The flow rates from each tube are shown on Figures IV-4 and IV-5.

The RELAP flows from each tube end are then added together to get the total flow rate since TRANSWRAP requires a single input. This flow rate was then corrected to determine the TRANSWRAP input because: 1) the RELAP code simulated the nitrogen injection with air, and 2) the TRANSWRAP II code can only accept water as an input. The correction is based on equating the volumetric generation rate of hydrogen in the TRANSWRAP code to the volumetric rate of nitrogen injected in the test. Since the TRANSWRAP code generates 1 molecular weight (mole) of hydrogen for each mole of water injected, and the RELAP code simulated the nitrogen injection with air, the multiplying factor for weight ratio is $\frac{M_{H_2O}}{M_{Air}}$. TRANSWRAP also predicts an adiabatic reaction zone temperature rise from the initial sodium temperature (1040°R) to an average bubble temperature (3120°R) so the ratio $\frac{^{\circ}R_{Na}}{^{\circ}R_{Bubble}}$ is used to correct for temperature. The TRANSWRAP water injection rate is shown on Fig IV-6. This was used for both Test A-1a and A-1b. An outline of the calculational sequence employed for the analyses is shown in Figure IV-7.

C. SODIUM SYSTEM MODELING WITH TRANSWRAP

The TRANSWRAP model used for the post test analysis is shown in Figure IV-8, along with the pressure transducers (P numbers) and the flow meteres (F numbers). A complete listing of the TRANSWRAP input for each test is given in Appendix D. The post test analyses use flow rates calculated from RELAP, and converted to an equivalent water flow rate as described in Section IVB.

The time step used in TRANSWRAP models was 0.0001 seconds for both tests. The length of each pipe and the number of nodes in TRANSWRAP were selected so that the Courant stability criterion, $1.0 < (\frac{\Delta X}{C\Delta t}) < 1.05$ was met for all models. The rupture disc model is based on the SWAAM elastic model, (Reference 7). A single disc model was used for Series II Test A-1a and a double disc model was used for Series II Test A-1b.

The double rupture disc model was obtained from the copy of SWAAM-I, transmitted to GE from Argonne in May 1979. This double rupture disc model was modified in the same manner as the single disc model as reported in Appendix III of Volume II of the Series I report (reference 8).

1. Effect of Sonic Velocity in LLTV on Pressures

The rate of pressure rise calculated by TRANSWRAP is a function of the sonic velocity used for the analysis. Since the LLTV has a thin-walled inner shell (the shroud) concentrically located within the thicker outer shell of the vessel, sonic velocity calculations in the LLTV were made based on both shell geometry and shroud geometries for comparison with test results. The calculated sonic velocity in the LLTV is 6850 ft/sec using the shell inside diameter of 44.38 inches with a shell wall thickness of 4.5 inches, while the sonic velocity is reduced to 5224 ft/sec using the shroud diameter of 36.5 inches and the shroud wall thickness of 1.0 inch. Typical calculated and measured pressure vs. time histories for Test A-1a are shown in Figure IV-9 to IV-11 for 5224 ft/sec and in Figures IV-12 to IV-14 for 6850 ft/sec. In general, a better prediction is made using the lower sonic velocity.

An effort was also made to determine the sonic velocity in the LLTV from test data by measuring the differences in the arrival time of the initial pressure pulse at various pairs of transducers. That time difference divided by the difference in distance from the leaksite to each of the transducer pairs gives the velocity. Table IV-1 shows the calculated velocities between various transducer locations and also gives the distance of each transducer from the leaksite. Because of the central leaksite location in the relatively short LLTV (~20 ft from lower to upper tubesheet), the measured time increments are relatively short. The maximum difference in arrival time was 2.38 msec (P-01-1 to P-01-9) and the minimum was 1.08 msec. The determination of the arrival time is made difficult by the initial relatively high noise and by differences in the shape of the initial wave front as recorded by the transducers, as shown on Figures IV-15 to IV-17. Because of these problems, the time differences determined by this method may be in error by 0.2 to 0.3 msec; the corresponding error in velocity determination would then be 25% to 40% for the shorter distances in the table.

The range of individual measurements of sonic velocity shown in Table IV-1 is from 4877 ft/sec to 8281 ft/sec with the higher velocities corresponding to the shorter distances. The average measured sonic velocity for test A-1a is 6572 ft/sec and the average for Test A-1b is 6410 ft/sec. For comparison the maximum sonic velocity in sodium at 580°F is 7032 ft/sec for an infinite medium. Because of the uncertainty in the measurements, it was decided to base the TRANSWRAP evaluation of the A-1a and A-1b test results on the 5224 ft/sec determined from the LLTV shroud geometry, since this provided a good match to the measured pressure data in conjunction with the water injection rates previously determined.

Since, in the time period prior to rupture disc failure, the calculated pressures depend on both the TRANSWRAP water injection rate (determined from RELAP calculations) and the sonic velocity in the LLTV, it may be possible to improve modeling by revising both these parameters. Stronger pressure pulses from the sodium-water reaction in Test A-2 may permit improved determination of acoustic velocity within the vessel from Test A-2 data. A reevaluation of both the acoustic velocity in the LLTV and the rupture tube flow rate from RELAP will be undertaken as part of the Test A-2 data evaluation.

2. Rupture Disc Modeling/Performance

The rupture discs were modeled in TRANSWRAP using the SWAAM-I, elastic finite element model, modified at GE to allow partial disc opening at disc rupture. In order to match the measured disc response with TRANSWRAP, the disc thickness had to be reduced from its actual value of .060 inch to .046 inch for test A-1a and to .045 inch for test A-1b. This parallels the treatment of the disc thickness for the Series I test where the ratio of TRANSWRAP disc thickness to actual disc thickness ranged from 0.64 to 0.81 and modeling of recent SRI tests where the ratio of TRANSWRAP to actual disc thickness was ~0.6. There appears to be a step discontinuity in disc response in the range of disc thickness needed to match the test data. Figures IV-18 to IV-20 show measured and calculated pressure time histories for test A-1a upstream from the rupture disc (P-525) for 3 disc thicknesses: 0.045, 0.046 and 0.047 inches. The .045 thick disc buckles at 32 milliseconds, whereas the 0.46 and .047 discs buckle at 57 milliseconds. The calculated peak pressures at buckling are 360, 400 and 405 PSIA for the .045, .046 and .047 in discs, respectively. The measured peak pressure at buckling is 390 PSIA at 49 milliseconds for test A-1a, and 305 PSIA at 29 milliseconds for test A-1b.

In order to match the response of the double disc system in the period following first disc failure in test A-1b, the first disc was opened to 15 percent of the maximum area. Post-test examination of this disc measured a 50 percent opening. With a 30 percent open area on the first disc, TRANSWRAP predicts the second disc to buckle and open in less than 200 milliseconds. The measured opening time for the second disc is about 12.7 seconds. This indicates that the first disc is only partially opened by the initial pressure pulse, and is opened to its maximum area only after the second disc opens and sodium begins to discharge into the relief system. Figure IV-21 shows the pressure time history at the rupture disc for a 15% open area for the first second of the test. Long term modeling necessary to predict the failure time of the second disc is not practical on TRANSWRAP. Good agreement between calculated and measured pressures is achieved with the 15% initial open area assumption.

The difference in failure pressure and open area of the first rupture disc in Test A-1a and the disc in Test A-1b is not well understood. It is probably caused by small differences in disc geometry or mechanical installation, as the effect of the second rupture disc on failure characteristics of the first disc in Test A-1b should be negligible. The relatively small initial open area of the first disc used for the A-1b analysis (15%) is consistent with recent findings from SRI rupture disc testing (reference 12) which showed that low energy pressure pulses result in low disc opening areas. This low initial area did not then allow sufficient pulse energy to be transmitted to the second disc to cause failure. The second disc's failure at 12.7 seconds is a consequence of sodium system pressurization by nitrogen when the sodium level reached the top of the expansion tank.

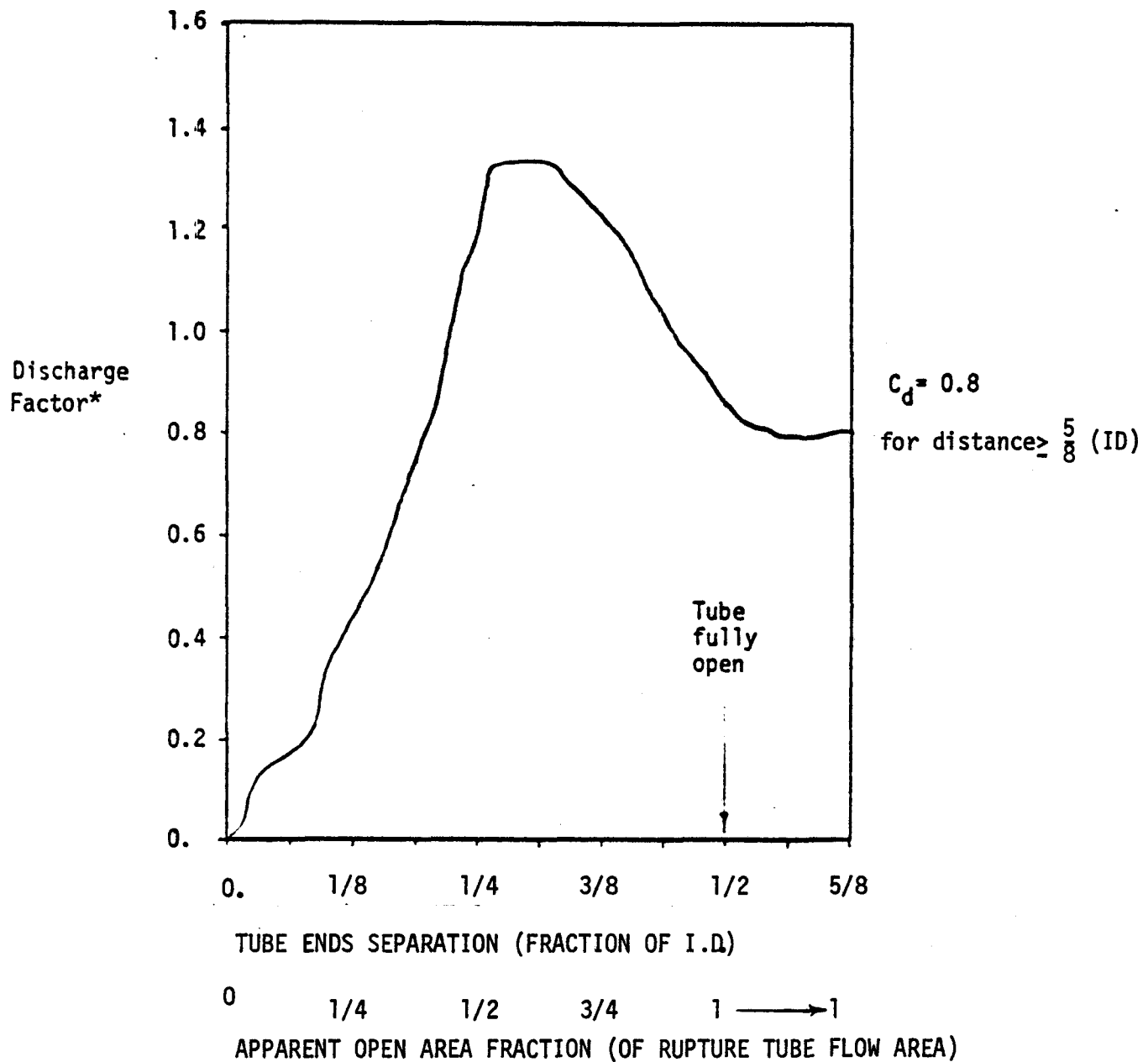
TABLE IV-1
 LLTV CALCULATED SONIC VELOCITIES
 (Distance of Transducer from Leaksite in Parenthesis)

TEST A1A

FROM/TO	P-A-10 (11.219)	P-A-11 (11.192)	P-A-12 (16.153)
P-01-3 (2.350)	5617	6262	6335
P-617 (1.945)	6955	7566	6695

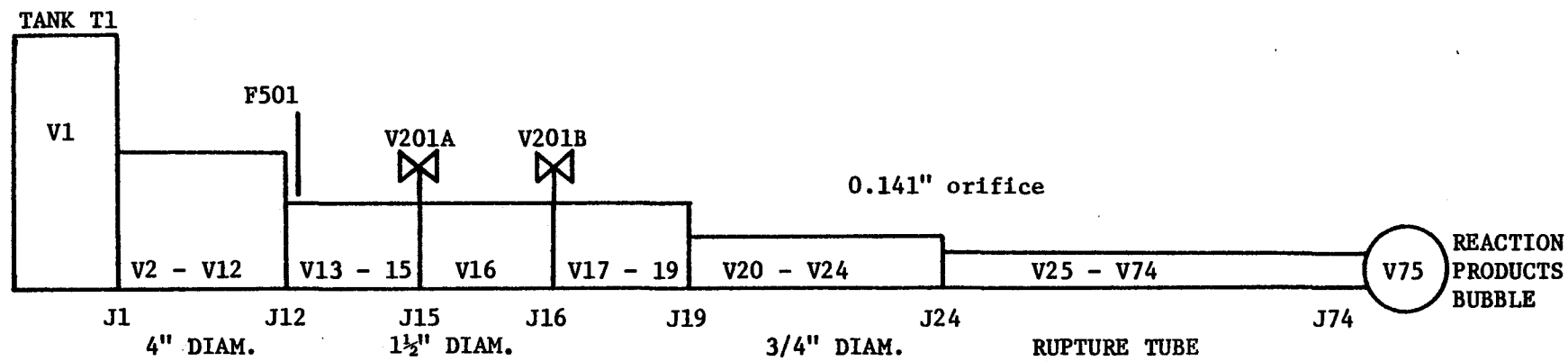
TEST A1B

FROM/TO	P-01-9 (14.152)	P-614 (13.935)	P-A-10 (10.804)	P-615 (10.313)	P-A-11 (10.776)	P-01-8 (10.153)
P-01-1 (1.756)	5213	5592	6463	5203	6494	6463
P-01-2 (1.851)	6150	6323	8058	6509	8281	8058
P-01-6 (2.184)	5495	5315	7388	5340	6846	7388
P-617 (1.859)	5477	5434	7188	4877	7102	7188



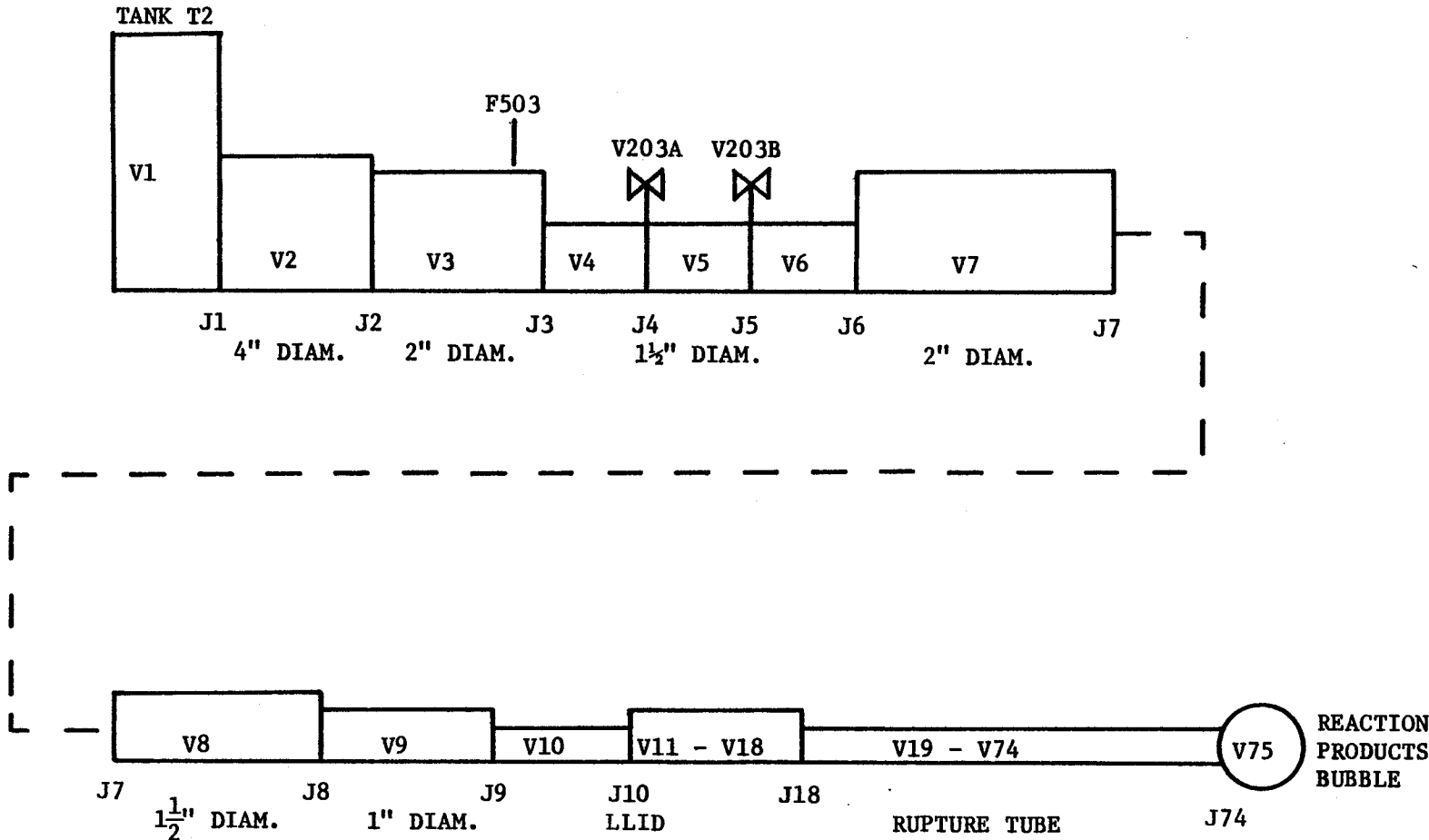
*"Discharge Coefficient" of Reference 8, Vol 1, Appendix I

FIGURE IV-1 Empirically-derived Discharge Factor for SWR-5 Leaksite



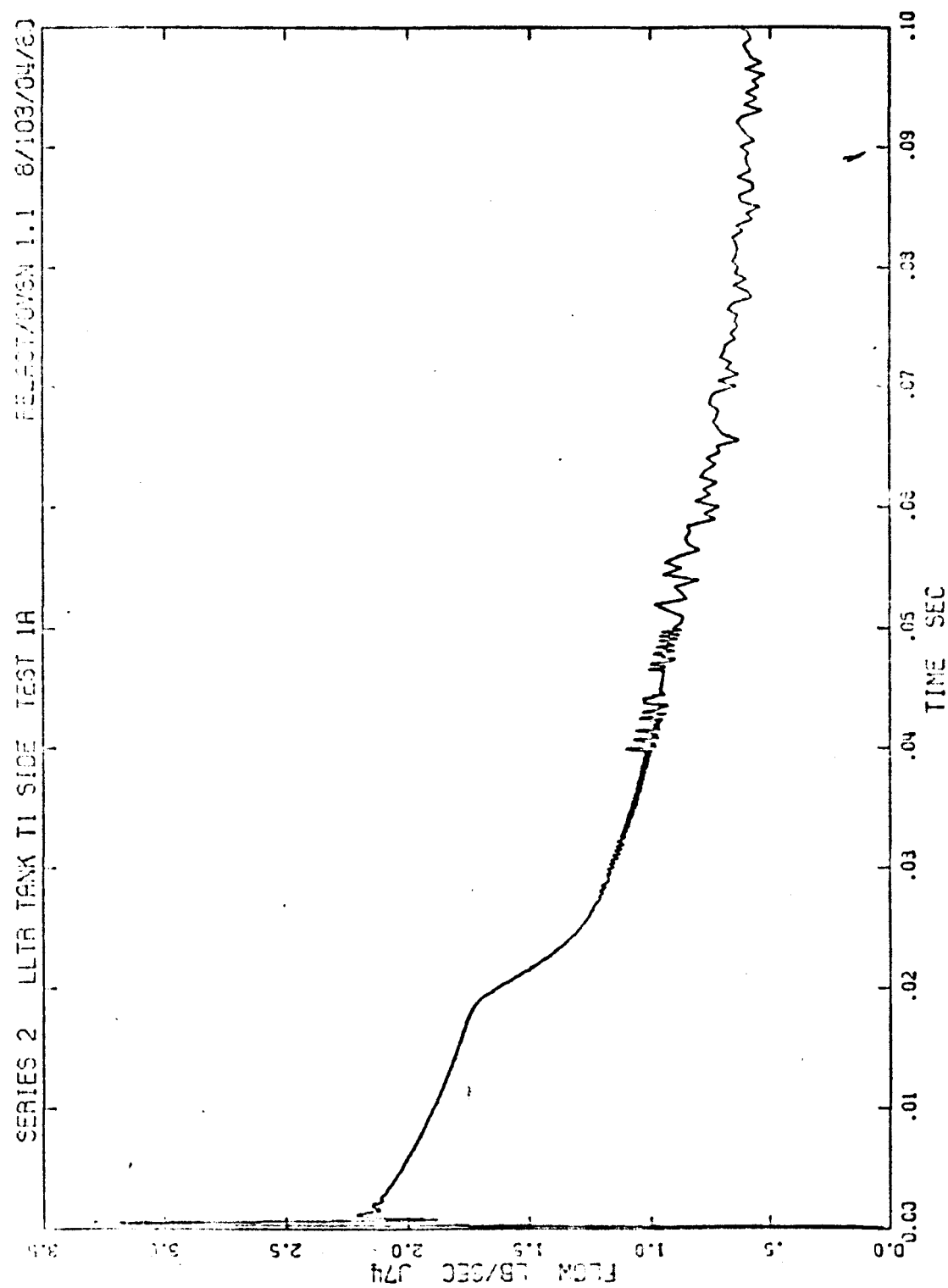
RELAP SCHEMATIC FOR TANK T1 SIDE OF RUPTURE TUBE

FIGURE IV-2



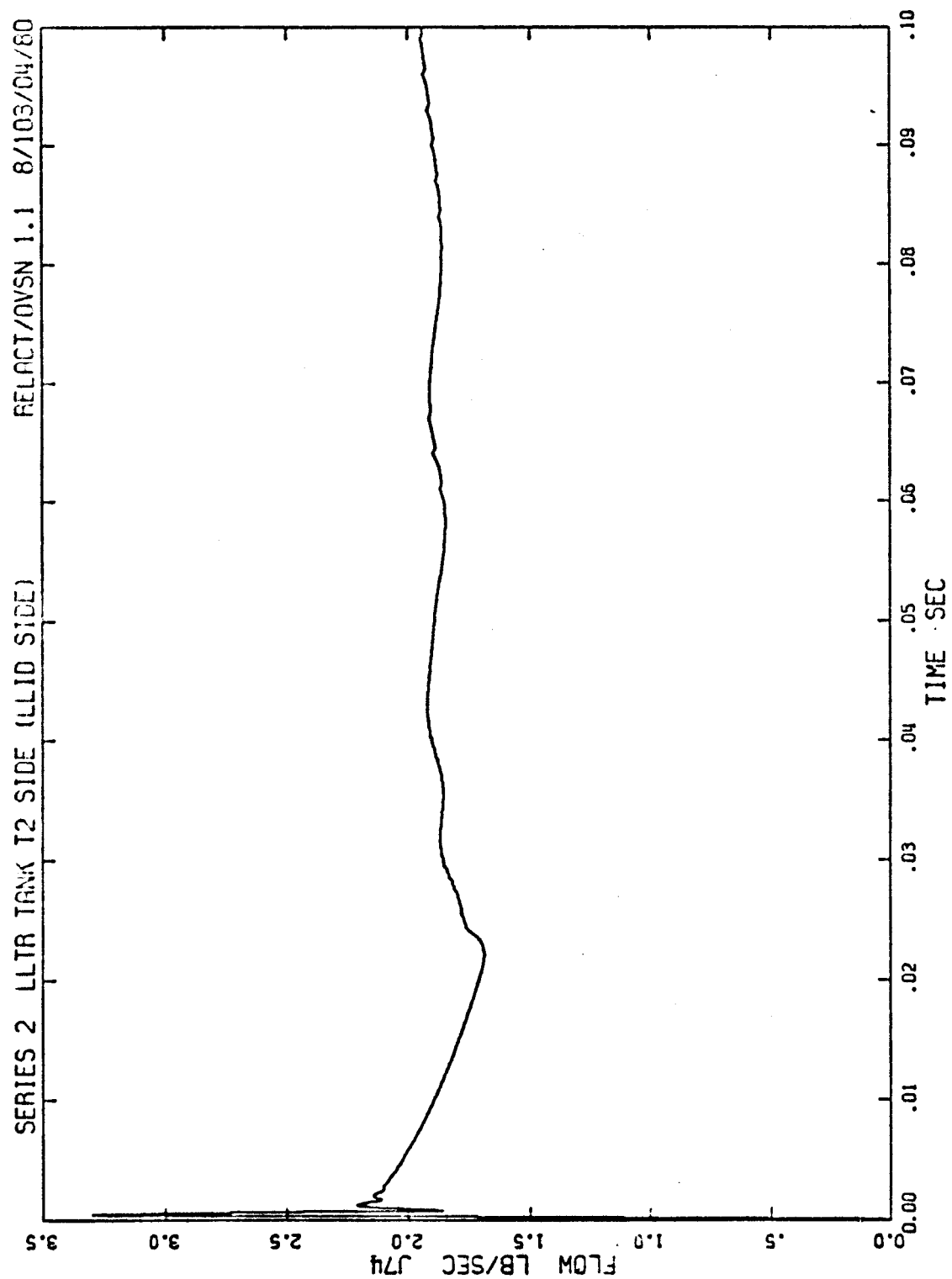
RELAP SCHEMATIC FOR TANK T2 SIDE OF RUPTURE TUBE

FIGURE IV-3



RELAP FLOW FROM TANK TI SIDE

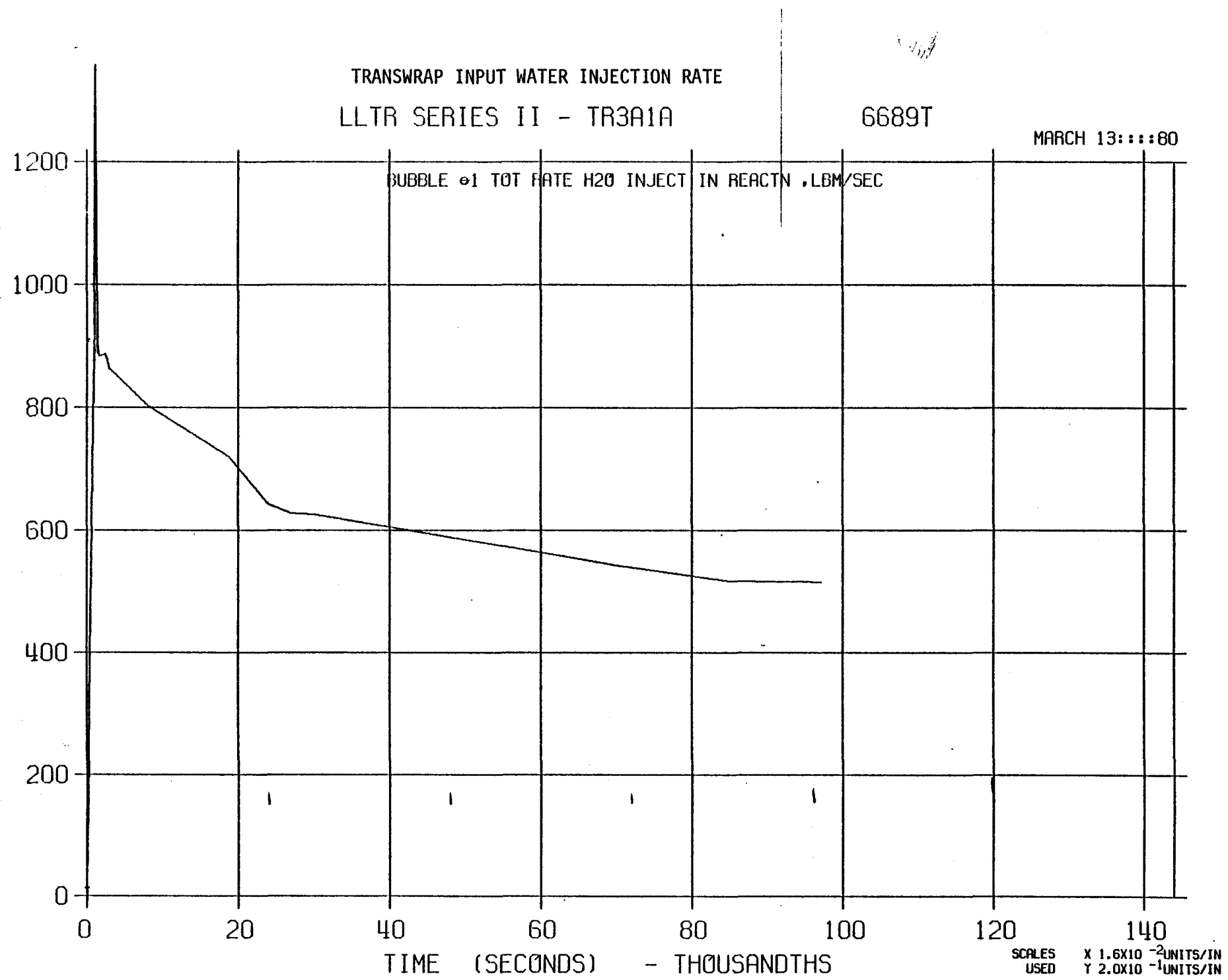
FIGURE IV-4



RELAP FLOW FROM TANK T2 SIDE

FIGURE IV-5

FIGURE IV-6
TRANSWRAP H₂O INJECTION - THOUSANDTHS (LB/SEC)



Calculational Methodology
for Test A-1a and A-1b Analysis

Calculation Sequence No.	Input	Code or Method	Output
1	Rupture tube geometry, properties, loading	NONSAP	Tube ends separation vs time
2	End separation (in diameters) vs time	FIGURE IV-1 Multiply rupture tube "area fraction" times "discharge factor"	Area ratio vs time for use in RELAP code rupture tube flow model
3	Nitrogen system geometry, operating temp., press., rupture tube area history and discharge pressure	RELAP 4/MOD 5 -Containment option (1 calculation for each broken end of tube)	RELAP flow vs time from each rupture tube
4	Sum of RELAP air flows from each tube end	Multiply by $\frac{M_{H_2O}}{M_{Air}} \times \frac{R_{Na}}{R_{Bubble}}$ (where M = molecular weight)	Water injection rate for TRANSWRAP analysis
5	Water injection rate, TRANSWRAP model parameters	TRANSWRAP modified to include SWAAM dynamic double rupture disk model	Sodium and relief system pressure and flow histories

FIGURE IV-7

TRANSWRAP MODEL

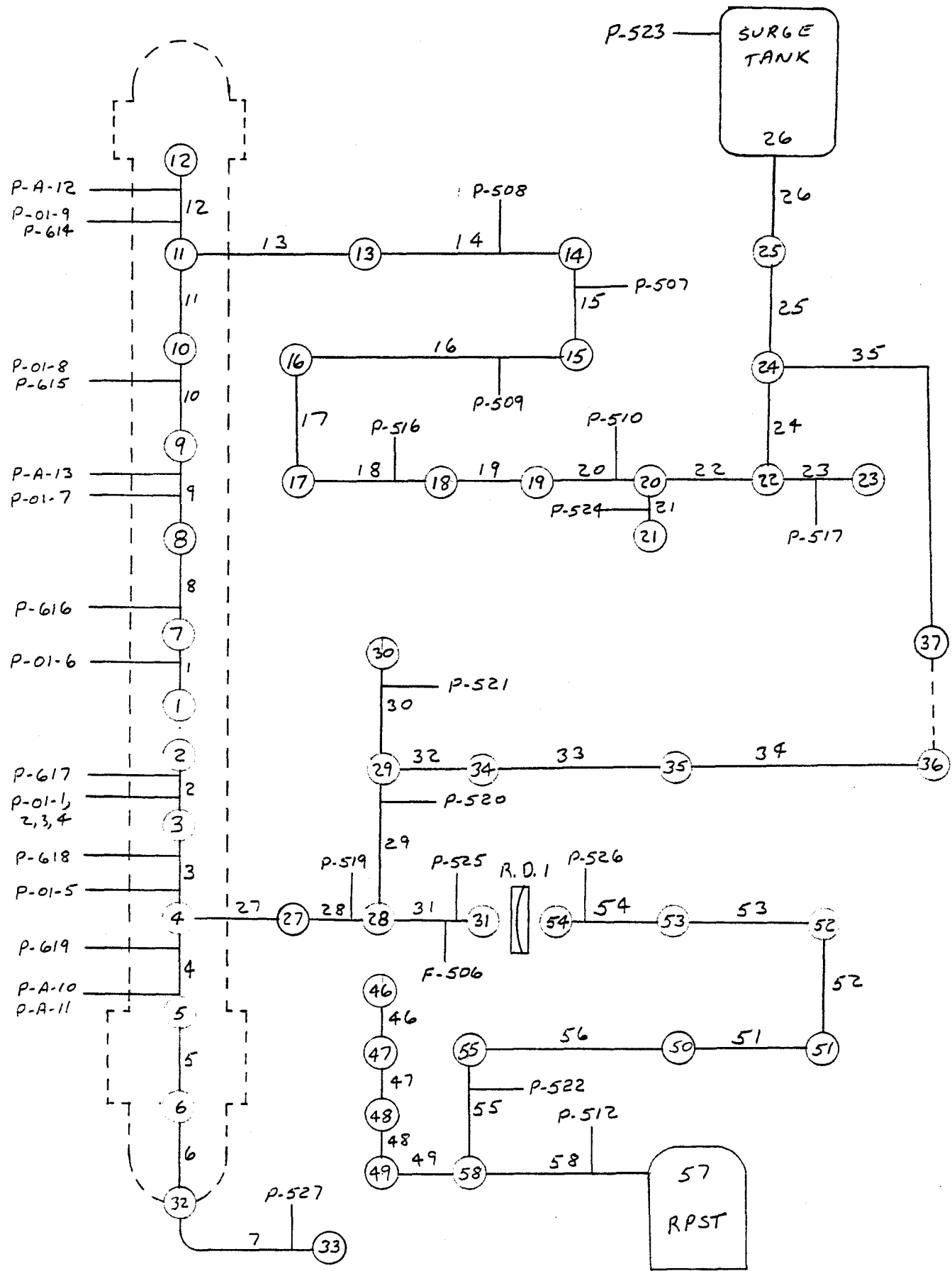


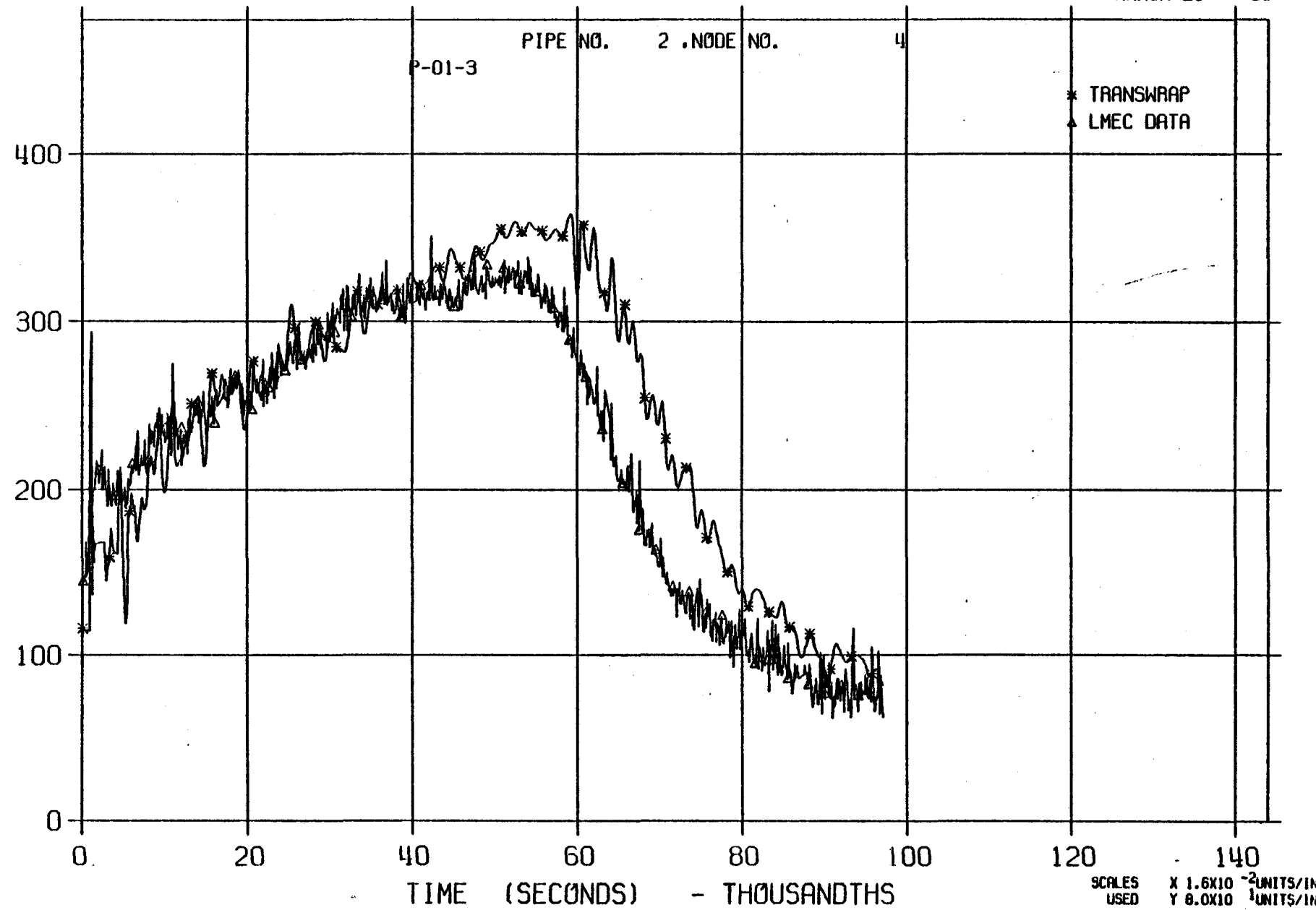
FIGURE IV-8

LLTR SERIES II - TR3A1A

7125T

MARCH 21:::80

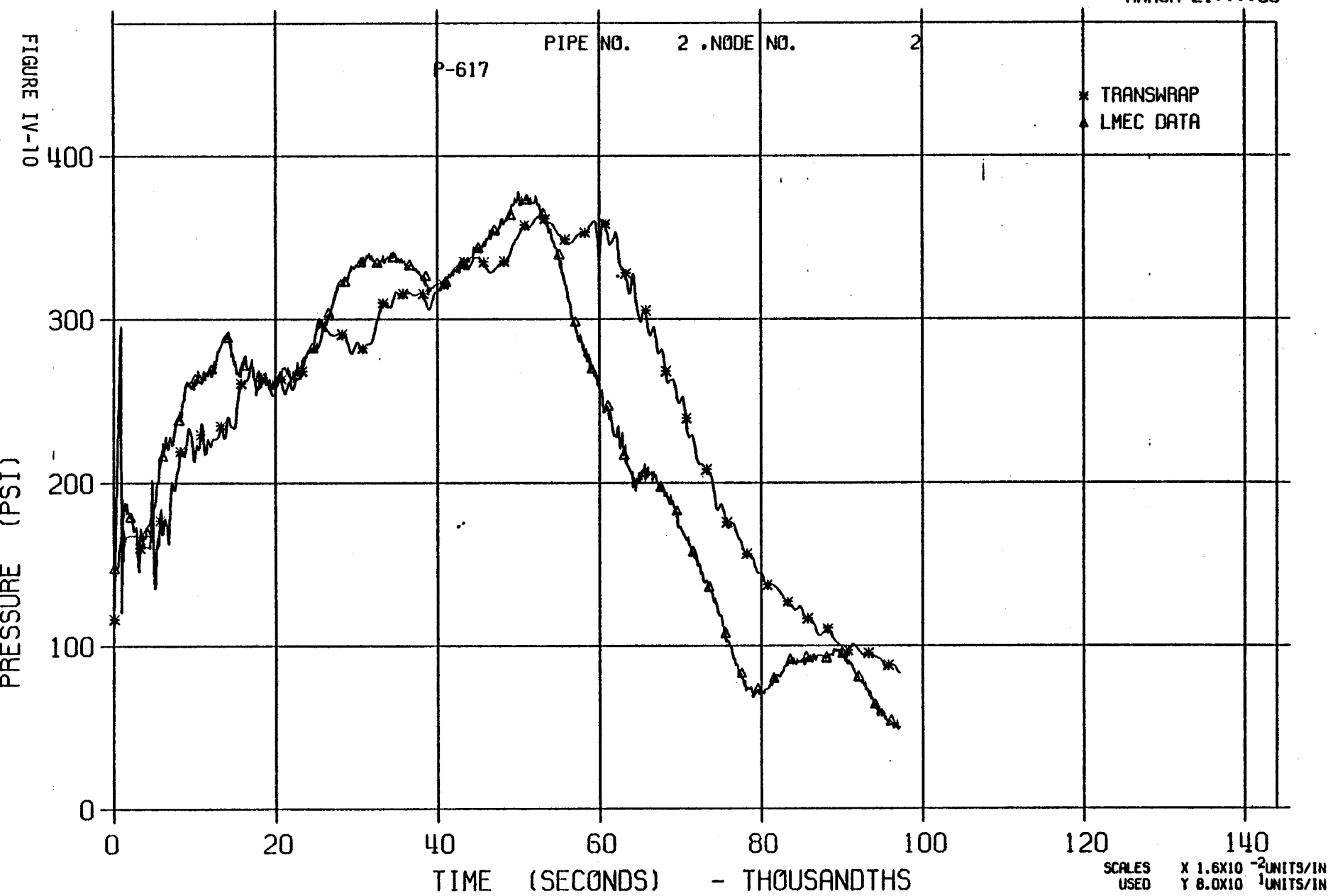
FIGURE IV-9



LLTR SERIES II - TR3A1A

7125T

MARCH 21:::80

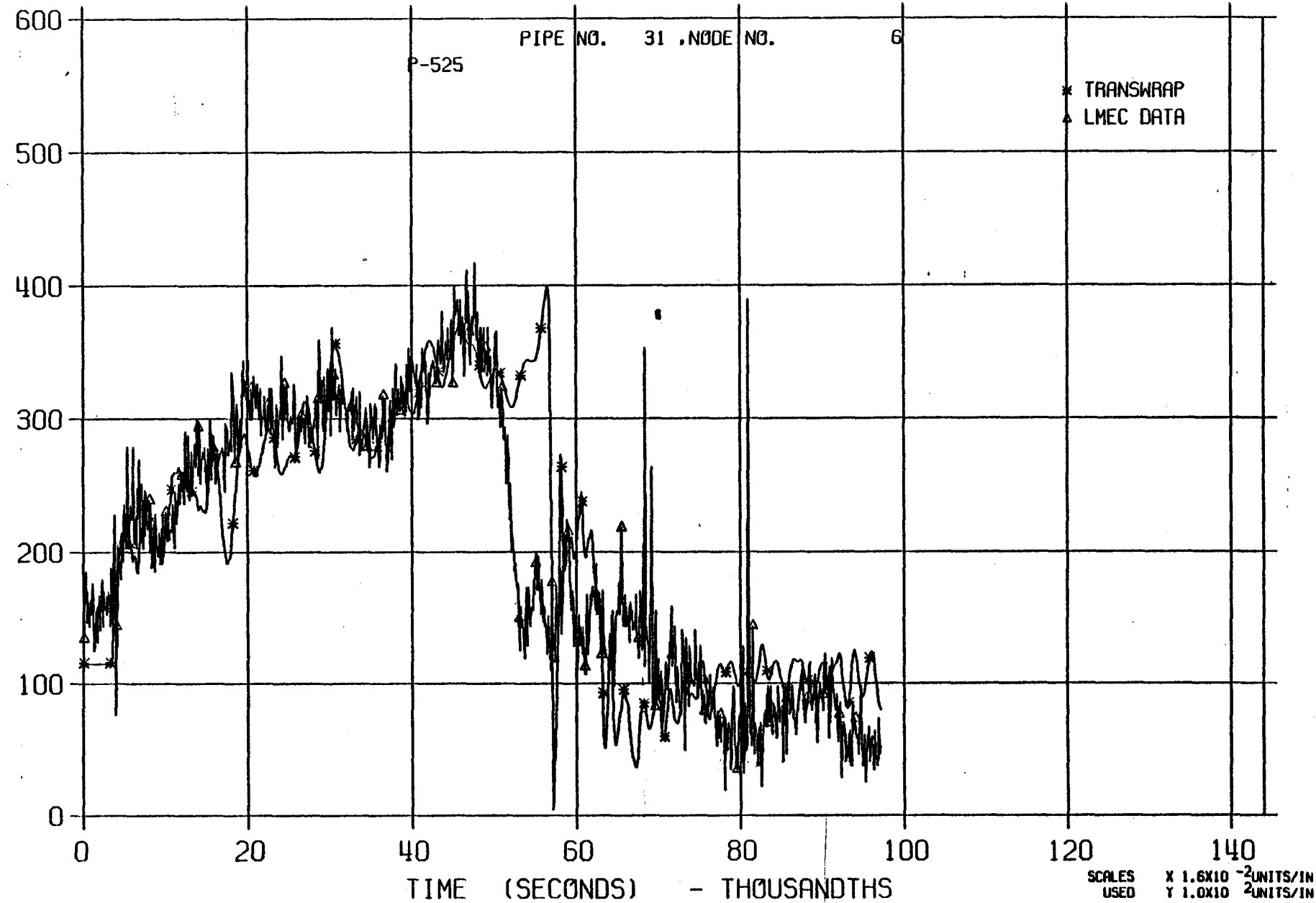


LLTR SERIES II - TR3A1A

7125T

MARCH 21:::80

FIGURE IV-11



LLTR SERIES II - TR3A1A

2730T

MARCH 21:::80

FIGURE IV-12

43

PRESSURE (PSI)

400

300

200

100

0

P-01-3

PIPE NO.

2 NODE NO.

4

* TRANSWRAP
▲ LMEC DATA

TIME (SECONDS) - THOUSANDTHS

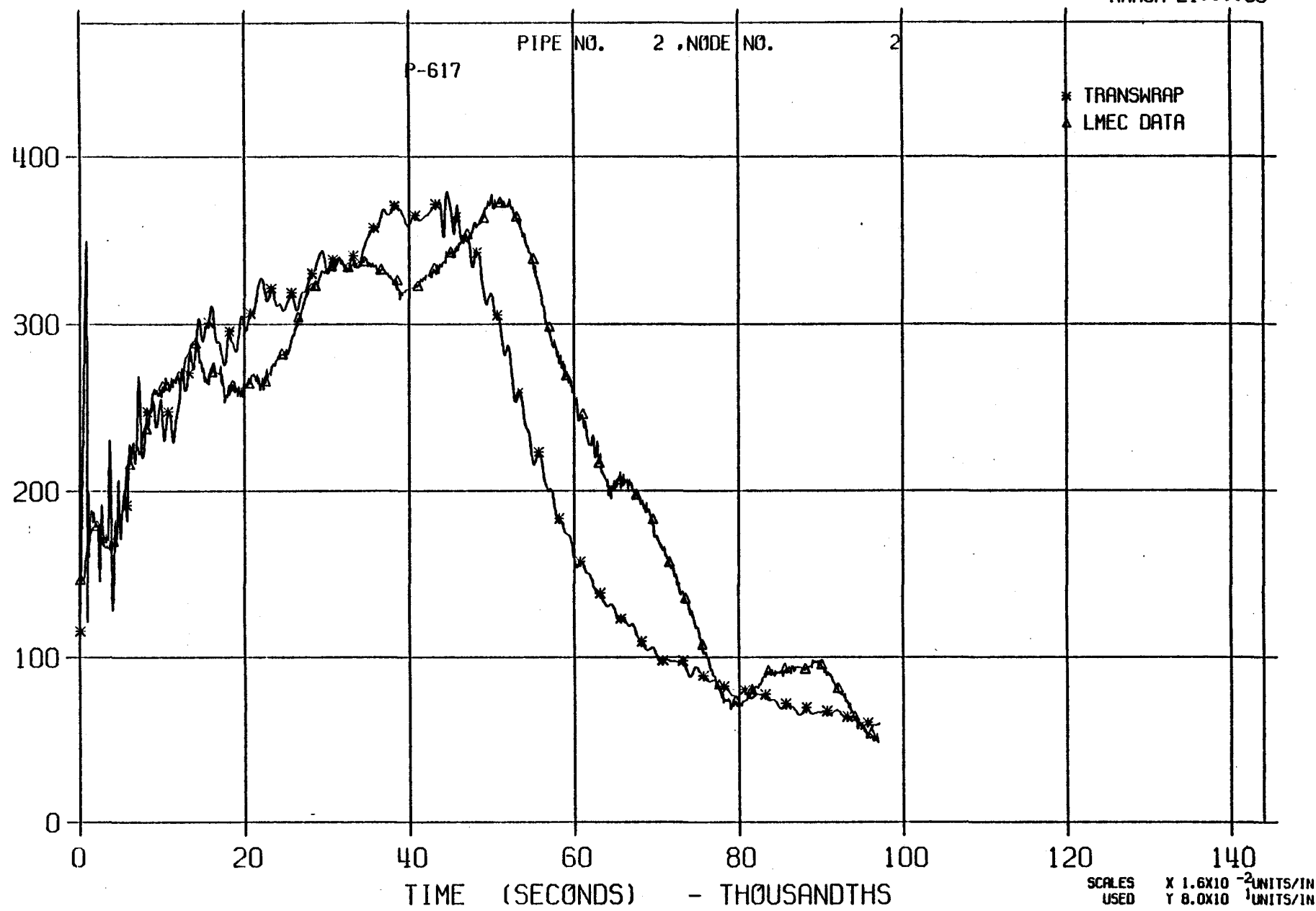
SCALES USED X 1.6×10^{-2} UNITS/IN
Y 0.0×10^1 UNITS/IN

LLTR SERIES II - TR3A1A

2730T

MARCH 21:::80

FIGURE IV-13

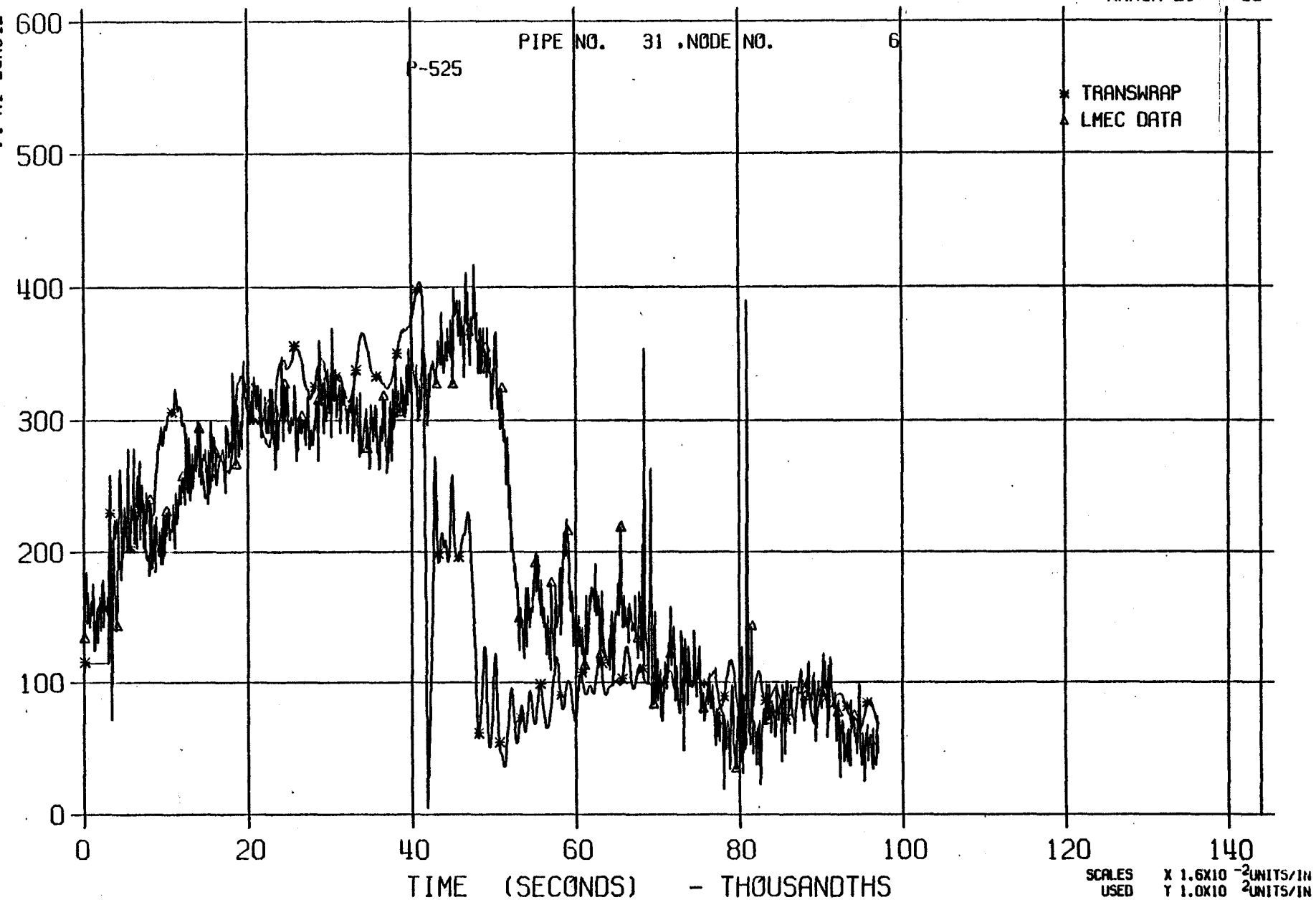


LLTR SERIES II - TR3A1A

2730T

MARCH 21:::80

FIGURE IV-14



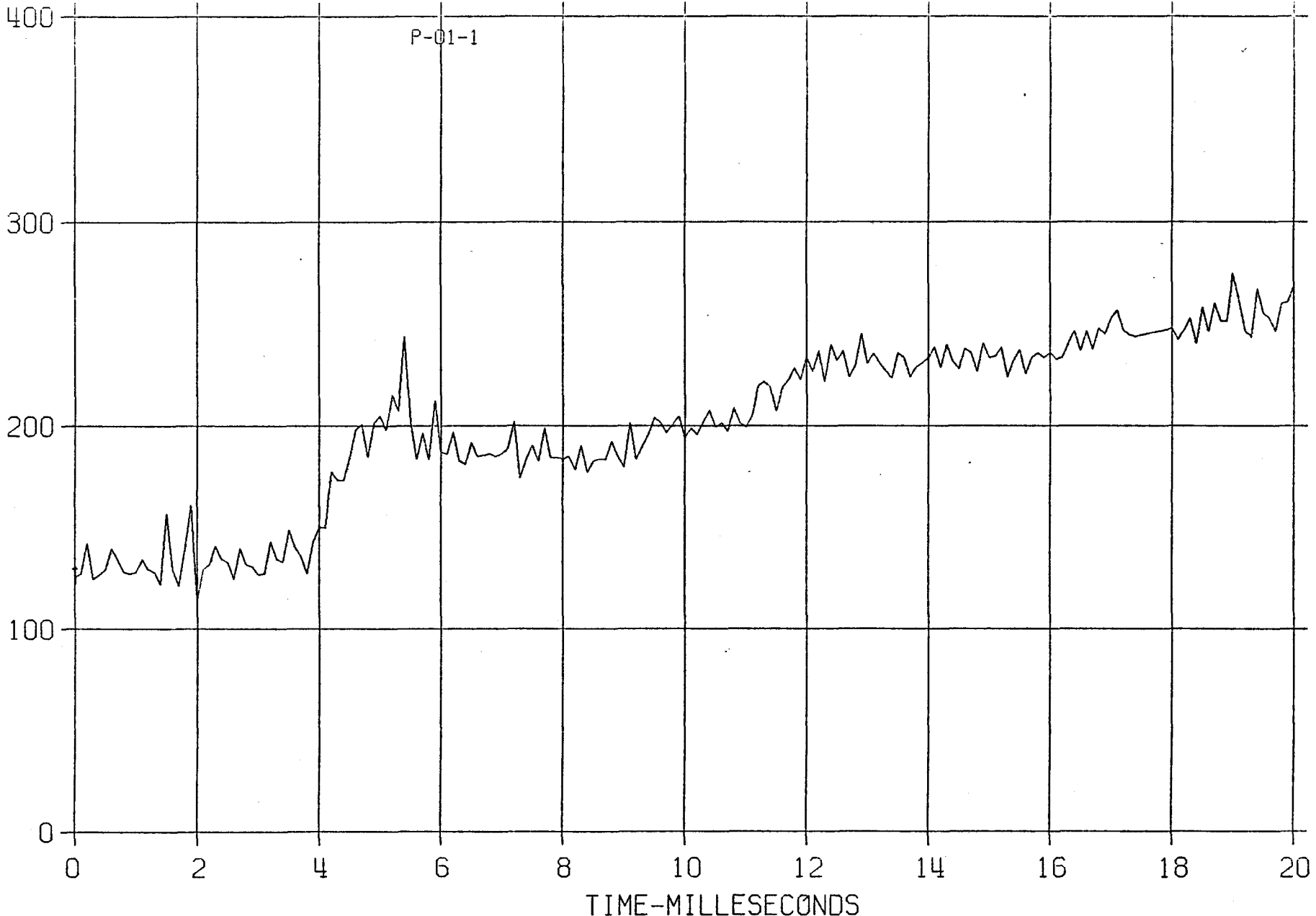
SER2 TEST A1B 46.069

MARCH 17:::80

FIGURE IV-15

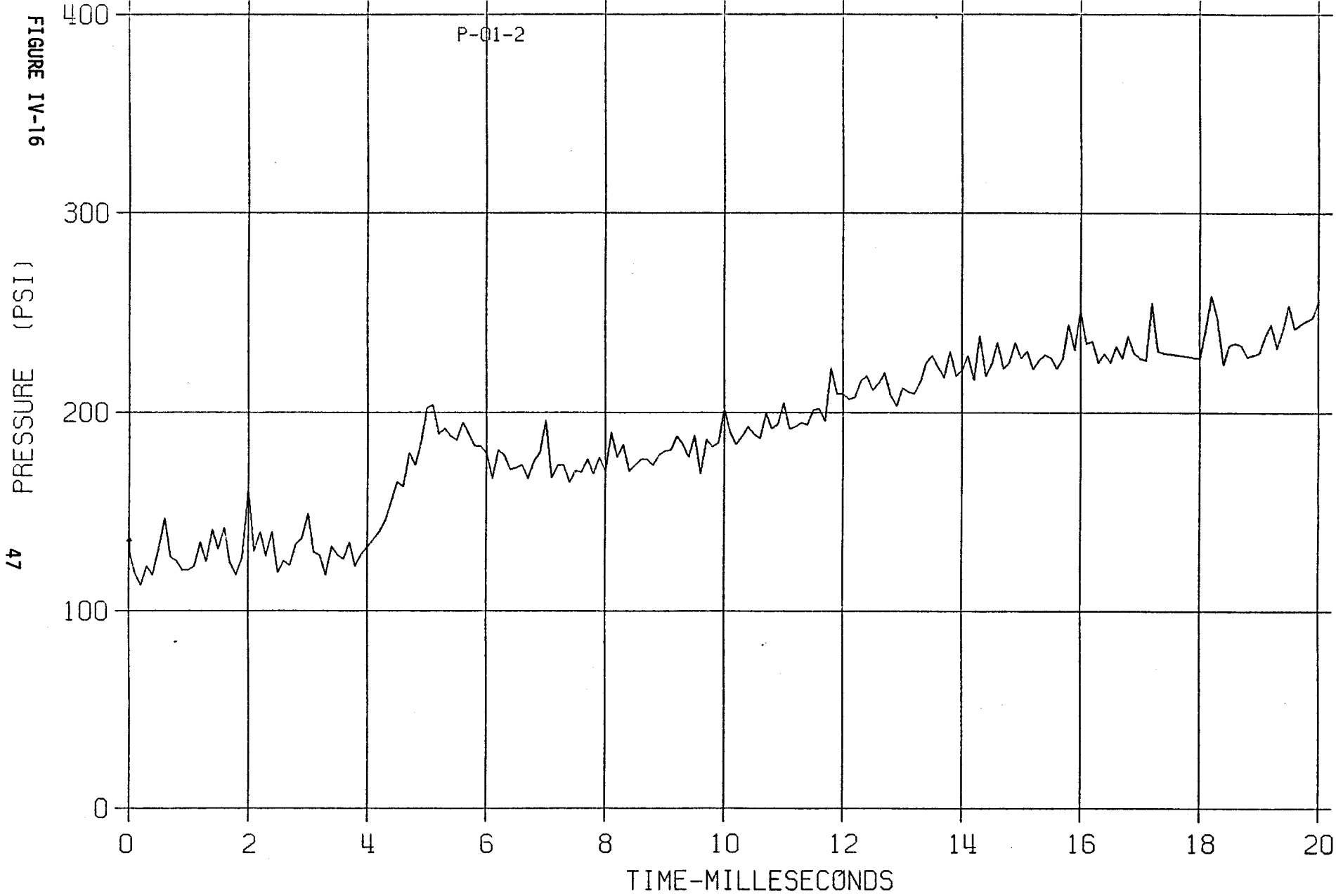
PRESSURE (PSI)

46



SER2 TEST A1B 46.069

MARCH 17:00:00

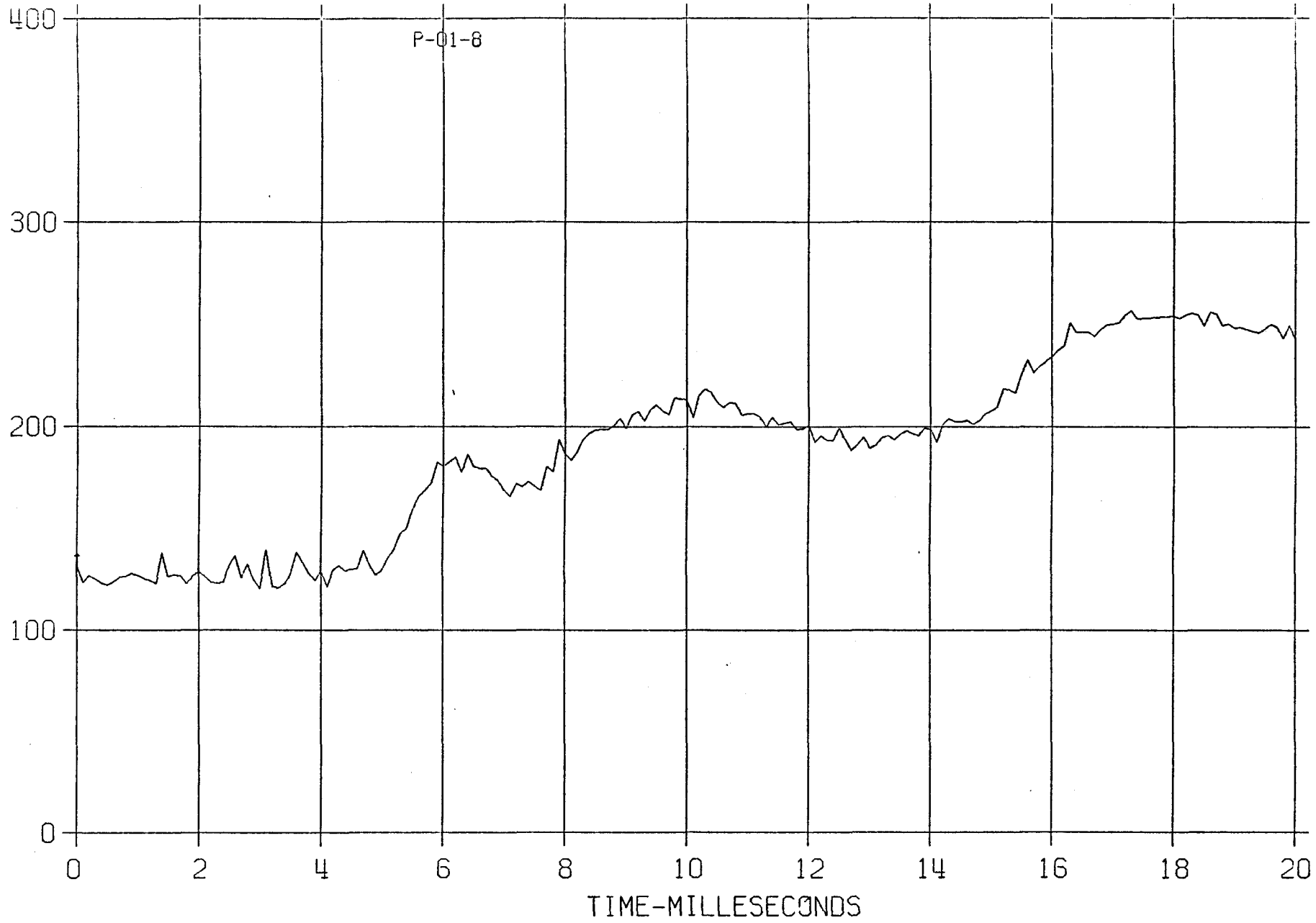


SER2 TEST A1B 46.069

MARCH 17::::80

FIGURE IV-17

PRESSURE (PSI)

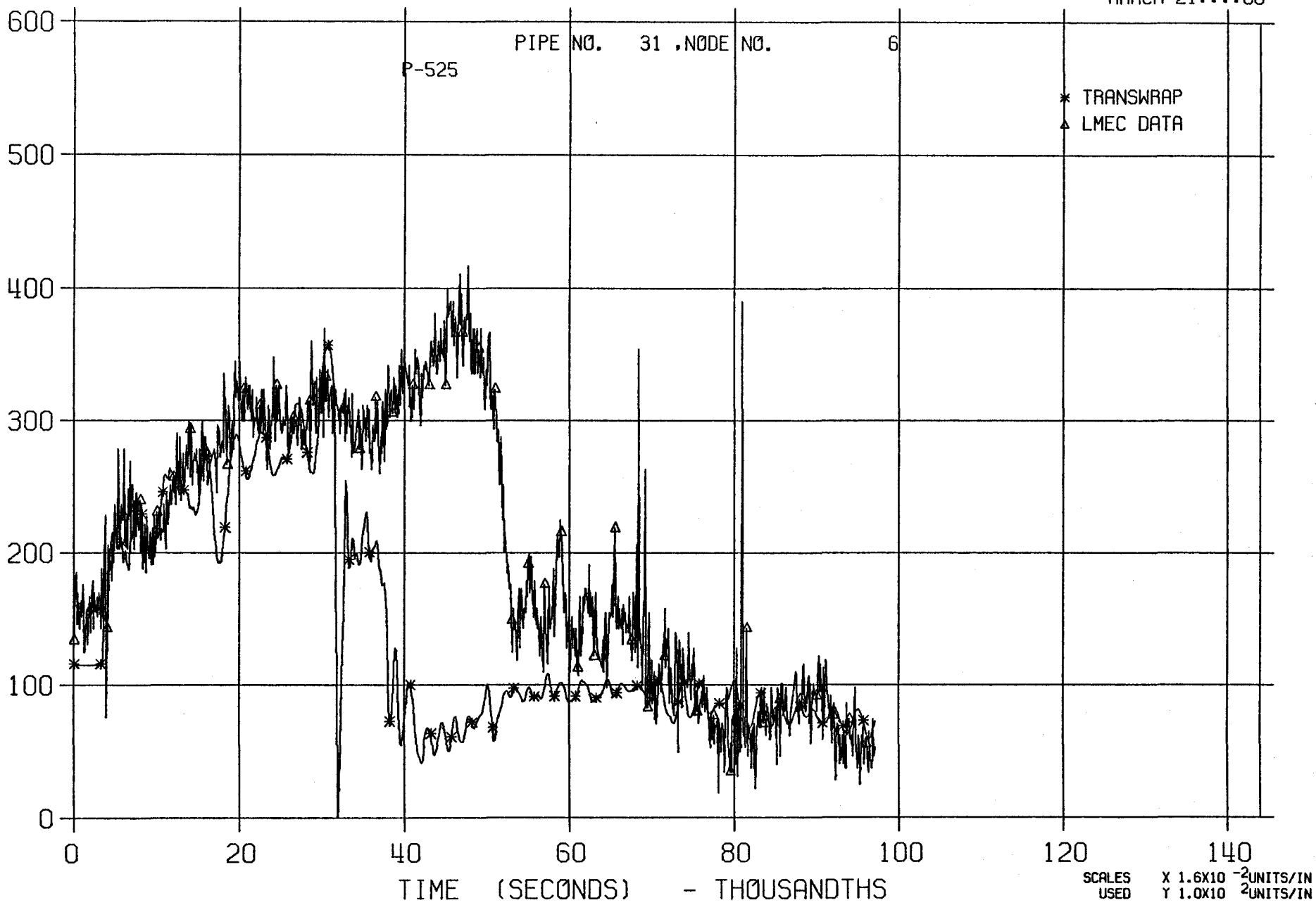


LLTR SERIES II - TR3A1A

7121T

MARCH 21:::80

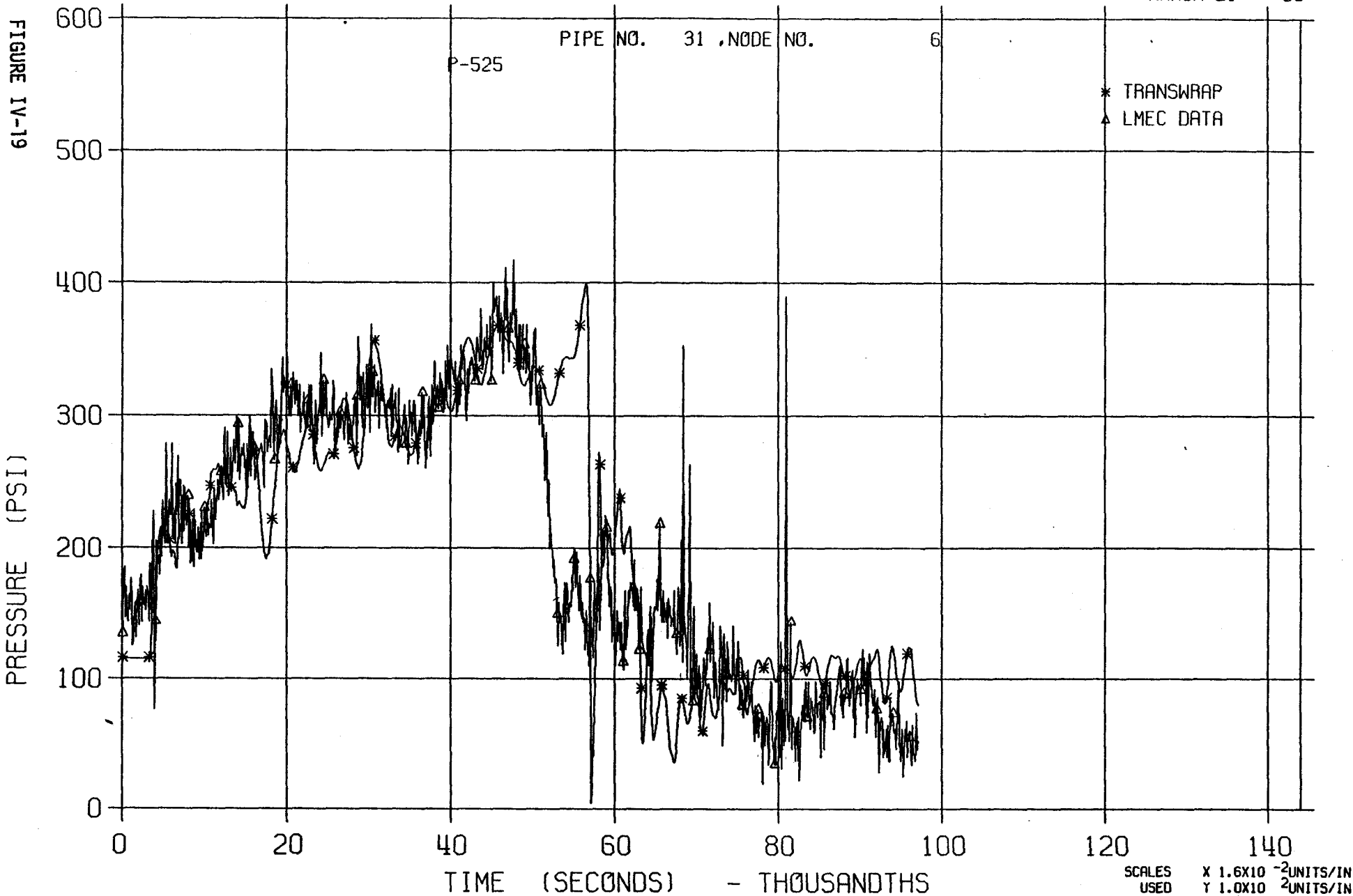
FIGURE IV-18



LLTR SERIES II - TR3A1A

7125T

MARCH 21:::80

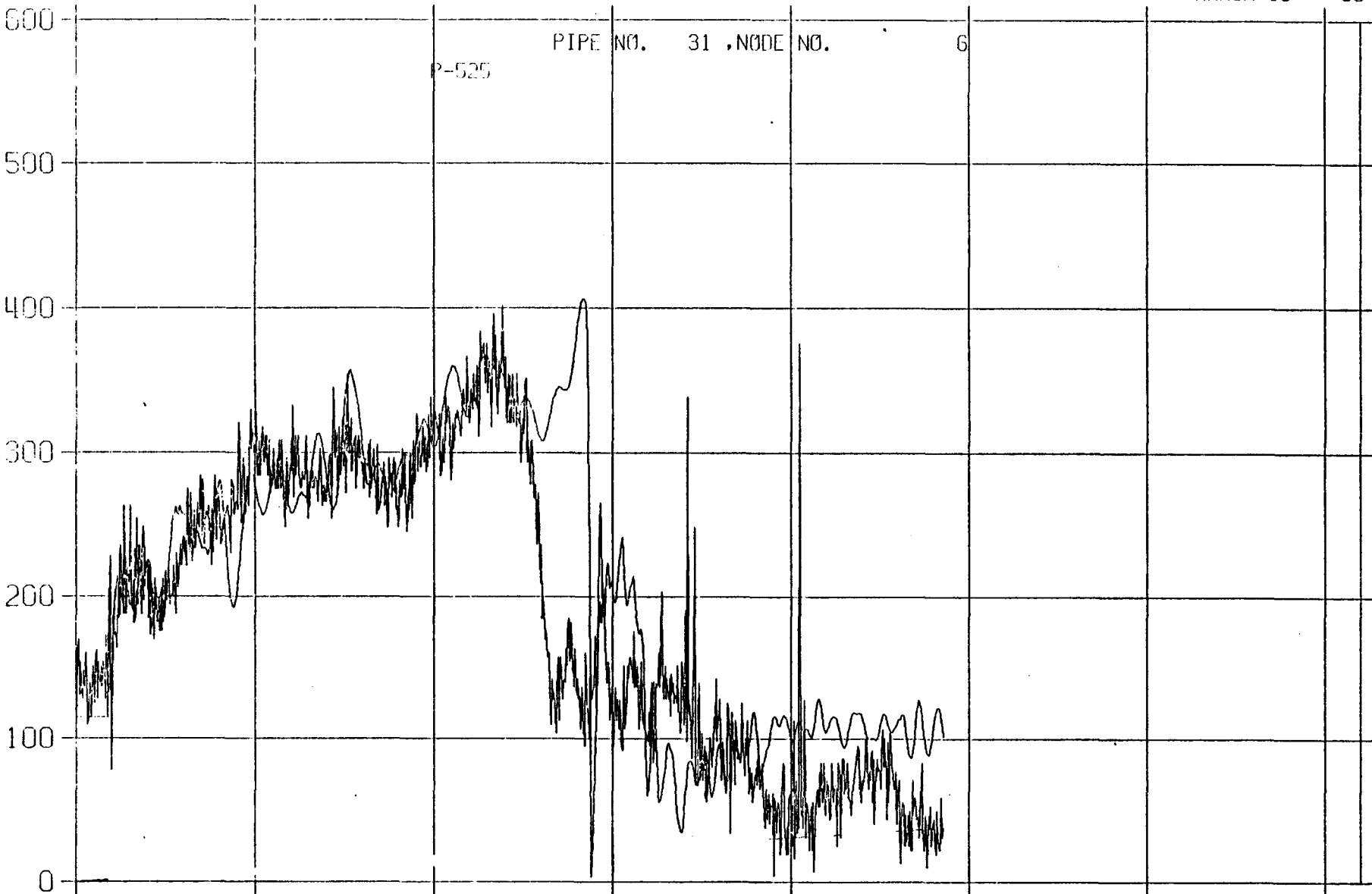


LLTR SERIES II - TR3A1A

6691T

MARCH 13:::80

FIGURE IV-20

100
200
300
400
500
600

TIME (SECONDS) - THOUSANDTHS

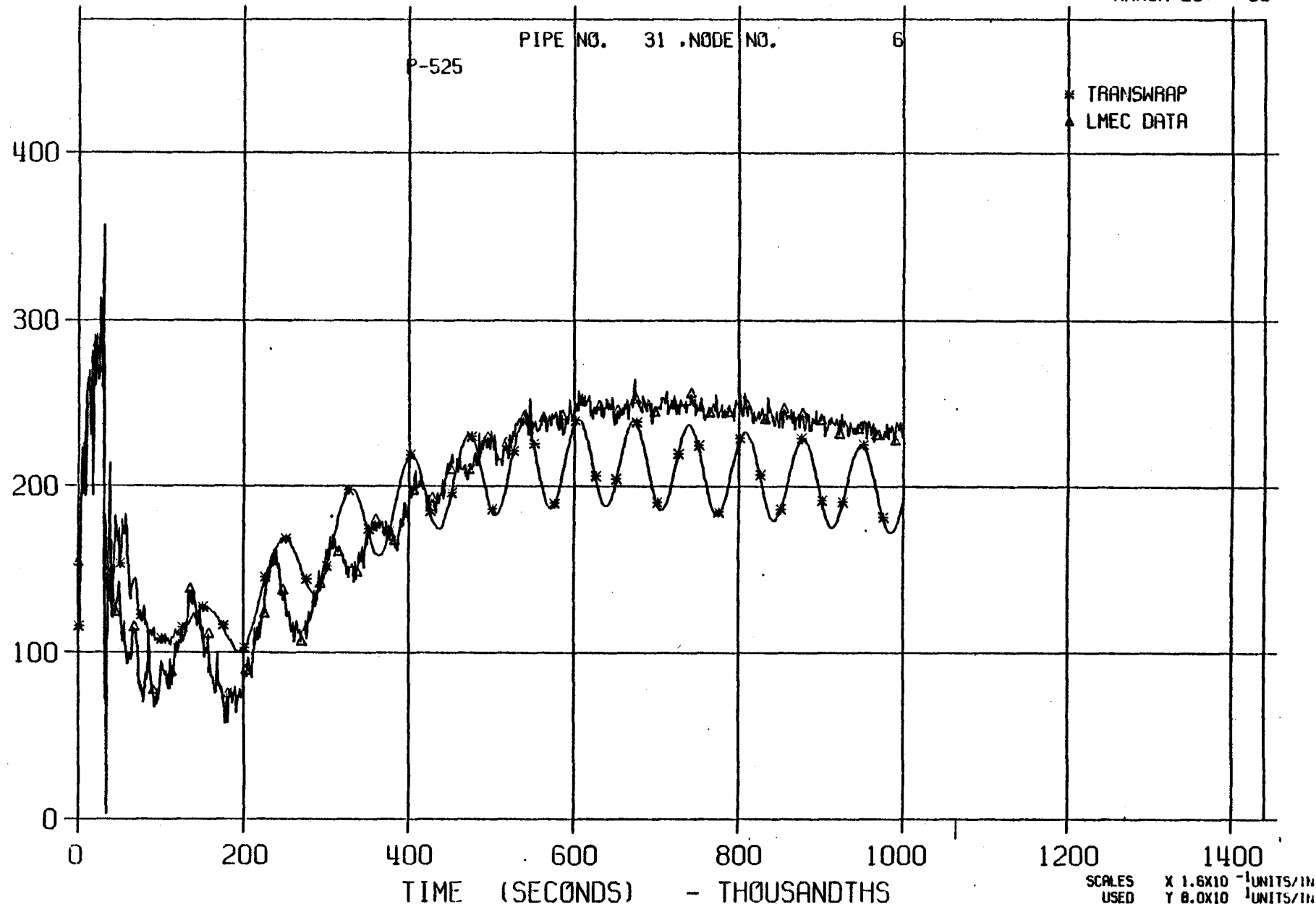
SCALE
USED X 1.6×10^{-2} UNITS/IN
Y 1.0×10^{-2} UNITS/IN

LLTR SERIES II - TR3A1B

2452T

MARCH 25:::80

FIGURE IV-21



V. EVALUATION OF TEST RESULTS

A. LLTV AND SYSTEM PRESSURES

Summaries of calculated maximum pressures using the standard methodology vs measured maximum pressures in the LLTV and sodium piping during the first second of the tests appear in Table V-1 and V-2 for test A-1a and A-1b respectively. The results show good agreement between the calculated and measured maximum pressures. Comparative pressure histories for these two tests are plotted on Figures V-1 thru V-14 for test A-1a and Figures V-10 thru V-27 for test A-1b. Additional figures and discussion of pressures in the lower sodium piping upstream of the rupture disc(s) may be found in Section IVC on rupture disc modeling. A complete set of figures showing TRANSWRAP vs measured values of test parameters may be found in Appendices A and B. For locations of pressure transducers, the reader should refer to Figures III-3 and III-4 in Section III. All sensors in these tables except the 500 series measure pressures within the vessel.

1. Leaksite Pressures

The pressure transducers closest to the leaksite within the shroud are P01-3 for test A-1a and P01-1 for A-1b. Pressure sensors P01-1, 2, 3 and 4 were installed to measure radial distribution at the leaksite elevation. Data was not obtained from P01-1, 2 and 4 in test A-1a and P01-3 in A-1b. The peak leaksite pressure, which is determined by the failure pressure of the first rupture disc, is slightly over predicted by TRANSWRAP; by 30 psi for test A-1a and by less than 15 psi that for A-1b. Except for times less than 10 msec close to the leaksite location (Figure V-1) there is also good agreement between the calculated and measured pressure change. About 60% of the discrepancy between TRANSWRAP calculations and the data during this early time interval is a consequence of TRANSWRAP pressures having been (incorrectly) initialized 30 psi below the test pressures. A sample calculation with the correct initial pressures decreased the discrepancy in pressure shown on Figure V-1 to about 20 psi without significant effect on longer time pressures. This early time region may also be improved by modifications to the rupture tube discharge rates calculated by RELAP and to LLTV sonic velocity. As previously indicated, changes to these parameters

will be considered during planned Test A-2 evaluations. At about 0.8 msec, TRANSWRAP calculates a pressure "spike" not recorded. The "spike" remains below the maximum leaksite pressure and is caused by discontinuities in the bubble pressure initialization routine in TRANSWRAP.

Radial pressure attenuation measured by P-01-1, 2, and 4 located about 2 feet below the leaksite (Table V-2) totals 15 psi over the 12 inch radial distance separating P-01-1 and P-01-4. P-01-4 is about 3.5 inches from the shroud. These measured small radial gradients support the one dimensional model in the TRANSWRAP code.

2. Pressure Distribution within the LLTV

Pressure transducer P617, which is on the vessel wall nozzle close to the leaksite, is the only vessel transducer which indicated a higher than calculated pressure (by 10 psi for test A-1a). P617 measured 20 psi lower than predicted for test A-1b. The calibration of P617 seems suspect since pressure measurements at P618 and P619 are 30 and 20 psi lower than P617 for test A-1a. Also, P619 is only 10 psi lower for test A-1b though the A-1b leaksite is relatively closer to P617 for the latter test.

Radial attenuation through the shroud is best determined by comparing P01-8 and P615 for tests A-1a and A-1b. These are at the same elevation, the former being less than 5 inches from the center line while the latter is on the vessel wall. For each test, P615 reads slightly higher (by 5 and 10 psi) but within the accuracy of the measurements. Comparing figures V-7 and V-8, there seems to be only a slight difference in the shape of the pressure waves recorded at these locations. Note that PA-13 (Fig. V-11) records over 600 psig and is believed to be giving an erroneous reading since it is inconsistent with all other transducers in the vessel.

The TRANSWRAP predicted pressures at the tube sheet locations, i.e. PA10, 11, and 12, are slightly higher than the leaksite measured pressures (~15 to 20 psi). For test A-1b the recorded pressures at PA-10 and PA-11 (10 inches and 5 inches from the center line of the lower tube sheet, respectively) are lower by 10 to 15 psi than at the leaksite. The upper tube sheet pressure was not available for this test. In general, TRANSWRAP does a good job of predicting system pressures within the LLTV.

3. Pressure Attenuation in Sodium-Filled Piping

Pressure sensors P507, 508, 509 and 516 are located along the 10 inch diameter sodium piping connected to the upper nozzle of the LLTV (see Figure III-3). Tables V-1 and V-2 show the maximum predicted and measured pressures for the above transducer which were functioning in each test. Note, in general, that both predicted and measured maximum pressures increase with distance from the leaksite as a consequence of internal reflections. The agreement between the predicted and measured pressures is considered good based on the complexity of the wave pattern. The complex wave pattern makes it very difficult to determine elbow attenuation effects from this data. Further studies are planned as part of the A-2 post-test evaluation.

B. RELIEF SYSTEM PERFORMANCE

A comparison of TRANSWRAP vs measured relief system flows is presented on Figure V-28 for test A-1a. Volumetric sodium flows are plotted as determined by three different methods. The upper curve represents the volume of sodium piping downstream of the rupture disc which has sufficient sodium to actuate the pair of flow spark plugs marked on the curve as F508A, B, C, D, E, and G (F not available). Note that the apparent volumetric flow rate (the slope of the curve) decreases downstream of 508C. The first three sensors are almost directly in-line with any spray of sodium from the failed rupture disc; the others are well downstream of the first bend and the two-component fluid flow pattern in this downstream region is more likely to have a lower fluid velocity than exists in the upstream region.

On the same figure, integration of drag disc flowmeter F506 located upstream of the rupture disc shows the volume of piping which would be occupied by the sodium if it moved down the piping as a "slug", completely filling the cross section. The ratio of ordinates of the flowmeter F506 data to the F508 spark plug data at any given time is a rough measure of the piping volume fraction occupied by sodium (the actual volume fraction would depend on how much sodium is required to trip the flow spark plugs and on the accuracy of flowmeter F506).

TRANSWRAP volumetric flow is also shown on this figure, with calculated and measured sodium velocities shown on Figure V-29. Note, that calculated

velocities and volume flows are higher than those measured by flowmeter F506 upstream of the rupture disc. Further studies are planned, as part of the test A-2 evaluation, to compare measured and predicted loads which result from these velocities on the relief system piping.

C. PRE-TEST PREDICTIONS

Pre-test predictions were based on a static rupture disc model and constant rupture tube discharge coefficient. Figure V-30 and V-31 are leak location and rupture disc pressure histories compared with data for test A-1a. The "old" static rupture disc model predicts a much faster decrease in pressure upstream of the rupture disc compared to the test data, with a corresponding rapid decrease in pressure at the leak location. The dynamic rupture disc model shows a much better agreement between predicted and measured data (see Figures IV-8 and IV-10).

TABLE V-1

SUMMARY OF CALCULATED VS MEASURED MAXIMUM PRESSURES FOR TEST A1A

<u>Location</u> (Transducer No.)	<u>TRANSWRAP</u>		<u>TEST DATA</u>	
	PRESSURE (psig)	TIME (msec)	PRESSURE (psig)	TIME (msec)
P01-3 (Leaksite)	345	59	315	53
P617	345	52	355	50
P618	350	55	325	49
P619	360	56	335	51
PA10	370	56	340	51
PA11	370	56	330	52
P616	360	52	335	51
P615	345	55	335	54
P01-8	345	57	330	53
PA12	360	58	340	54
P508	360	58	330	51
P507	360	32	360	33
P509	385	32	350	33

TABLE V-2

SUMMARY OF CALCULATED VS MEASURED MAXIMUM PRESSURES FOR TEST A1B PRIOR TO FAILURE OF THE SECOND RUPTURE DISC*

<u>Location</u> (Transducer No.)	TRANSWRAP		TEST DATA	
	PRESSURE (psig)	TIME (msec)	PRESSURE (psig)*	TIME (msec)
P01-1 (Leaksite)	305	37	295	28
P01-2	305	37	290	30
P01-4	305	37	280	30
P617	305	33	285	28
P619	315	30	275	28
PA10	315	38	280	28
PA11	315	38	280	28
P616	310	35	295	31
P615	310	36	300	29
P01-3	310	38	290	32
P614	310	38	300	31
P01-9	315	38	295	32
P508	355	33	295	31
P516	400	33	370	38

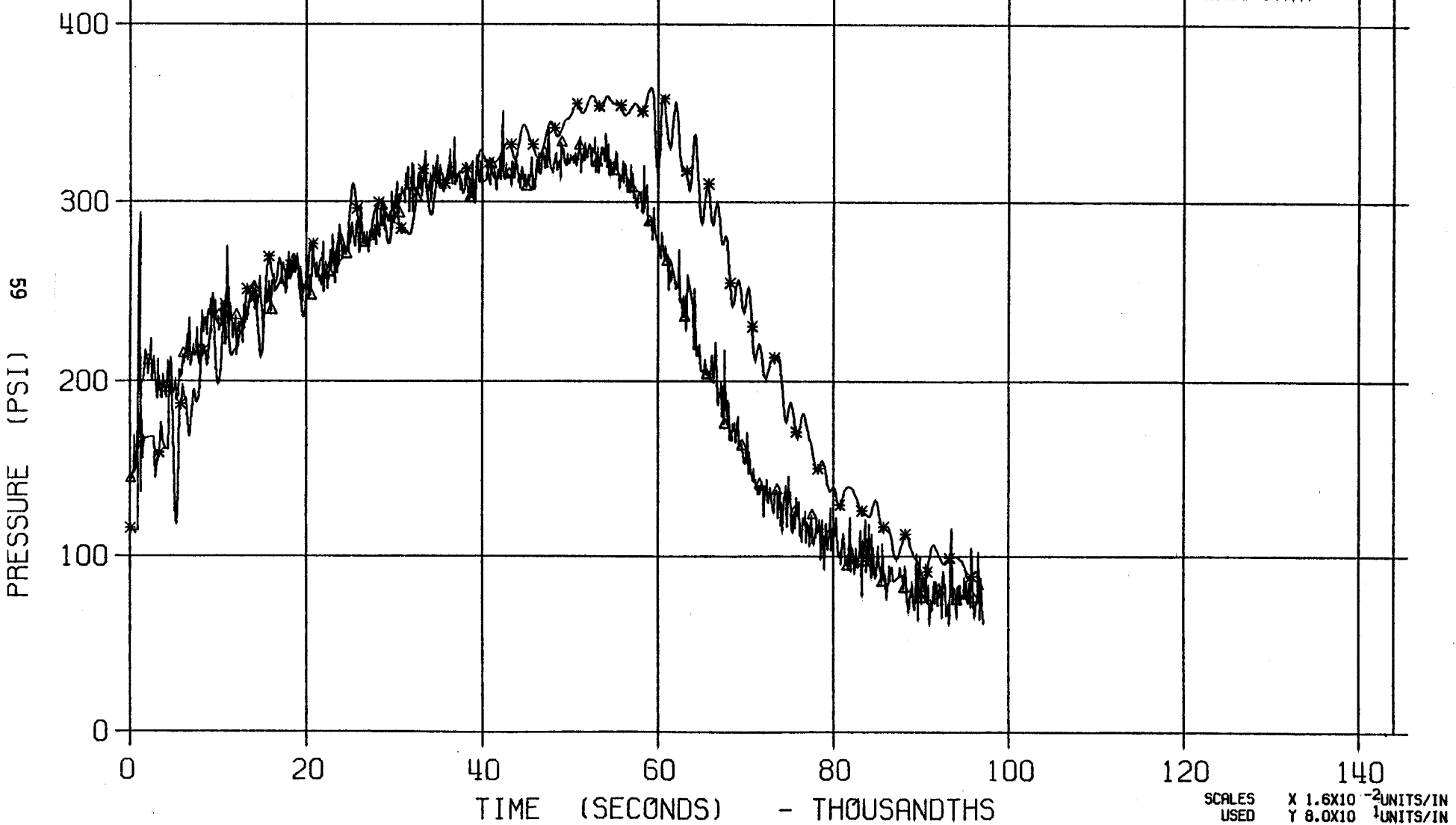
* Maximum measured sodium pressures at the time of second rupture disc failure (12.7 sec) were ~ 330 psig.

LLTR SERIES II - TR3A1A

7125T

MARCH 21:::80

FIGURE V-1

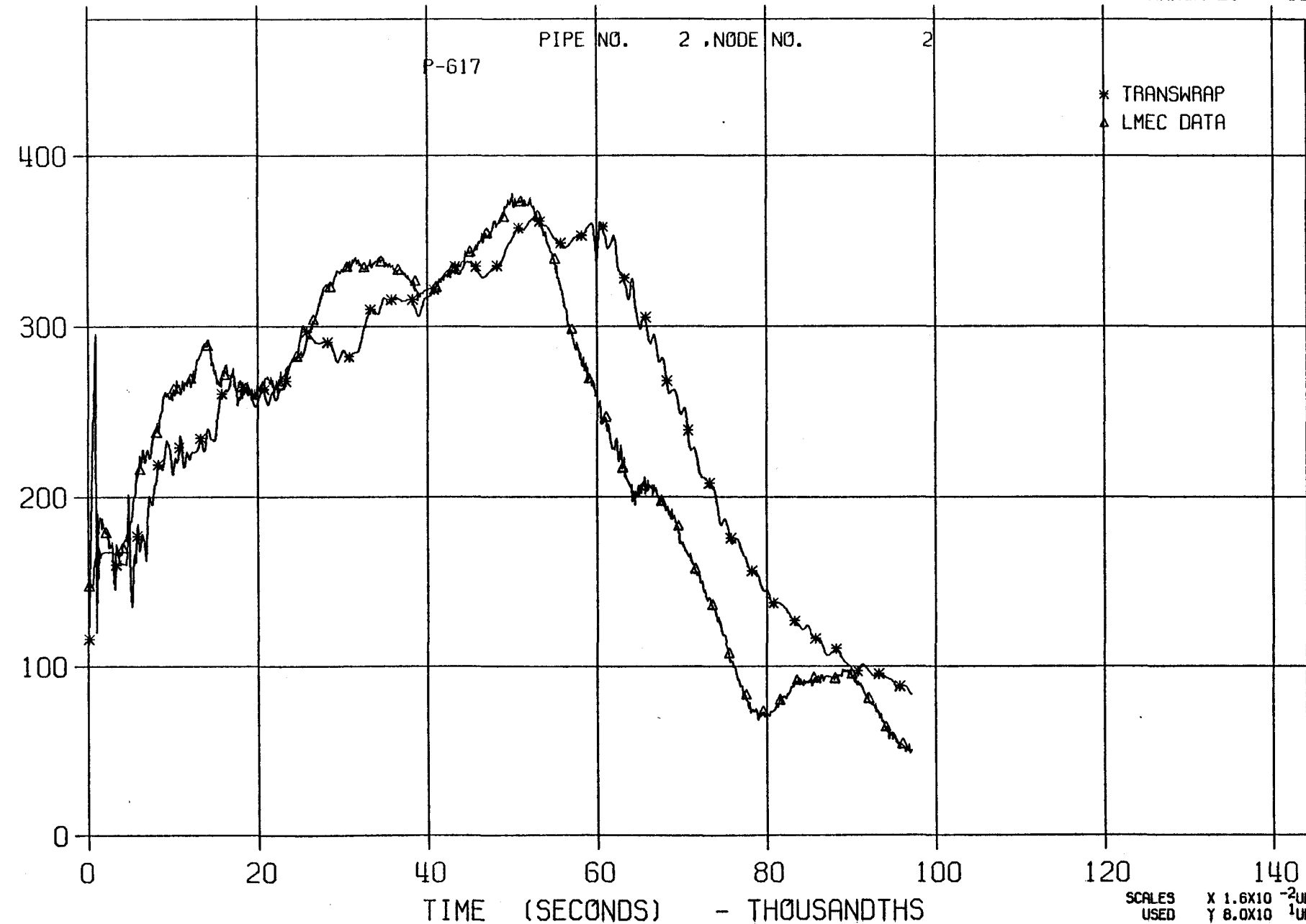


LLTR SERIES II - TR3A1A

7125T

MARCH 21:::80

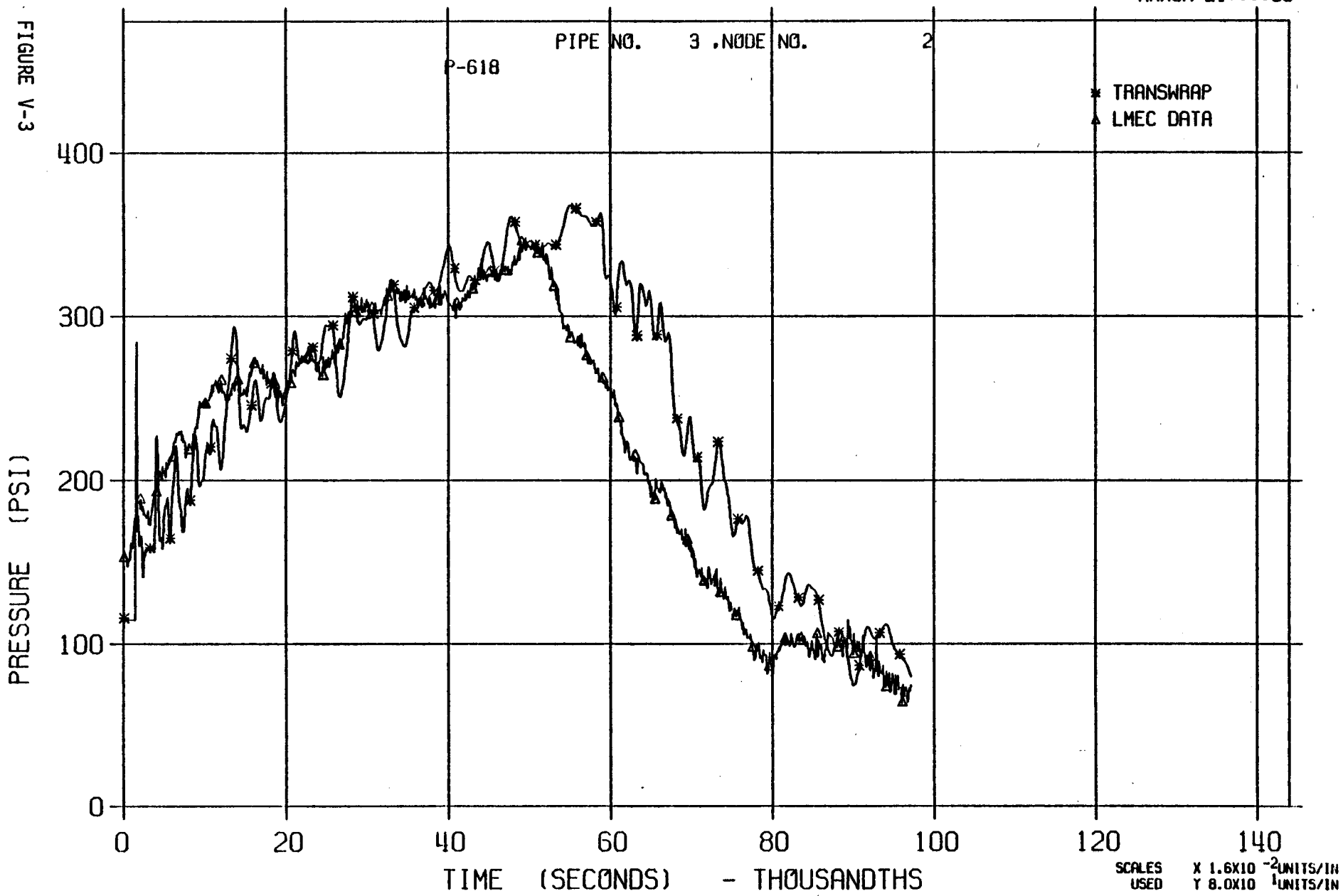
FIGURE V-2



LLTR SERIES II - TR3A1A

7125T

MARCH 21:::80

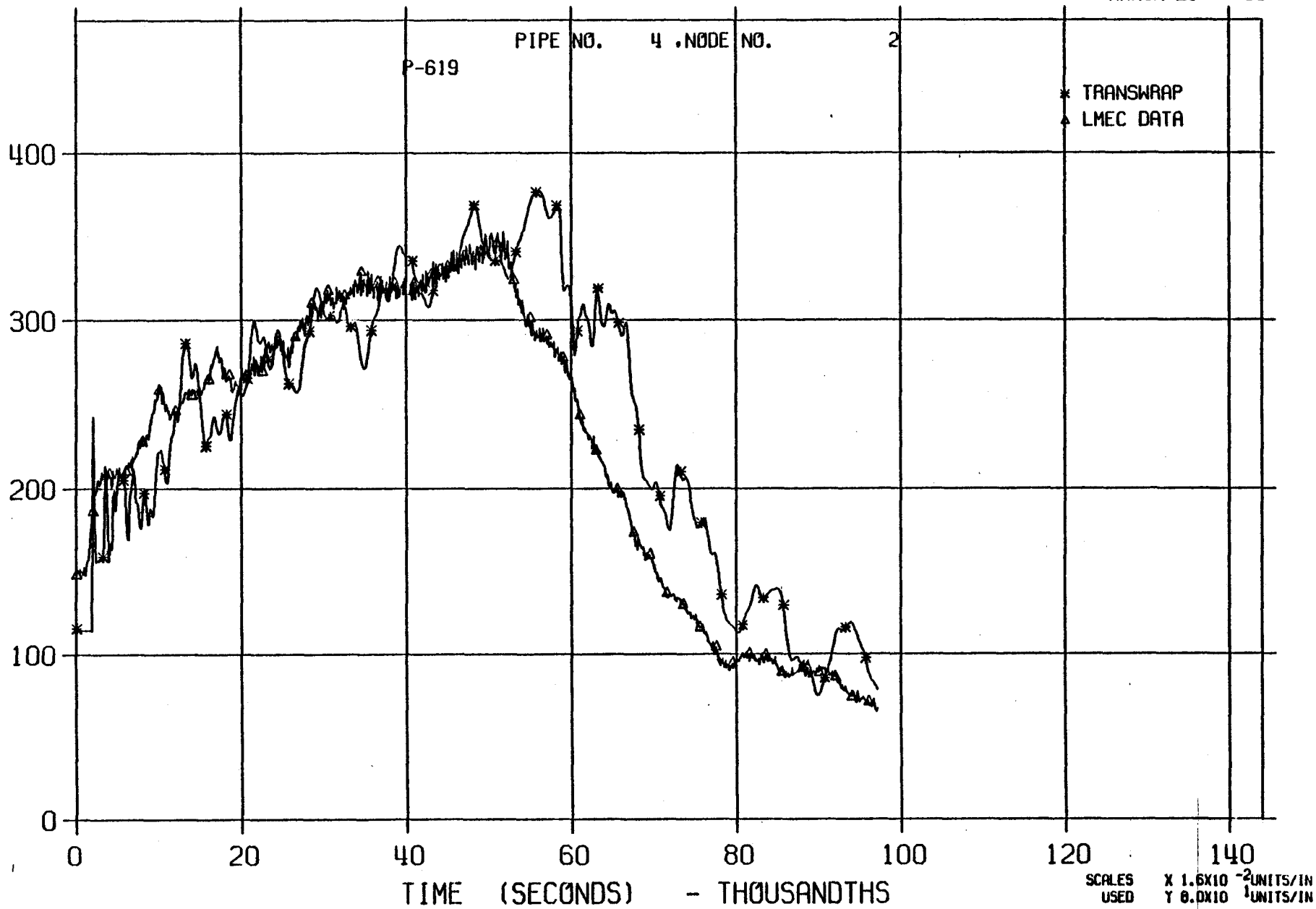


LLTR SERIES II - TR3A1A

7125T

MARCH 21:::80

FIGURE V-4

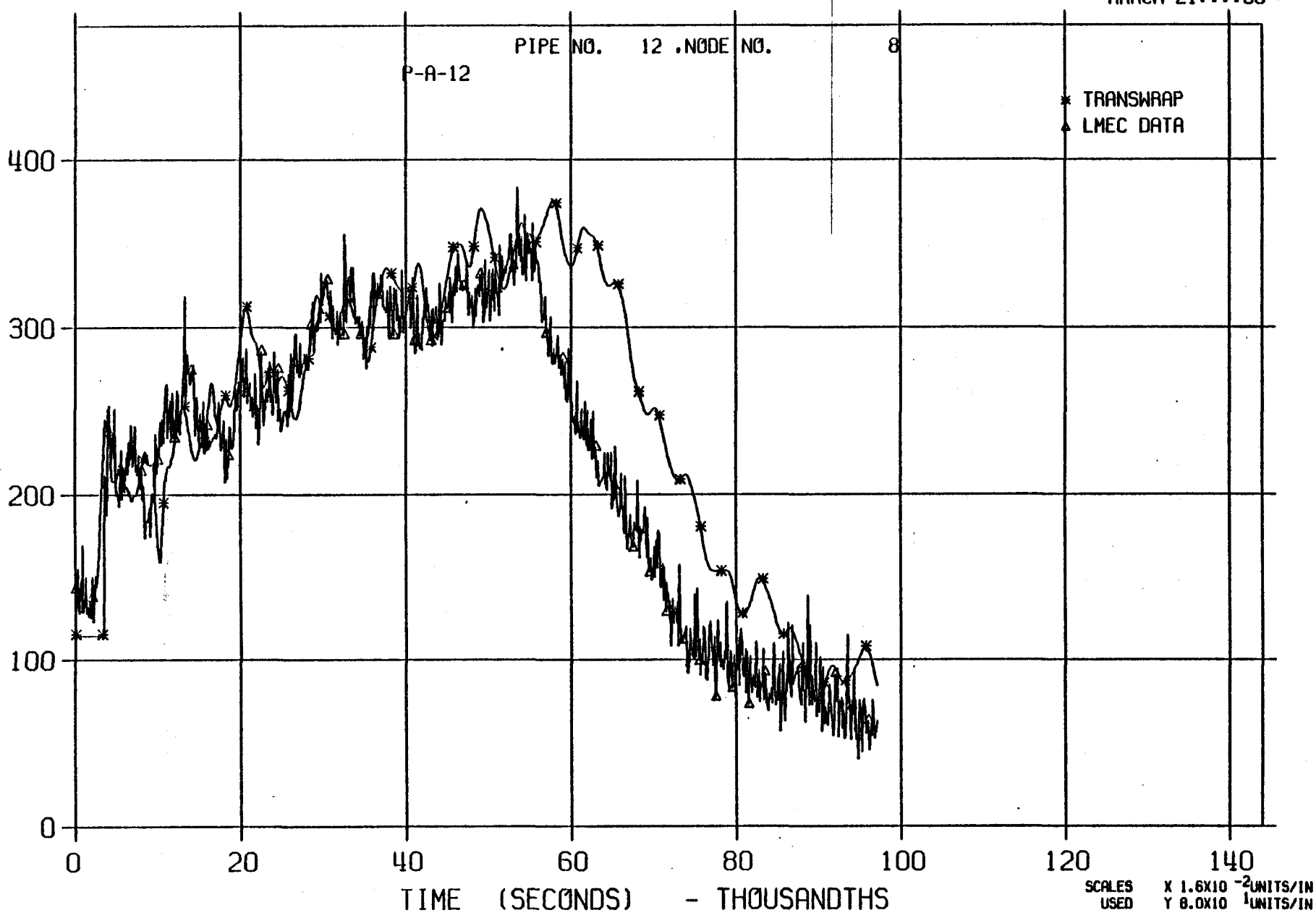


LLTR SERIES II - TR3A1A

7125T

MARCH 21:::80

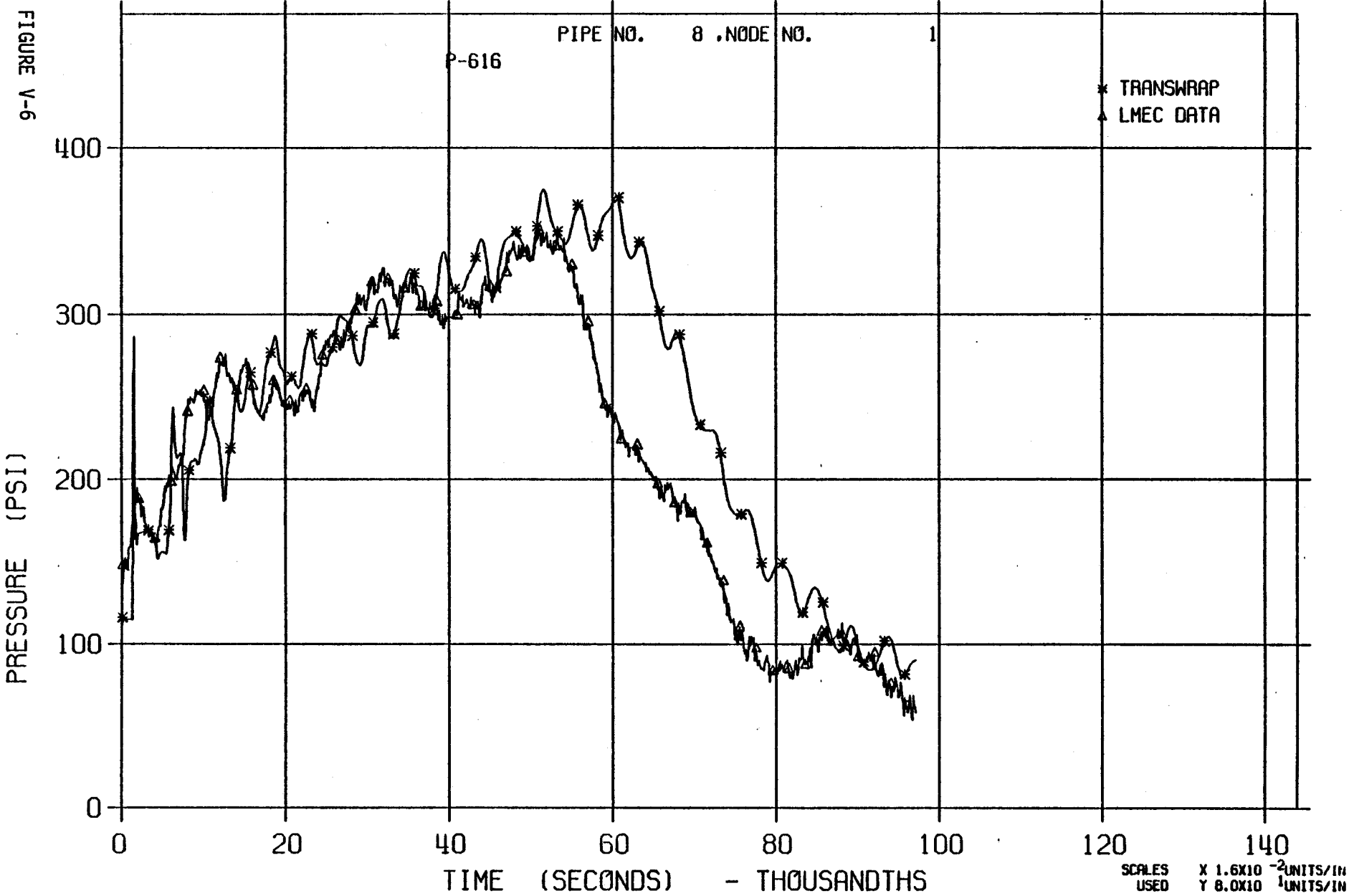
FIGURE V-5



LLTR SERIES II - TR3A1A

7125T

MARCH 21:1980

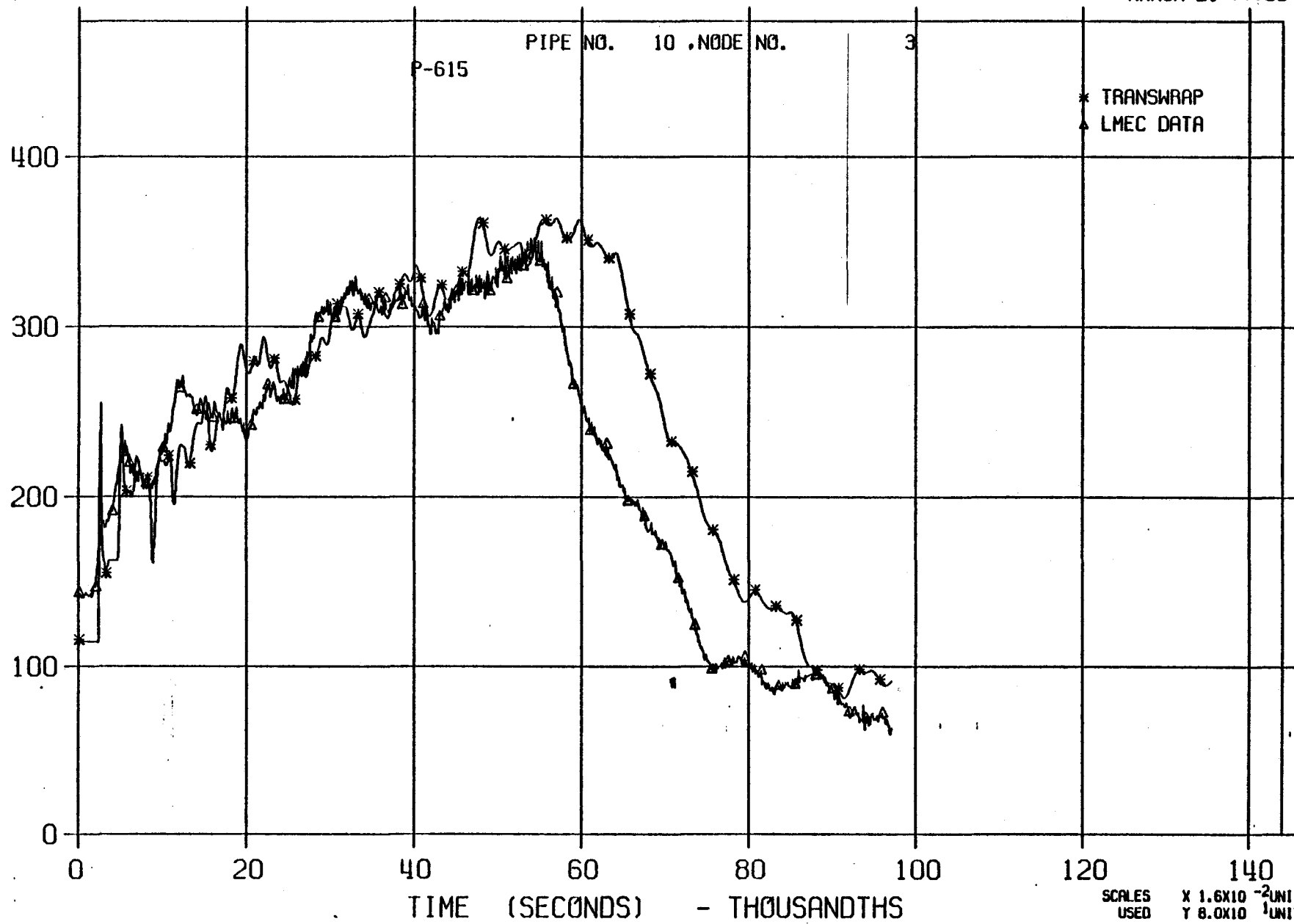


LLTR SERIES II - TR3A1A

7125T

MARCH 21::::80

FIGURE V-7

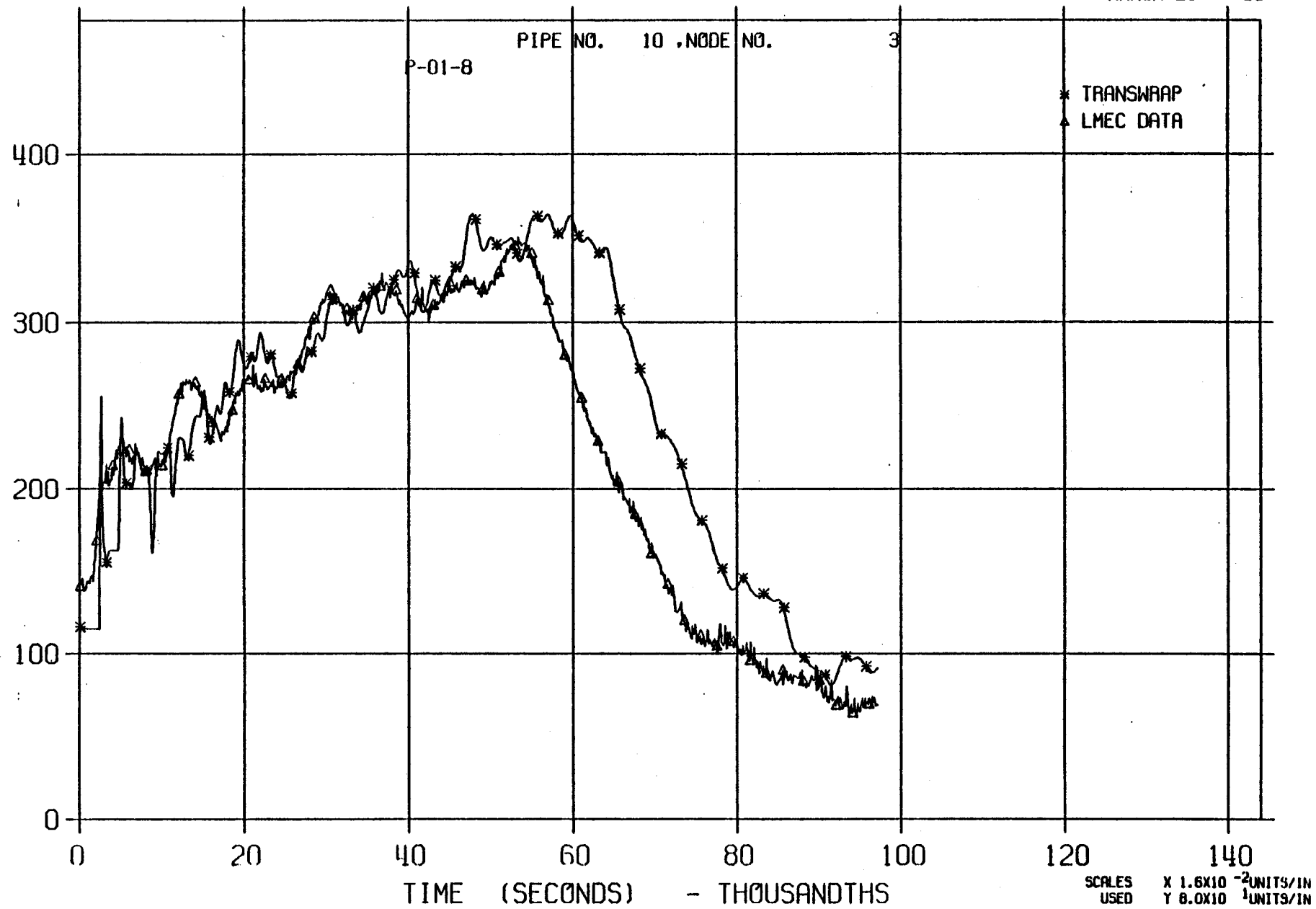


LLTR SERIES II - TR3A1A

7125T

MARCH 21:::80

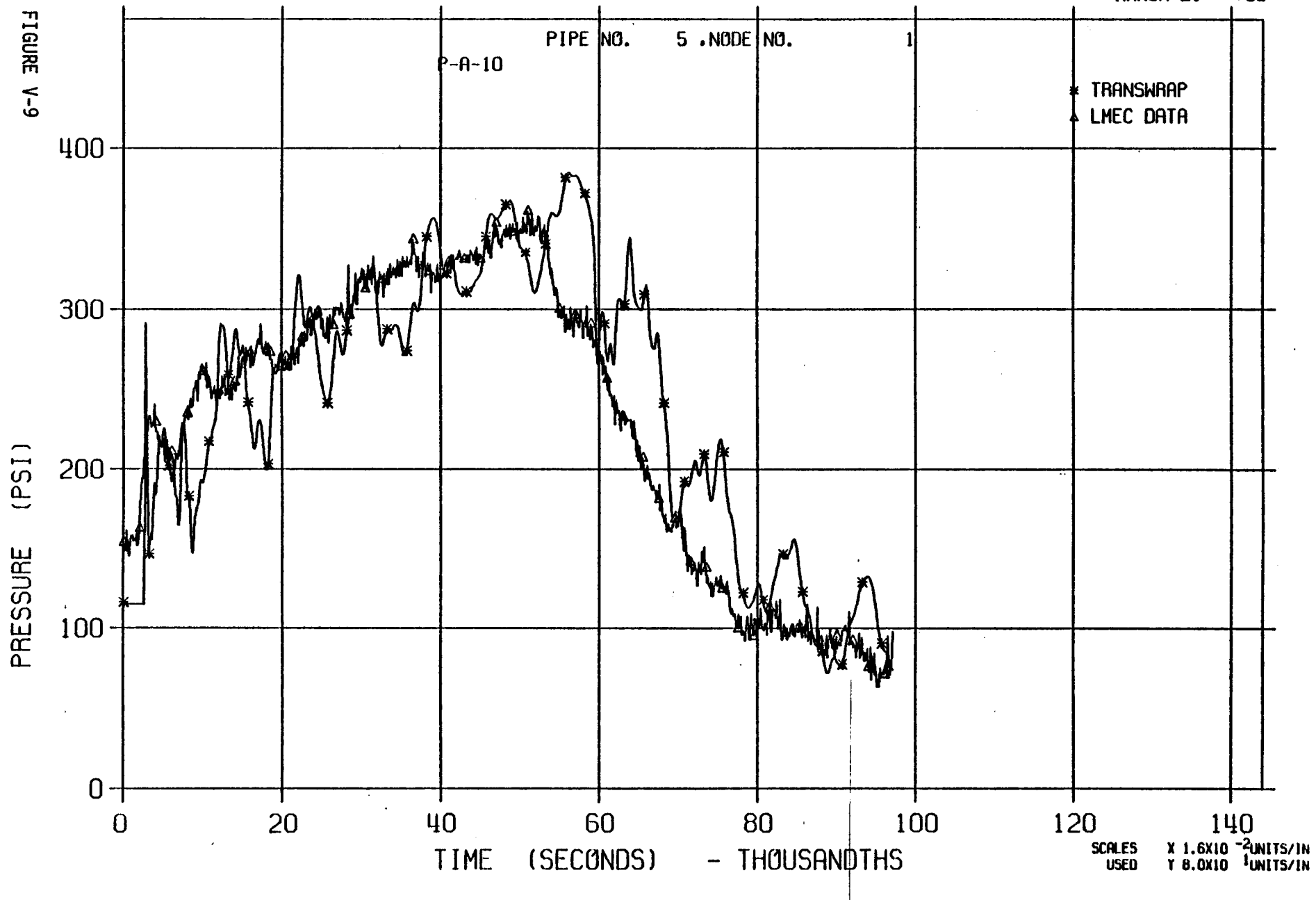
FIGURE V-8



LLTR SERIES II - TR3A1A

7125T

MARCH 21:80



LLTR SERIES II - TR3A1A

7125T

MARCH 21:::80

FIGURE V-10

89

PRESSURE (PSI)

400
300
200
100
0

P-A-11

PIPE NO. 5 . NODE NO.

1

TRANSWRAP
LMEC DATA

TIME (SECONDS) - THOUSANDTHS

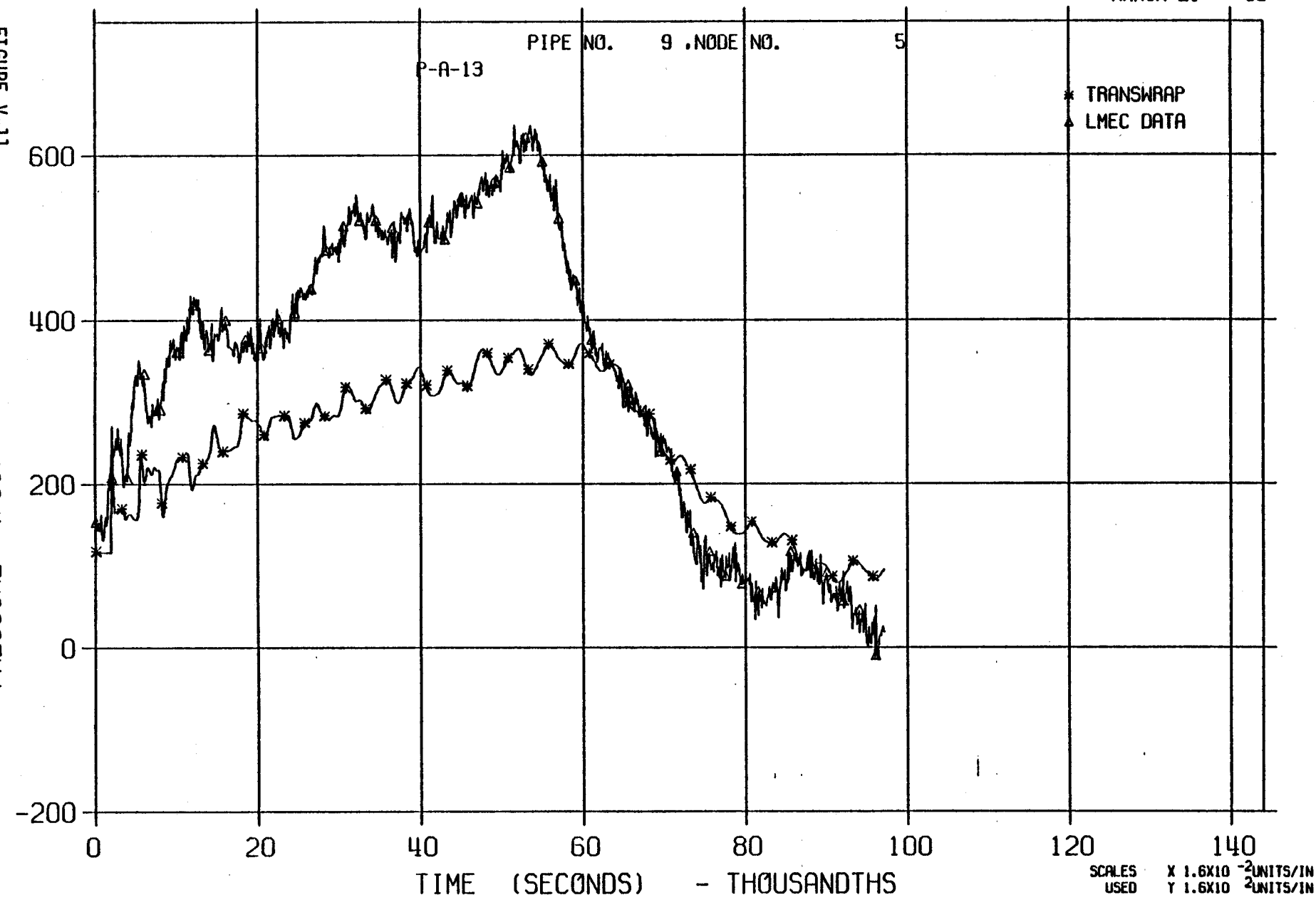
SCALES
USED X 1.6×10^{-2} UNITS/IN
Y 8.0×10^{-1} UNITS/IN

LLTR SERIES II - TR3A1A

7125T

MARCH 21:11:00

FIGURE V-11

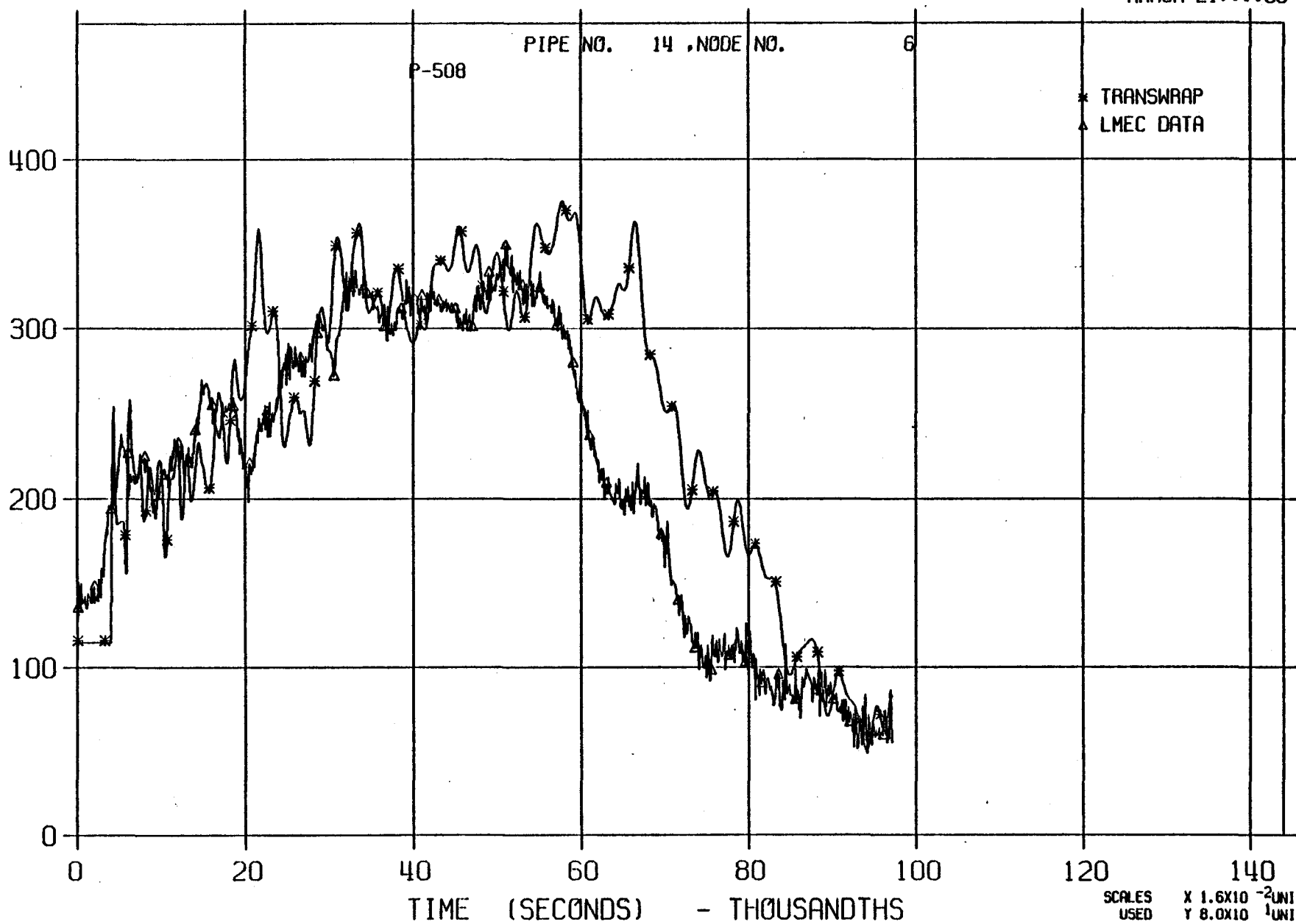


LLTR SERIES II - TR3A1A

7125T

MARCH 21:::80

FIGURE V-12

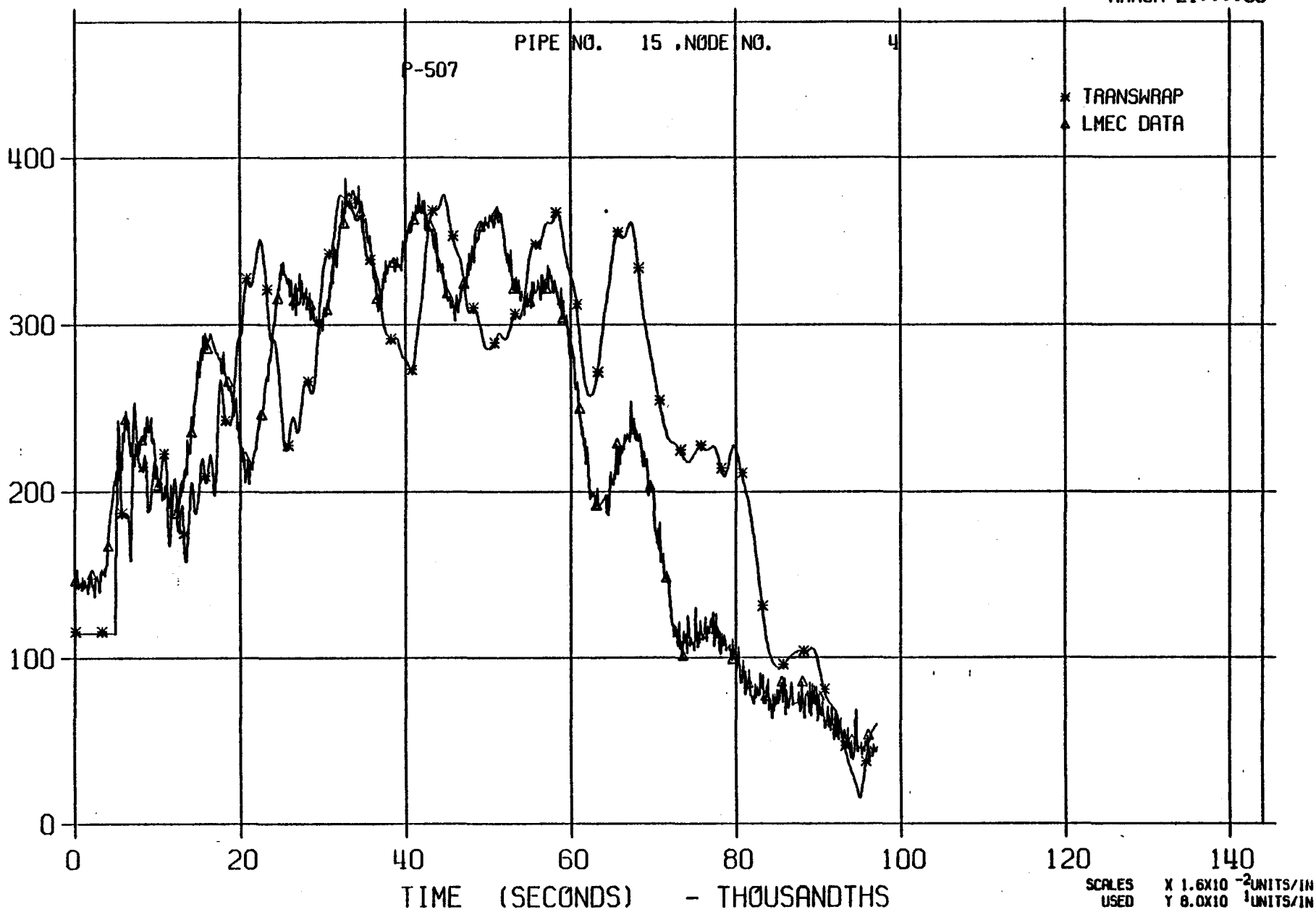


LLTR SERIES. II - TR3A1A

7125T

MARCH 21:::80

FIGURE V-13

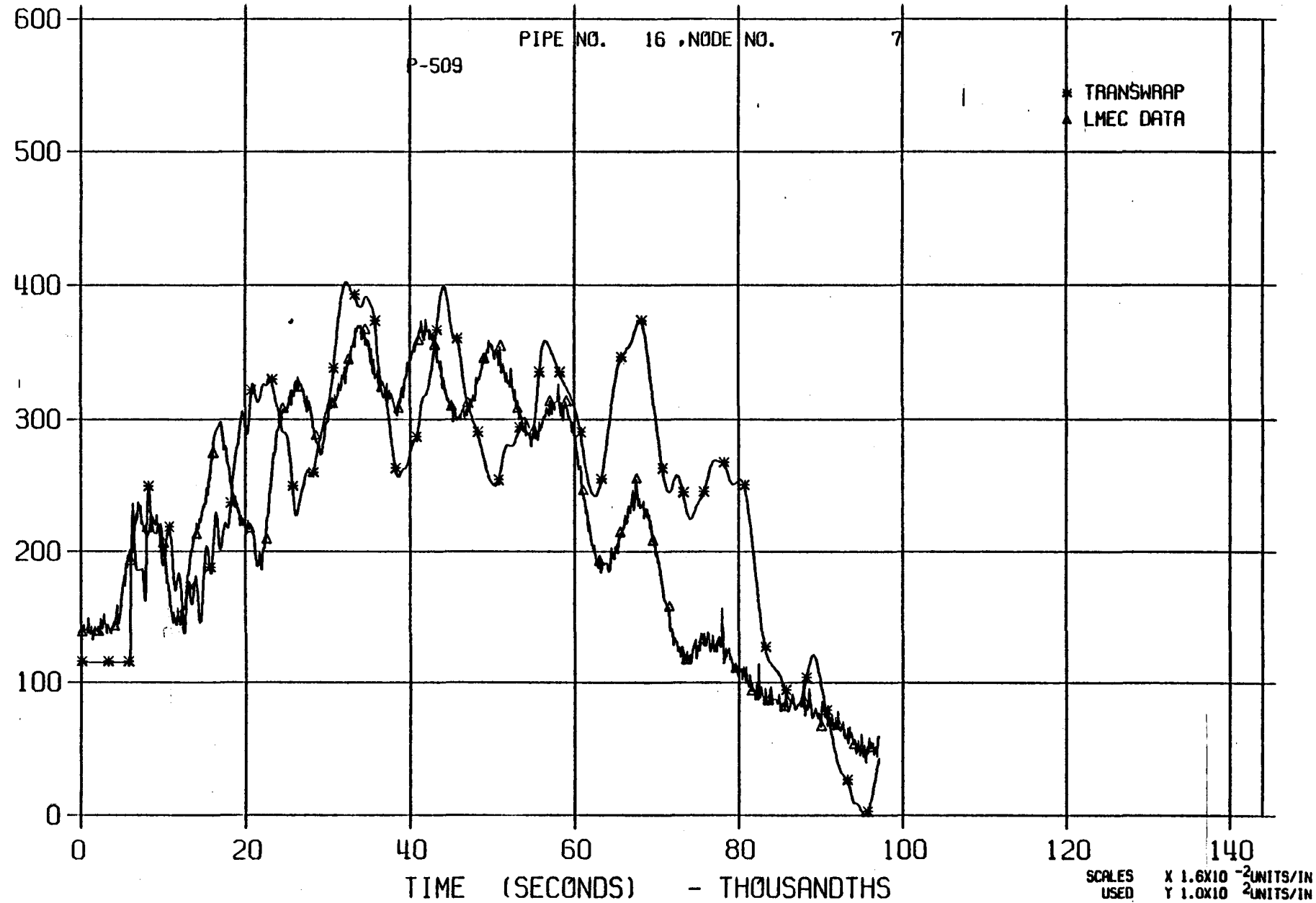


LLTR SERIES II - TR3A1A

7125T

MARCH 21:::80

FIGURE V-14

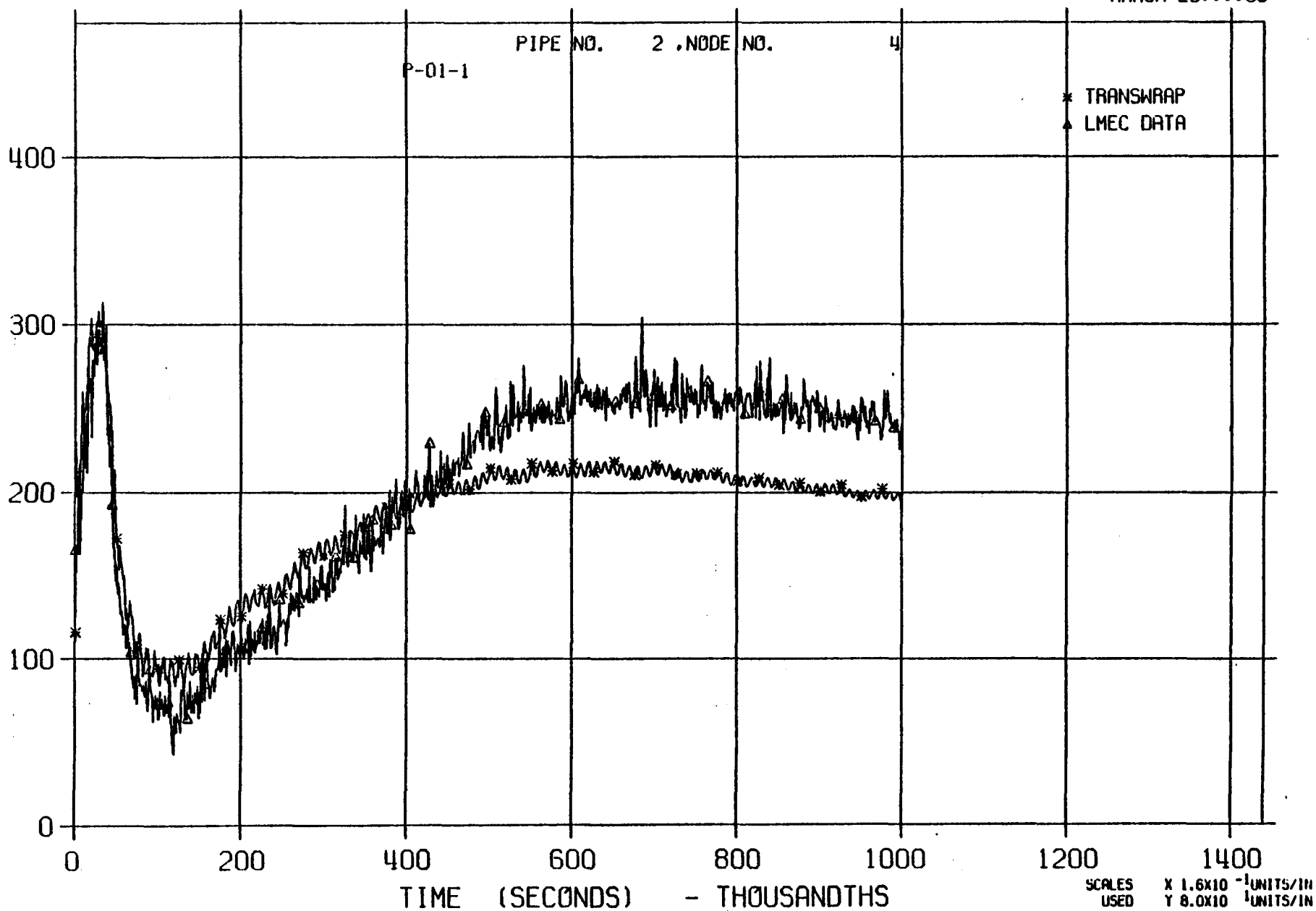


LLTR SERIES II - TR3A1B

2452T

MARCH 25:::80

FIGURE V-15

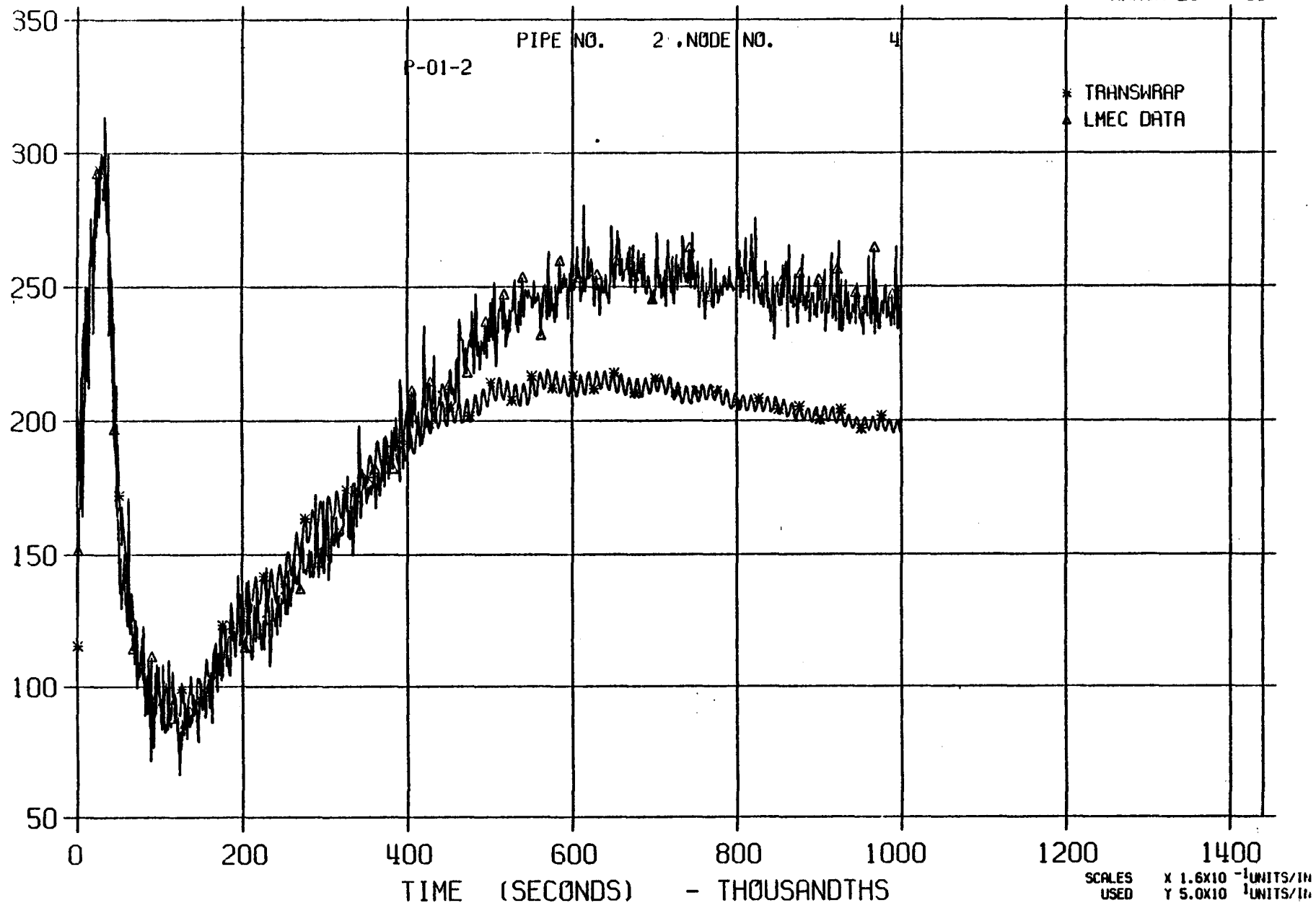


LLTR SERIES II - TR3A1B

2452T

MARCH 25:::80

FIGURE V-16

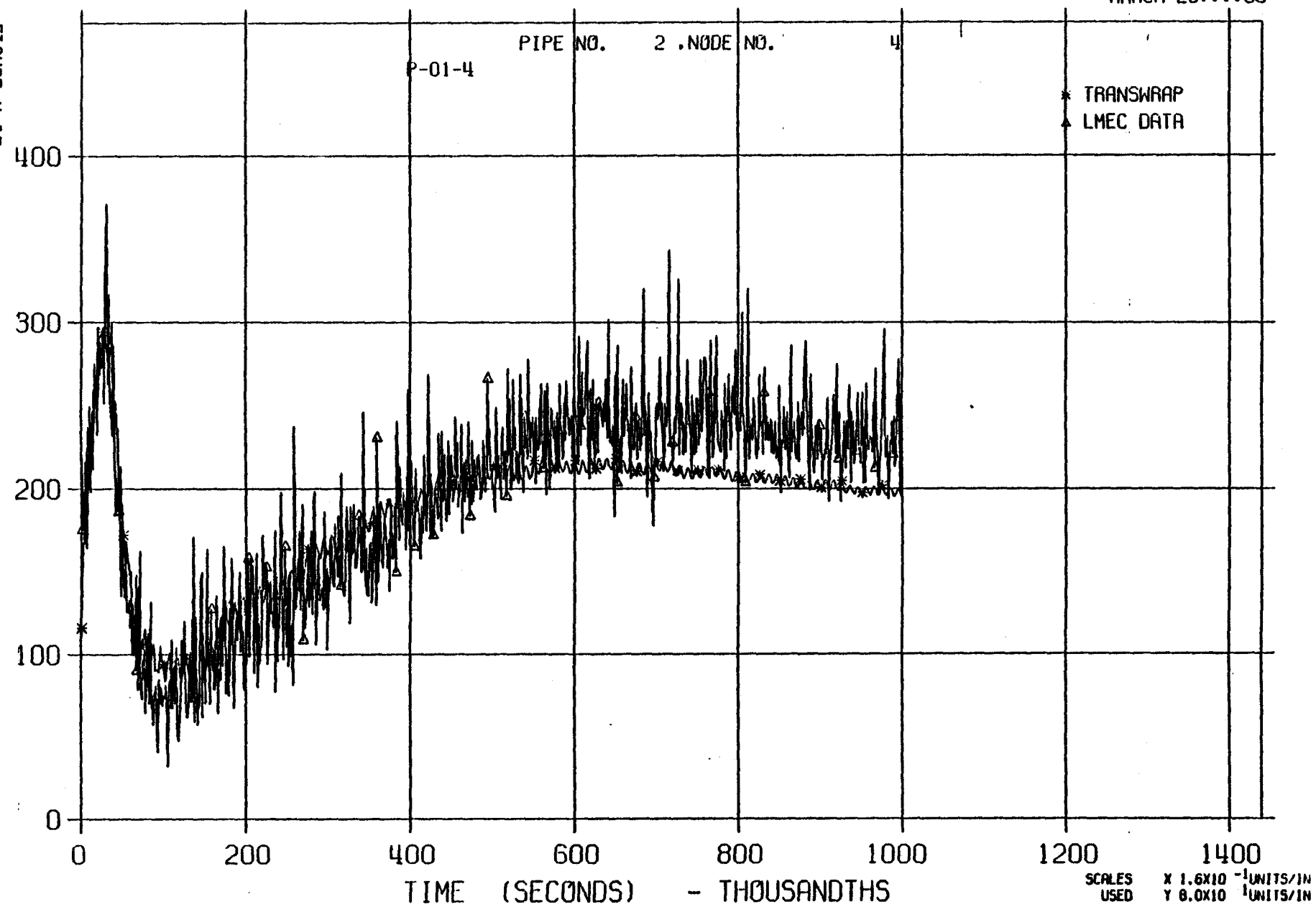


LLTR SERIES II - TR3A1B

2452T

MARCH 25:11:80

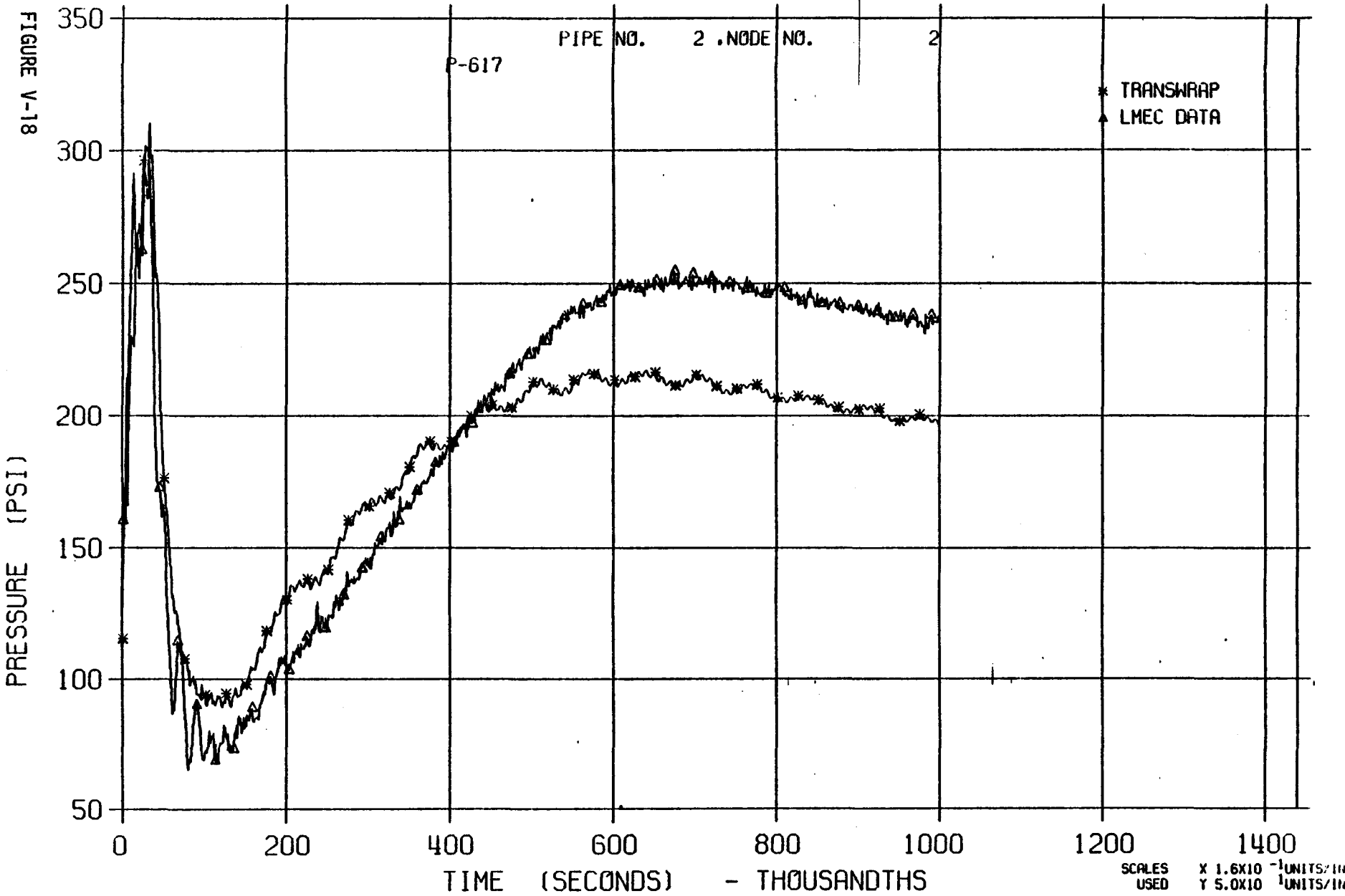
FIGURE V-17



LLTR SERIES II - TR3A1B

2452T

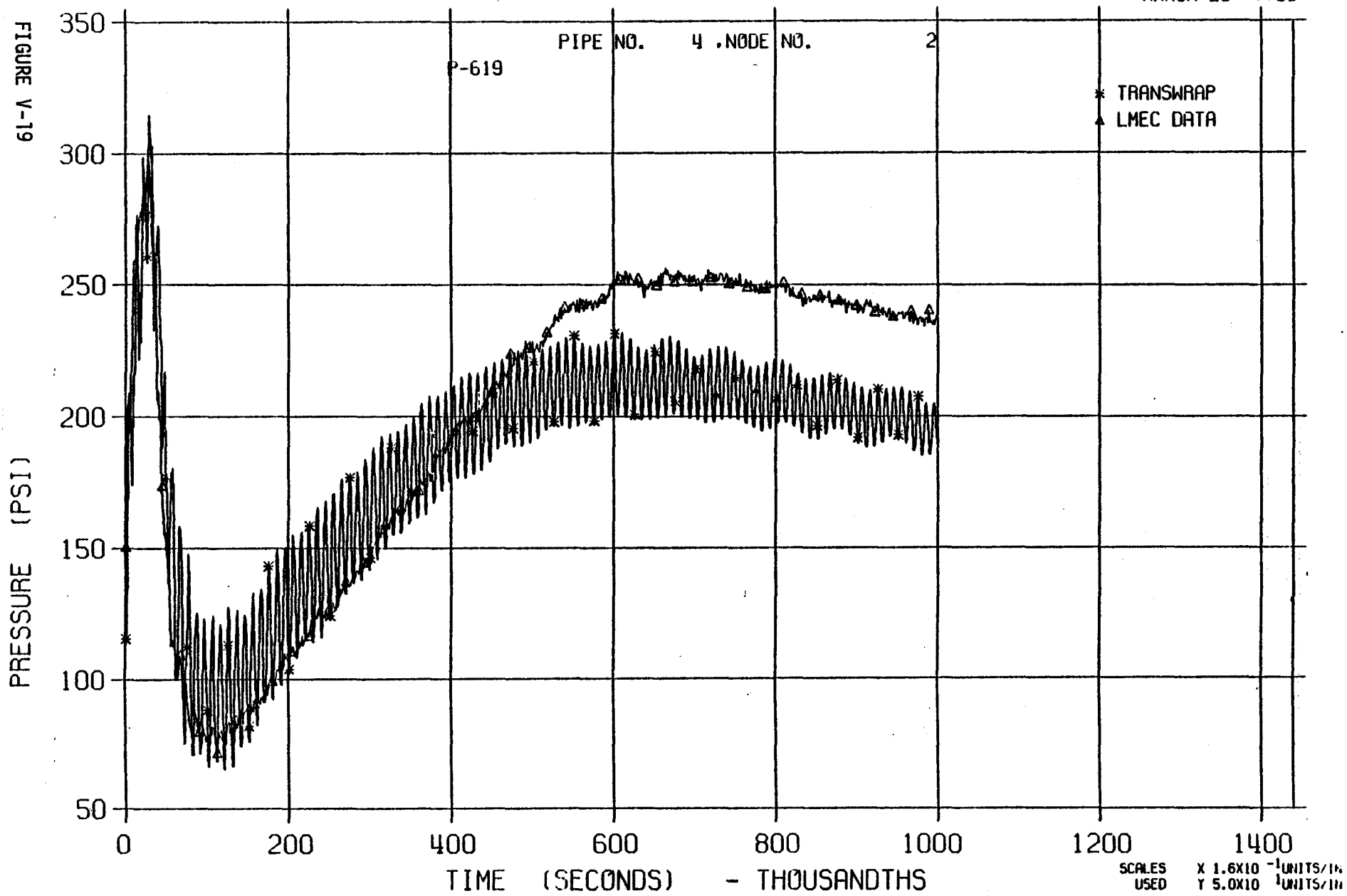
MARCH 25:::80



LLTR SERIES II - TR3A1B

2452T

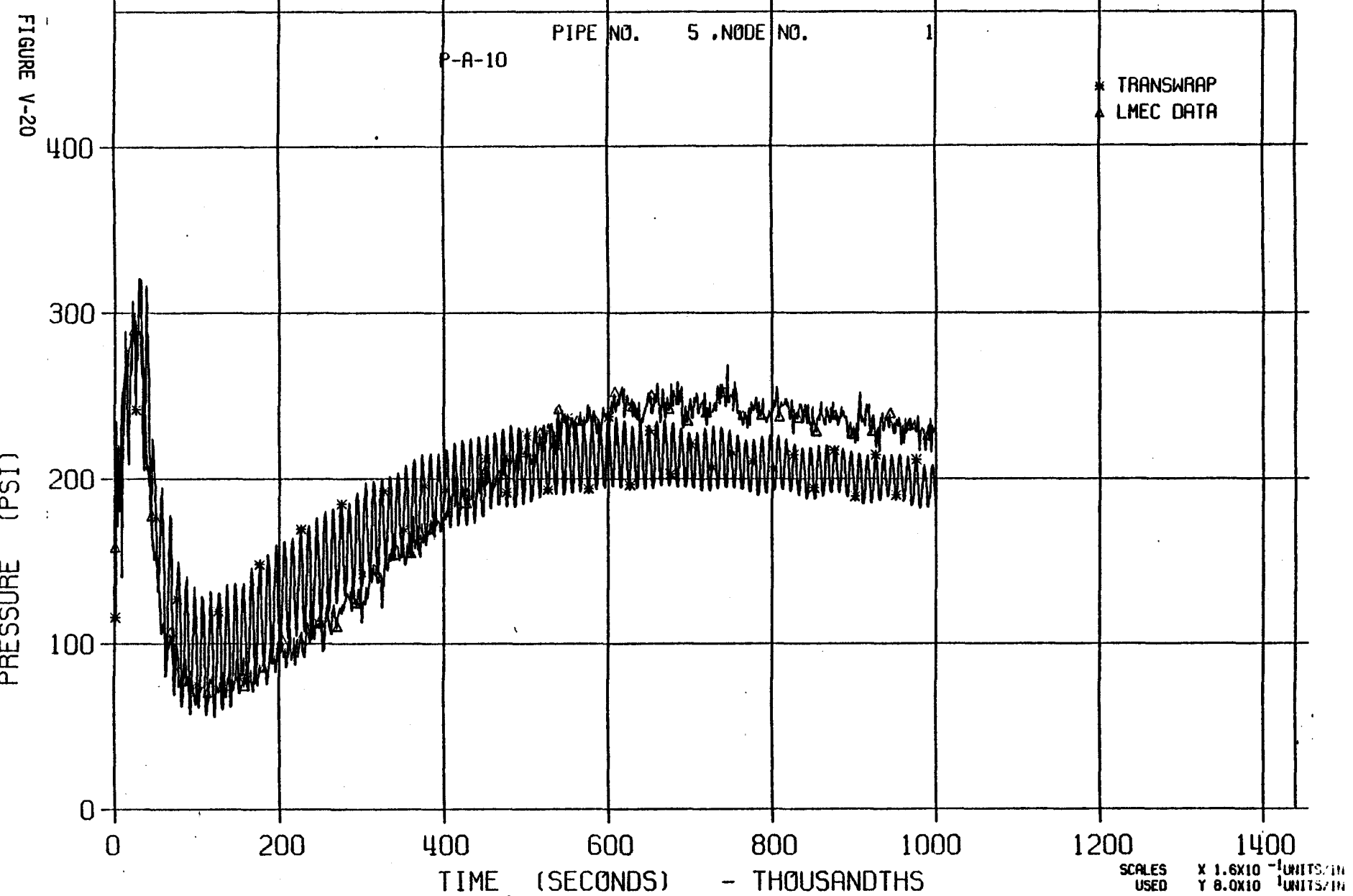
MARCH 25:::80



LLTR SERIES II - TR3A1B

2452T

MARCH 25:::80

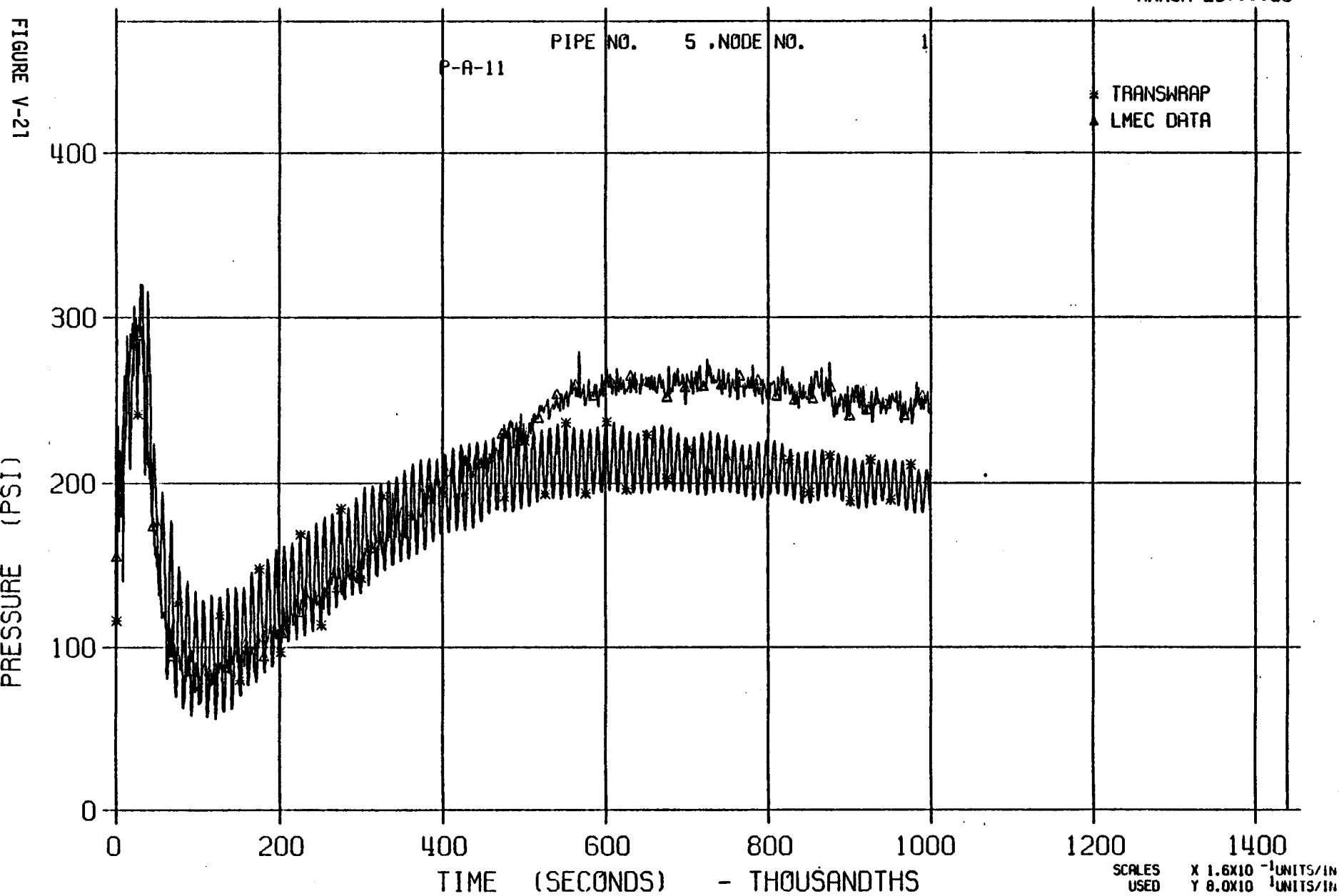


LLTR SERIES II - TR3A1B

2452T

MARCH 25:11:80

FIGURE V-21

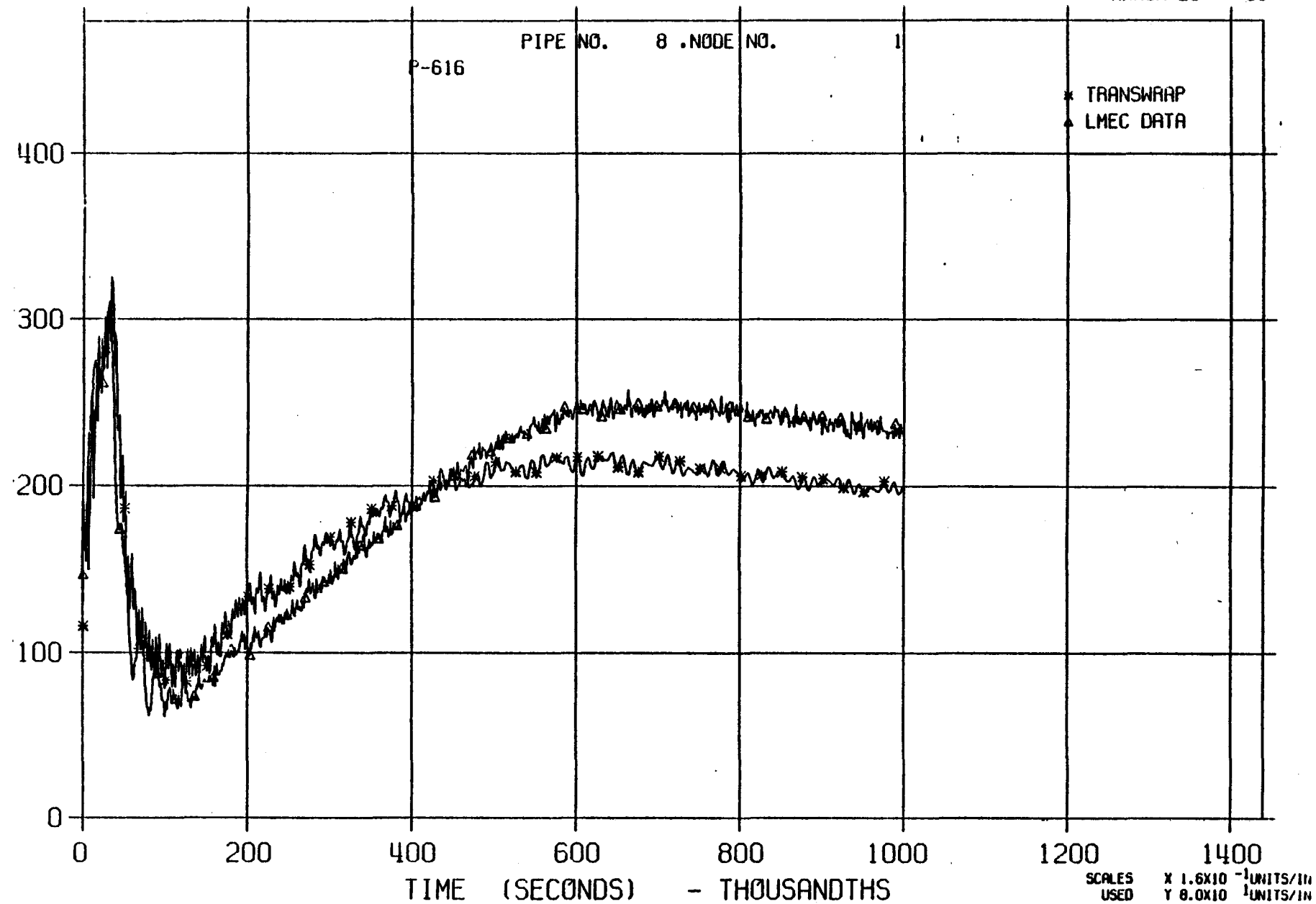


LLTR SERIES II - TR3A1B

2452T

MARCH 25:11:00

FIGURE V-22



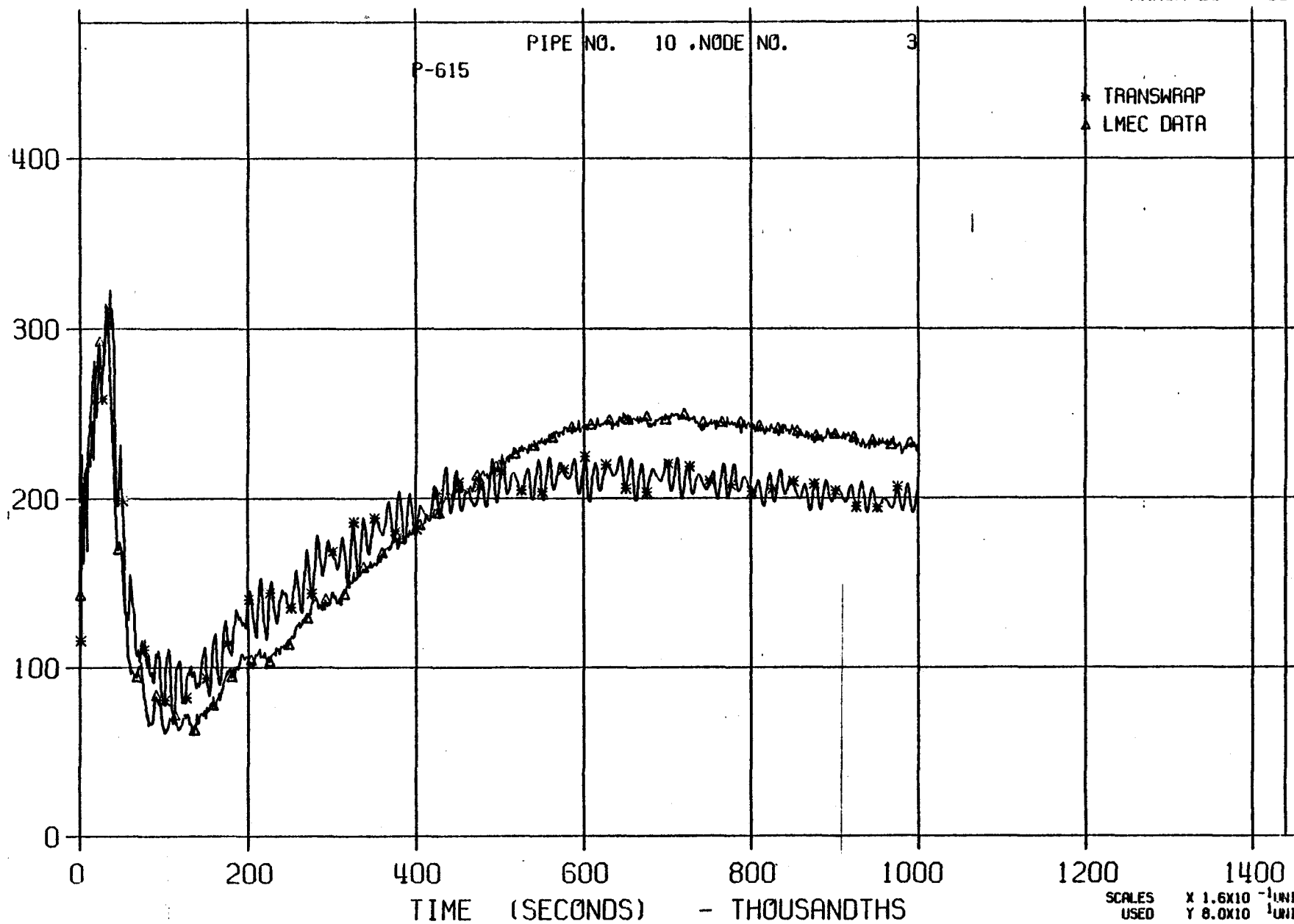
LLTR SERIES II - TR3A1B

2452T

MARCH 25:::80

FIGURE V-23

81

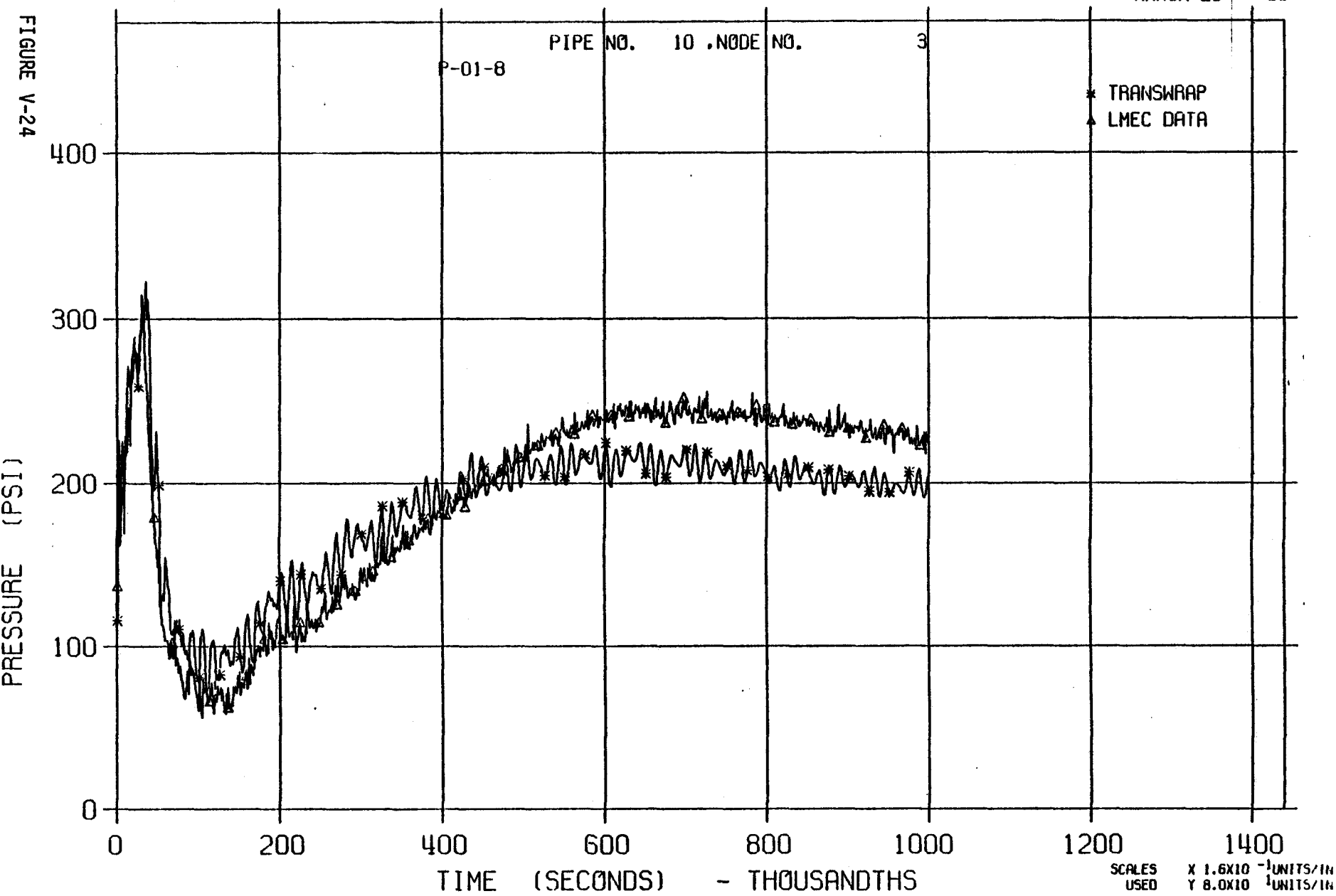


LLTR SERIES II - TR3A1B

2452T

MARCH 25, 1980

FIGURE V-24

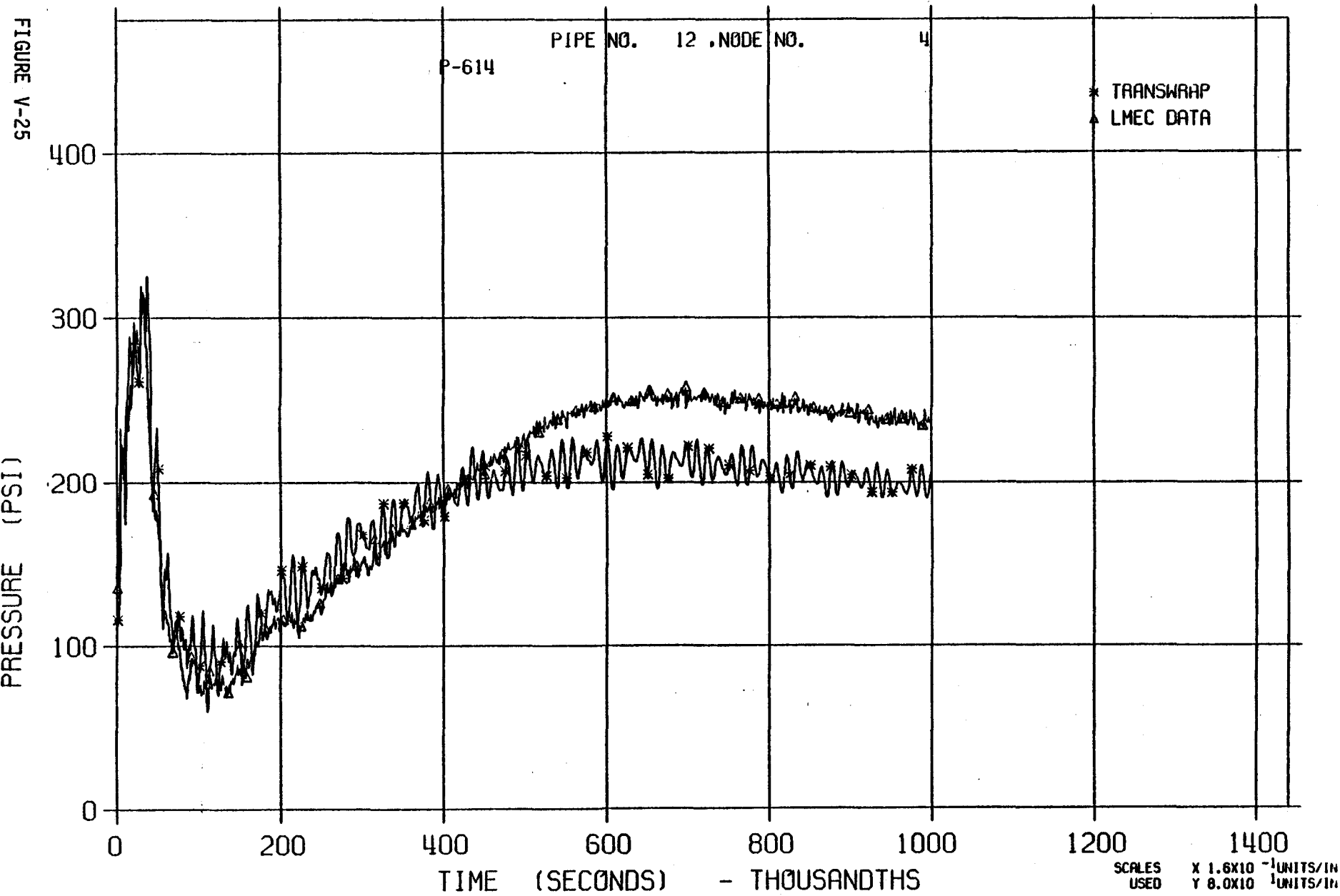


LLTR SERIES II - TR3A1B

2452T

MARCH 25:11:80

FIGURE V-25

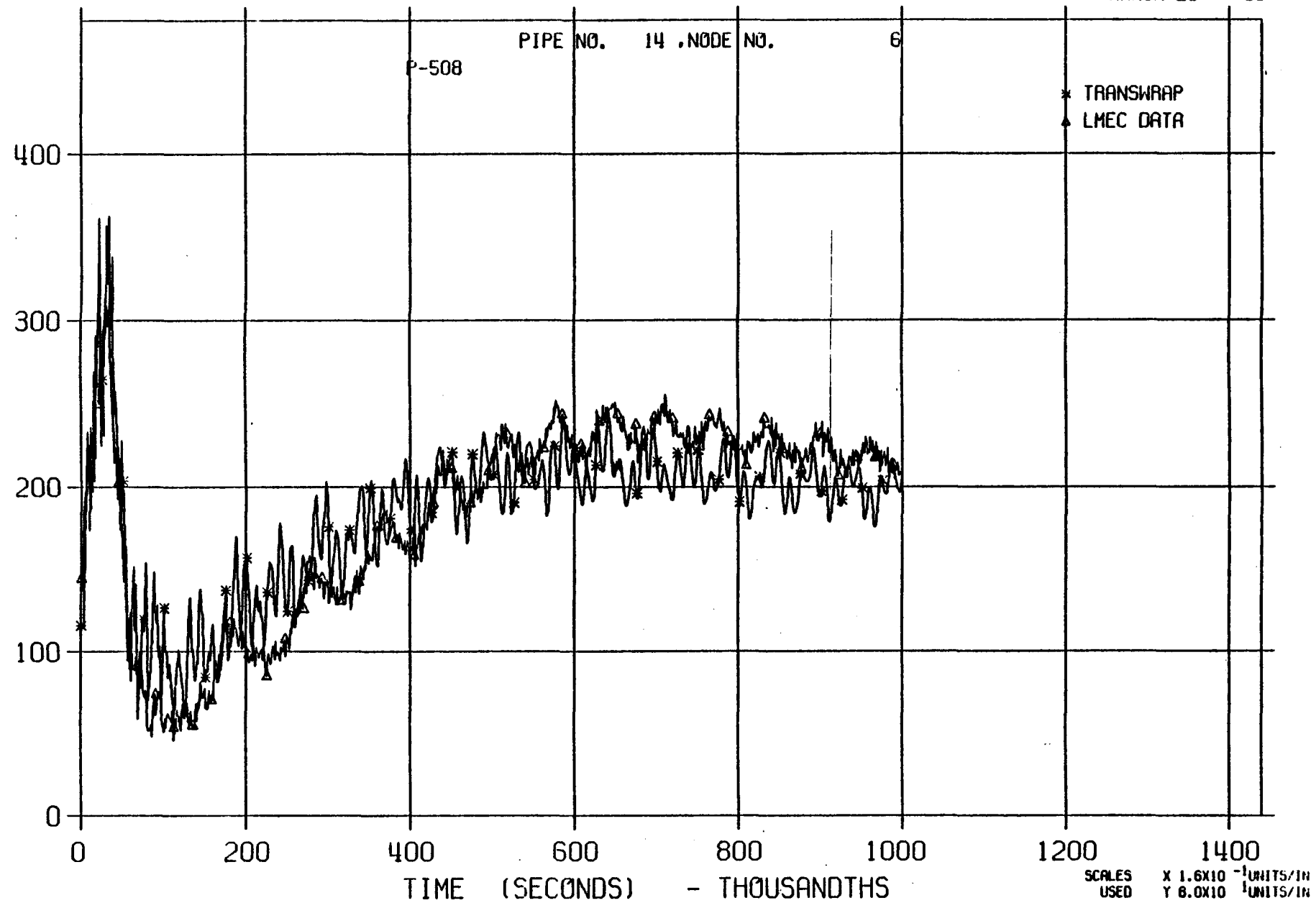


LLTR SERIES II - TR3A1B

2452T

MARCH 25:::80

FIGURE V-26



LLTR SERIES II - TR3A1B

2452T

MARCH 25:::80

FIGURE V-27

58

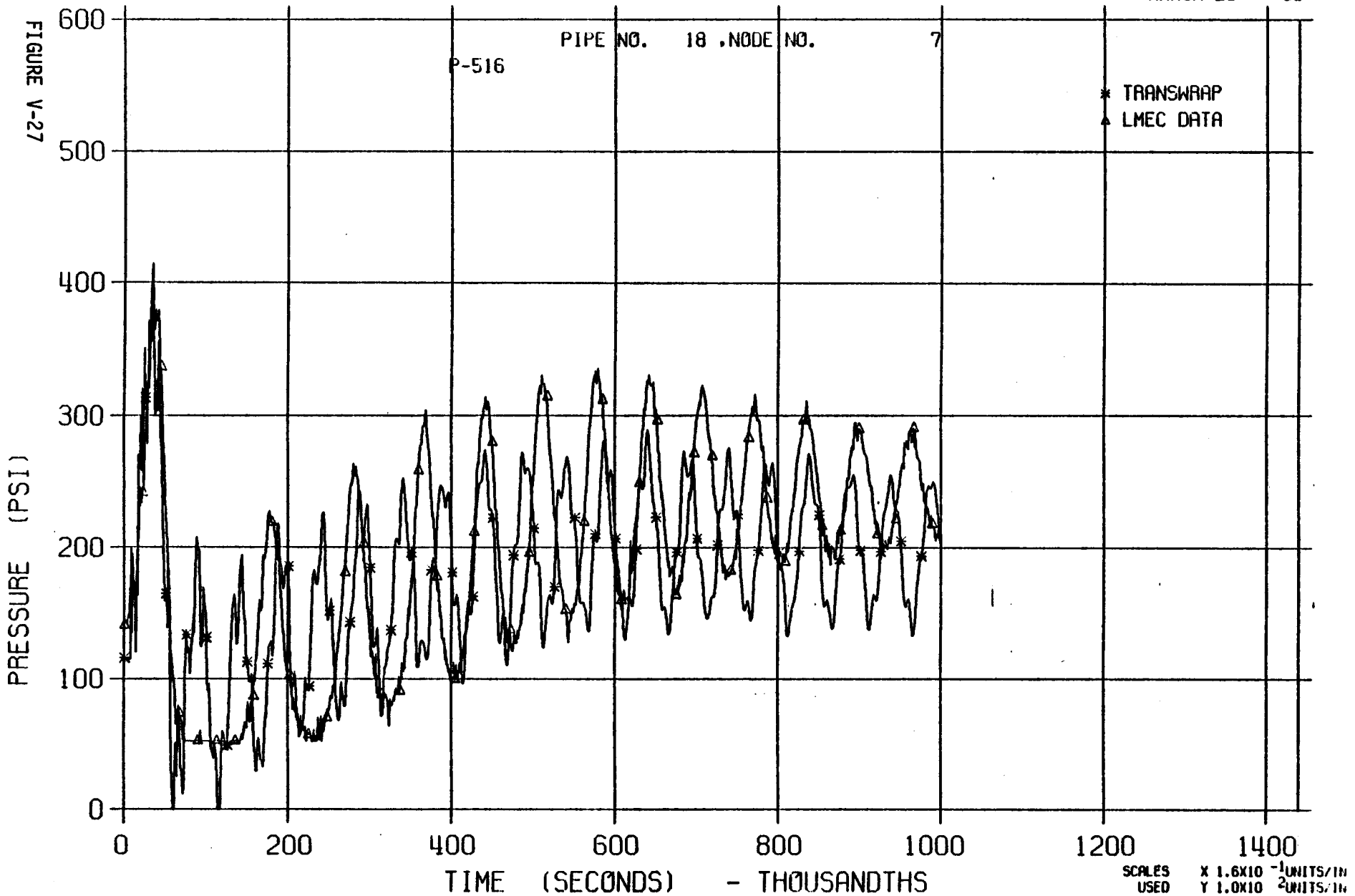
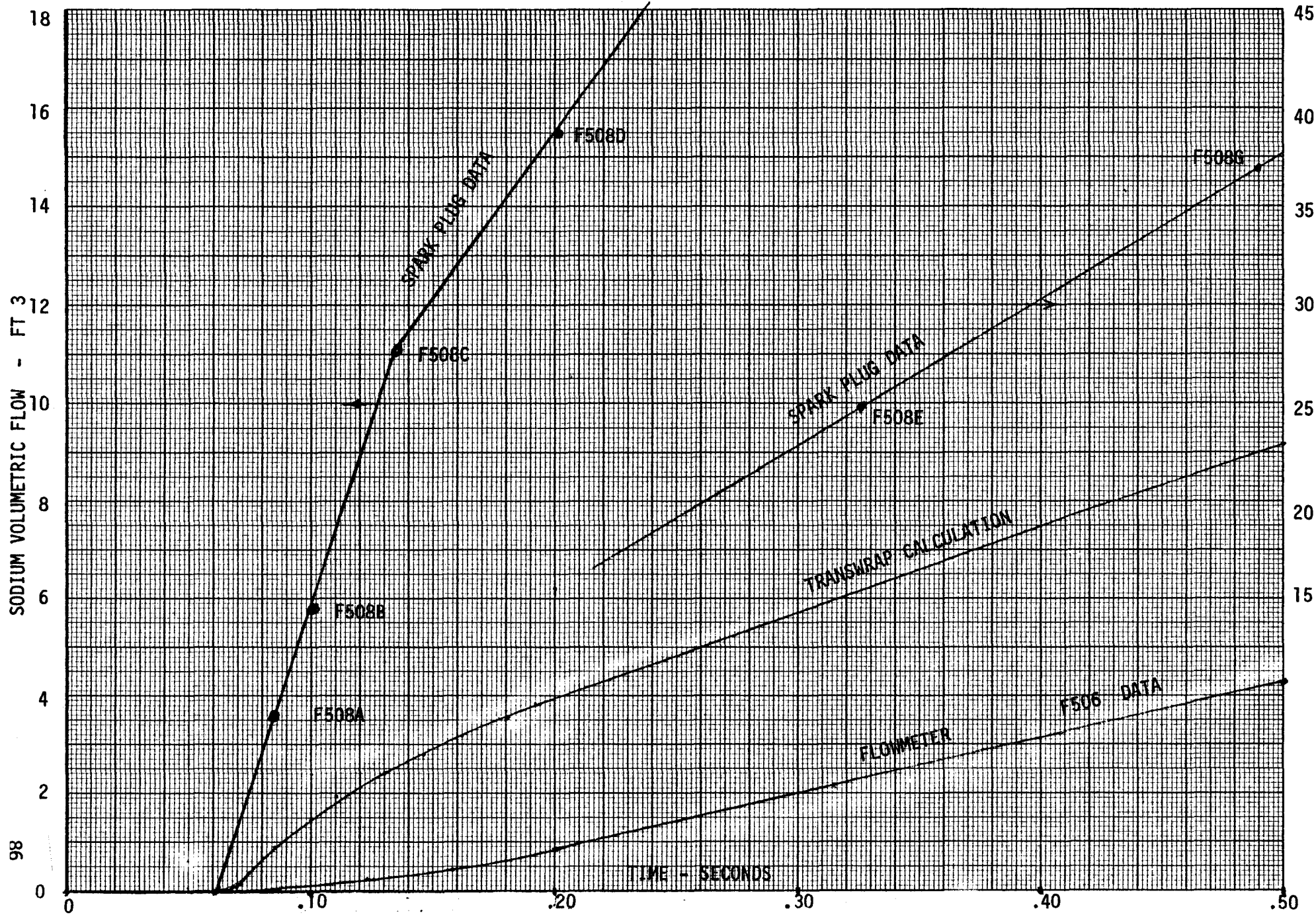


FIGURE V-28 RELIEF SYSTEM FLOW

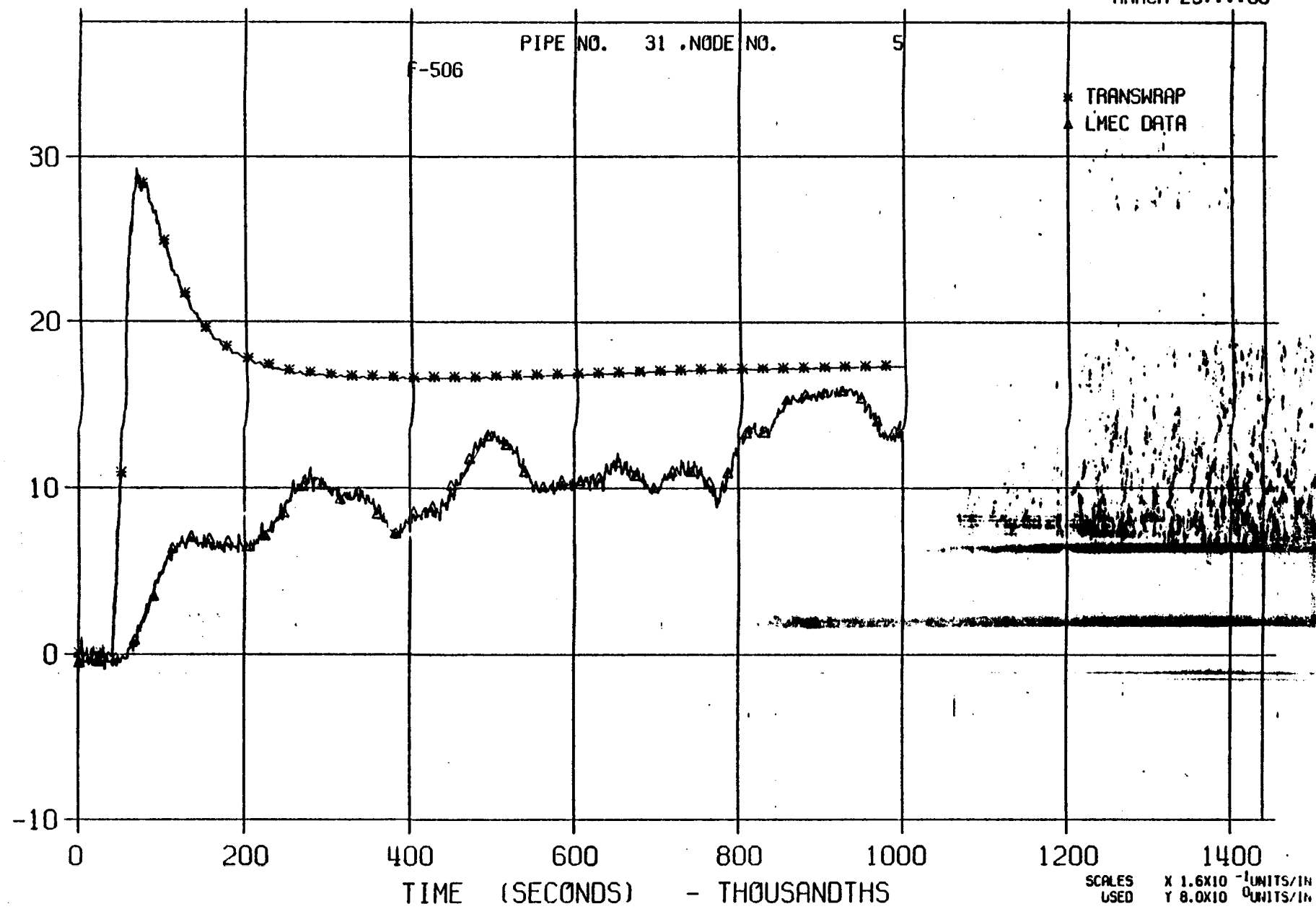


LLTR SERIES II - TR3A1A

2924T

MARCH 25:11:80

FIGURE V-29

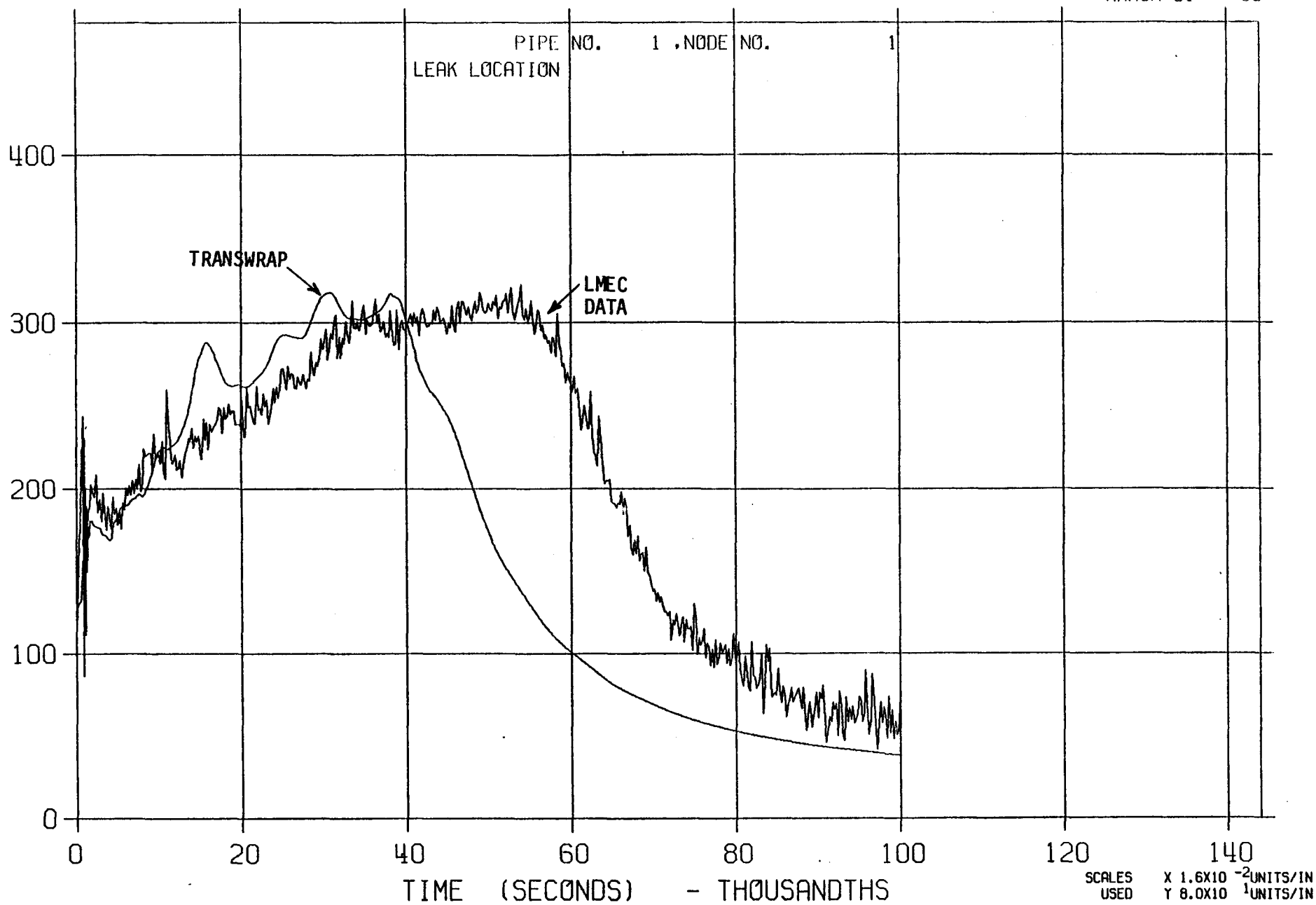


LLTR SERIES II - CASE 1C

2437T

MARCH 01:::80

FIGURE V-30



LLTR SERIES II - CASE 1C

2437T

MARCH 01:::80

FIGURE V-31

